Investigating the Neural Circuitry of Methamphetamine Addiction, and Prelimbic Cortex GABA Involvement in the Treatment Effect of Oxytocin

Katherine Jane Robinson

Bachelor of Medical Sciences

A thesis submitted in partial fulfillment of the requirements for the degree of

Master of Research

Department of Psychology, Macquarie University

November 2018

Table of Contents

Appendices

List of Abbreviations

ANOVA	Analysis of Variance
Cg1	Anterior cingulate cortex
CNO	Clozapine N-oxide
Cre	Cre-recombinase enzyme
DAT	Dopamine Transporter
DIO	Double-floxed inverted open reading frame
DMEM	Dulbecco's Modified Eagle's Medium/Nutrient Mixture F-12 Ham
DREADD	Designer receptor exclusively activated by designer drugs
DSM	Diagnostic and Statistical Manual of Mental Disorders
FLEX	FLip and Excise
FR1	Fixed ratio 1 schedule
GABA	γ-amino-butyric acid
GAD	Glutamate-decarboxylase
GAD1	Glutamate decarboxylase gene
GAD67	Glutamate-decarboxylase, isoform 67
hM3D(Gq)	Human muscarinic receptor type 3, excitatory DREADD
hM4D(Gi)	Human muscarinic receptor type 4, inhibitory DREADD
IL	Infralimbic cortex
IP	Intraperitoneal
IV	Intravenous
IVSA	Intravenous self-administration

LO	Lateral orbitofrontal cortex
METH	Methamphetamine
MO	Medial orbitofrontal cortex
mPFC	Medial prefrontal cortex
NAc	Nucleus Accumbens
nNOS	Neuronal nitric oxide synthase
NO	Nitric oxide
NOS	Nitric oxide synthase
OFC	Orbitofrontal cortex
OTR	Oxytocin receptor
OTR-A	Oxytocin receptor antagonist
PBS	Phosphate buffered saline
PFA	Paraformaldehyde
PFC	Prefrontal cortex
PrL	Prelimbic cortex
PV	Parvalbumin
PVN	Paraventricular nucleus
ROI	Region of interest
SC	Subcutaneous
Veh	Vehicle
VMAT-2	Vesicular monoamine transporter 2
VO	Ventral orbitofrontal cortex
VTA	Ventral Tegmental Area

List of Figures

List of Tables

Statement of Originality and Ethical Approval

I, Katherine Jane Robinson, hereby confirm that all material contained in this project are my original authorship and ideas, except where the work of others has been acknowledged or referenced. I also confirm that the work has not been submitted for a higher degree to any other university or institution.

The research project was approved by Macquarie University Animal Ethics Committee.

Animal Research Authority: 2017/043

Ms Robinson was supported by the Research Training Pathway Scholarship Scheme for the duration of the project. Research studies were funded by internal funding from Macquarie University and NHMRC grants awarded to JLC.

Katherine Jane Robinson

Date: 17/11/2018

Co-Author Contribution

Cornish, J.L 5%

Contributed to research design, provided assistance with surgeries and manuscript editing

Baracz, S.J 4%

Contributed to the research design and provided assistance with surgeries, self-administration and perfusions.

Everett, N.A 3%

Contributed to the research design and provided assistance with self-administration and perfusions.

Turner, A.J 1%

Provided assistance with surgeries and perfusions.

Nedelkoska, T 1%

Provided assistance with self-administration.

Acknowledgments

Firstly, thank you to my supervisor Jen for welcoming me into your lab group and introducing me to the field of addiction. I am very grateful for your guidance. Thank you for giving me independence and the freedom to explore my ideas. Thank you to my mentors, Ann, Simon and Cara. Ann, without your initial support and guidance, I wouldn't be in research today. Thank you for giving me the opportunity. Simon, thank you for your endless wisdom and encouragement. You always know how to ignite passion and excitement. Cara, thank you for your ongoing support and friendship.

Thank you to everyone in the Cornish lab! Sarah and Nick: thank you for your endless guidance and friendship during the last 18 months. You are both very talented scientists and wonderful people. You both inspire me to strive for a successful career in research. I couldn't have gotten through this year without your continuous encouragement and guidance. Special thank you to Anita (and your old school iPod) for keeping me going during the long surgery days. Thank you to Eden for our morning coffee dates and for reminding me of why I love neuroscience. Thank you to Thea for helping me stay motivated and listening to my rants after a bad day in the lab.

Thank you to my parents for continually supporting me in all of my endeavors. Lastly, thank you to my partner Bowden for all of your love, support and encouragement. Thank you for putting up with me and understanding the demands of this challenging year.

I would like to dedicate this thesis to the beautiful rats that I have cared for this year. Without you, this thesis would not be possible.

Abstract

Abuse of methamphetamine (METH), a potent psychostimulant, elicits dysfunction of reward-associated brain regions such as the nucleus accumbens (NAc) and prefrontal cortex (PFC). Additionally, it is thought that METH disrupts the balance of excitation and inhibition in the brain, perturbing neurotransmitter systems and inducing neurotoxicity. Current pharmacotherapies act to reduce the acute rewarding effects of METH, however, existing treatments are largely ineffective with most abstinent users relapsing to drug-taking behaviour. Ineffective pharmacotherapies can, in part, be attributed to our limited understanding of the neurobiological mechanisms which underlie METH addiction. Preclinical models of addiction have evidenced the therapeutic potential of oxytocin, an endogenous neuropeptide, which may act to restore METH-induced disruptions to the excitatory/inhibitory balance. The present thesis utilized the intravenous drug-self administration model of reinstatement to investigate METH-induced neuroadaptations and the mechanistic action of oxytocin.

Existing published literature suggests increased neuronal activation in reward-associated brain regions following administration of addictive drugs or drug-associated cues. However, it is unknown precisely which neuronal populations are activated and how this may impact on functional connectivity. Chapter 2 investigated alterations to neuronal activity as indicated by Fos immunoreactivity and immunoreactivity of neuronal nitric oxide synthase (nNOS) and parvalbumin (PV), two populations of GABAergic interneurons. Injection of METH significantly increased Fos immunoreactivity in the NAc and many subregions of the PFC. Analysis also revealed reduced correlated activity between these regions in METH-exposed

animals. Analysis of nNOS immunoreactivity revealed increased number and activation of nNOS+ neurons at discrete areas of the NAc in chronic METH-exposed animals, suggesting increased activation of the nitrergic system. In contrast, no significant differences were noted in PV immunoreactivity. Furthermore, the lack of colocalisation of Fos with GABAergic markers suggests activation was most likely confined to excitatory populations. This study presents the first investigation of altered correlated activity following relapse to METH use in the intravenous self-administration paradigm, evidencing aberrant activation of excitatory neurons within subregions of the NAc and PFC.

It is hypothesized that oxytocin treatment interacts with GABA systems within the brain to restore the imbalance of excitation and inhibition, yet the precise mechanisms for this interaction are unknown. Chapter 3 used a chemogenetic approach to investigate the interaction between GABAergic neurons and oxytocin in the PFC during relapse. DREADDs were used to inactivate GABAergic neurons in the prelimbic subregion of the PFC (PrL) prior to pretreatment with systemic oxytocin. It was hypothesised that inactivation of GABAergic neurons would blunt the effect of systemic oxytocin treatment, eliciting robust reinstatement. While this study demonstrated attenuation of cue-induced and METH-primed reinstatement behaviours following treatment with systemic oxytocin, chemogenetic inactivation of GABAergic neurons did not reduce the efficacy of systemic oxytocin treatment. This suggests that oxytocin is not interacting with GABAergic neurons within the PrL to attenuate drug-seeking behaviours. The present thesis reveals new insights relating to the neurobiological mechanisms underlying METH addiction and enhances knowledge about the mechanistic actions of oxytocin which facilitates attenuatuation of drug-associated behaviours.

Chapter 1: Introduction

Drug addiction, also described as substance use disorder, is a compulsive, relapsing condition where maladaptive drug-seeking behaviours are maintained despite adverse outcomes (DSM-5, 2013). Drug addiction is associated with tolerance to drug effects, withdrawal symptoms and increased motivation to consume drugs (Hyman & Malenka, 2001), despite detrimental social and economic impacts.

Drug use is highly prevalent worldwide, with approximately 275 million people reporting drug use at some stage in 2016 (United Nations Office on Drugs and Crime [UNODC], 2018). Whilst not every drug-user will develop a compulsive drug addiction (DSM-5, 2013; Deroche-Gamonet, Belin, & Piazza, 2004; Volkow & Morales, 2015), approximately 31 million people suffered from addiction in 2016, most of which did not receive treatment (UNODC, 2018). Acute administration of addictive drugs can cause hedonic effects, however repeated or chronic abuse of drugs can cause pathological changes to brain circuitry and a myriad of medical, cognitive and psychosocial complications that persist despite cessation of drug-taking (Epstein, Preston, Stewart, & Shaham, 2006; Kalivas, 2009; Leshner, 1997; O'Brien & Kalivas, 2008). Drug-induced neurobiological changes are long-lasting and thought to drive the compulsive nature of addiction and high incidence of relapse (Leshner, 1997; O'Brien & Kalivas, 2008).

Methamphetamine (METH, “ice”) is amongst the most harmful of illicit drugs abused worldwide, detrimentally impacting on the drug-user and the broader community (Courtney & Ray, 2014; Degenhardt et al., 2017; Morley, Cornish, Faingold, Wood, & Haber, 2017). Recently, METH was reported as the second most used illicit drug in Australia (Stafford, Breen, & Burns, 2016), with 61% of surveyed drug users reporting METH as their drug of choice (Australian

Institute of Health and Welfare [AIHW], 2017). Whilst the prevalence of METH use has remained stable in the last five years, the proportion of crystalline METH ("crystal METH") users and frequency of use has increased (Degenhardt et al., 2017; Stafford et al., 2016). Increased use of crystal METH has corresponded with increases in the numbers of dependent users, METH-related harms and METH-related deaths (Darke, Kaye, & Duflou, 2017; Degenhardt et al., 2017). Abuse of METH places a significant burden on the Australian economy and healthcare system, as users often require medical attention due to medical and psychiatric comorbidities (Degenhardt et al., 2017; Morley et al., 2017).

1.1 Methamphetamine

1.1.1 Pharmacology

Methamphetamine (*N*-methyl-1-phenylpropan-2-amine) is a highly potent psychostimulant drug (Courtney & Ray, 2014; Cruickshank & Dyer, 2009; Panenka et al., 2013). METH is a synthetically produced molecule, derived from amphetamine (Courtney & Ray, 2014; Cruickshank & Dyer, 2009). Whilst both METH and amphetamine are structurally similar, METH is highly lipophilic and more permeable to the blood-brain barrier, increasing the potency and addictiveness of the drug (Courtney & Ray, 2014). METH can be injected, snorted, smoked or orally ingested (Courtney & Ray, 2014; Cruickshank & Dyer, 2009; Panenka et al., 2013).

1.1.2 Effects of METH Consumption

METH is highly addictive with users frequently and repeatedly administering the drug (Courtney & Ray, 2014). Users of METH typically experience behavioural disinhibition, increased energy, euphoria, increased sexual drive, enhanced confidence, short-term

improvements in attention and decreased appetite (Courtney & Ray, 2014; Cruickshank & Dyer, 2009; Hart, Ward, Haney, Foltin, & Fischman, 2001; Panenka et al., 2013).

Abuse of METH can alter behaviour and elicit negative symptoms such as psychosis, paranoia, anxiety, depression, suicidal ideation, aggression and hyperactivity (Courtney & Ray, 2014; Cruickshank & Dyer, 2009; Darke, Kaye, McKetin, & Duflou, 2008; Degenhardt et al., 2017; Panenka et al., 2013). Furthermore, prolonged use of METH can cause an array of neuropsychological and cardiovascular impairments including impaired executive function, impulse control, working memory, chronic hypertension, arrhythmia and increased incidence of cardiac infarction (Cruickshank & Dyer, 2009; Darke et al., 2008; Panenka et al., 2013).

1.1.3 Available Treatments

Currently available neuropsychological and pharmacological treatments, such as cognitive behavioural therapy, antidepressants or antipsychotics, have been ineffective in reducing METH relapse (Courtney & Ray, 2014; Everitt & Robbins, 2005; Morley et al., 2017). It is postulated that the enduring nature of drug-relapse is due to permanent drug-induced molecular and cellular adaptions in neuronal circuitry (Goldstein & Volkow, 2011; O'Brien & Kalivas, 2008; Sarnyai & Kovács, 2014; Shaham, Shalev, Lu, de Wit, & Stewart, 2003; Van den Oever, Spijker, Smit, & De Vries, 2010; Volkow & Morales, 2015). Given the high prevalence and the significant socioeconomic cost of METH addiction, there is a clear need to develop effective pharmacological treatments which promote abstinence and prevent abstinent users from relapsing (Courtney & Ray, 2014; Epstein et al., 2006; Everitt, Giuliano, & Belin, 2018; Morley et al., 2017). In order to develop effective pharmacotherapies for drug addiction and drug

relapse, it is critical to enhance our understanding of neurobiological mechanisms and neuroadaptations that underlie addiction (Van den Oever et al., 2010).

1.2 METH Addiction and Reward

1.2.1 Reward Circuitry within the Brain

Reward is defined as an event or action that induces a positive or pleasurable experience; where positive reinforcement acts to promote repetition of the behaviour that elicited feelings of reward (Ikemoto & Bonci, 2014; Koob, 1992). The brain has evolved to direct responding towards certain events and experiences that facilitate survival and continuation of the species, such as obtaining food and mating (Hyman, Malenka, & Nestler, 2006; Kelley & Berridge, 2002; Koob & Volkow, 2010). These natural stimuli are both rewarding and positively reinforcing, increasing the likelihood that these behaviours will be repeated (Hyman et al., 2006).

Under normal conditions, reward processing is governed by release of monoamines, such as dopamine, within the mesocorticolimbic system (Di Chiara, 2002; Hyman & Malenka, 2001; Kelley & Berridge, 2002; Koob, 1992; Koob & Volkow, 2010; Ridderinkhof, van den Wildenberg, Segalowitz, & Carter, 2004). In addition, consumption of rewards also initiates learning and memory processes that act to consolidate reward-associated behaviours (Hyman et al., 2006; Ikemoto & Bonci, 2014). The ‘reward circuit’ extends from the ventral tegmental area (VTA) within the midbrain, an area rich in dopaminergic cell bodies, and projects to regions such as the nucleus accumbens (NAc), prefrontal cortex (PFC), hippocampus and amygdala (Hyman & Malenka, 2001; Hyman et al., 2006; Ikemoto & Bonci, 2014; Kelley & Berridge, 2002; Koob, 1992; Figure 1.1). Previous evidence suggests that increased release of dopamine within the NAc

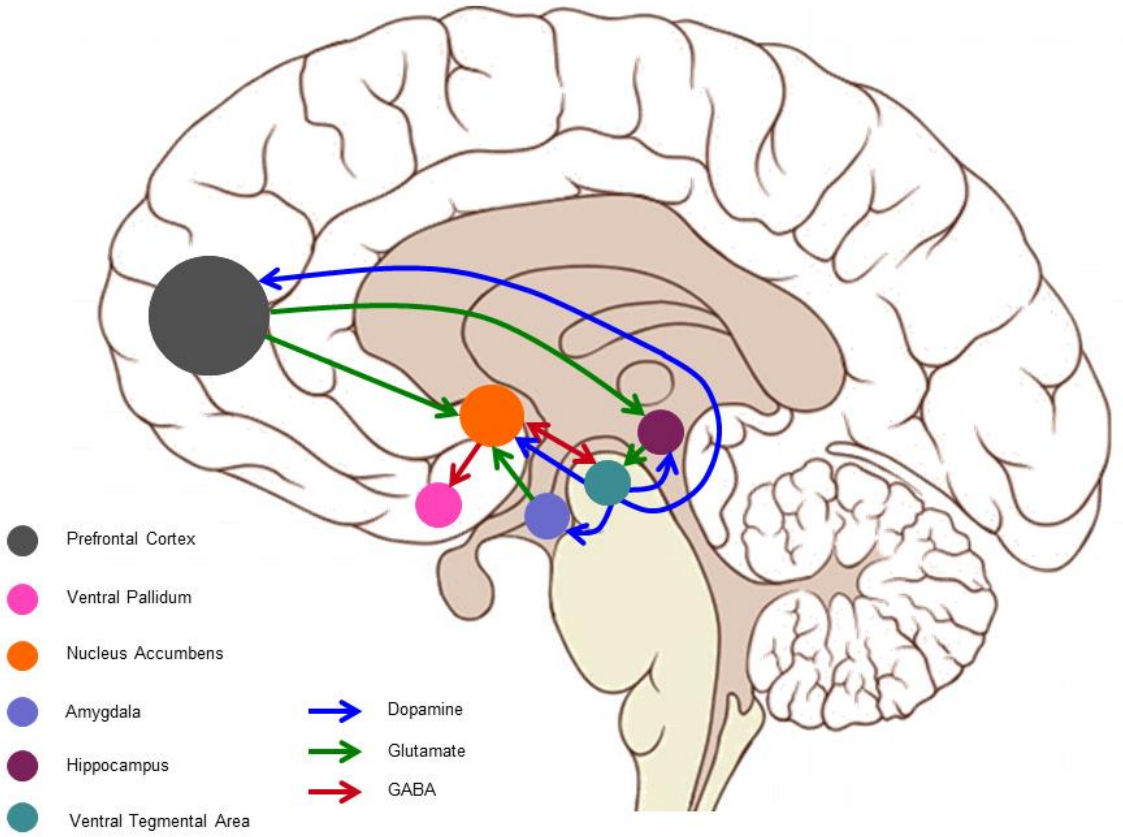

Figure 1.1. Diagram showing inputs and outputs of brain regions involved in processing reward.

may be critical for the hedonic and reinforcing effects experienced following consumption of rewards (Di Chiara, 2002; Hyman & Malenka, 2001; Koob & Volkow, 2010).

1.2.2 Acute Drug-induced Changes to Neurotransmission in Reward Circuitry

Drugs of abuse can usurp reward systems and act via the same mechanism as natural rewards to increase extracellular dopamine levels and elicit powerful hedonic effects (Di Chiara, 2002; Hyman & Malenka, 2001; Hyman et al., 2006; Kelley & Berridge, 2002; Koob & Volkow, 2010; Robinson & Berridge, 1993). The administration of addictive drugs causes supraphysiologic levels of extracellular dopamine, promoting a stronger hedonic state, which can cause drug rewards to be overvalued at the expense of other stimuli (Hyman & Malenka, 2001;

Hyman et al., 2006; Koob & Volkow, 2010; Volkow & Morales, 2015). The potent and prolonged rewarding effects of addictive drugs act to reinforce drug-taking behaviour, strengthening the motivation to seek and consume more drugs (Di Chiara, 2002; Hart et al., 2001; Hyman & Malenka, 2001; Hyman et al., 2006; O'Brien & Kalivas, 2008; Volkow, Wang, Fowler, & Tomasi, 2012).

The highly addictive and potent properties of METH can be attributed to strong and sustained effects on monoamine neurotransmission (Courtney & Ray, 2014; Cruickshank & Dyer, 2009). Once administered, molecules of METH can cross the blood brain barrier and bind with dopamine, serotonin and noradrenaline transporters, acting as an indirect agonist on monoaminergic systems (Cruickshank & Dyer, 2009). METH is structurally similar but more potent than monoamines, acting to decrease sequestration and increase the release of monoamines by reversing the functional activity of many monoamine transporters, including vesicular monoamine transporter 2 (VMAT-2) and dopamine transporter (DAT; Courtney & Ray, 2014; Cruickshank & Dyer, 2009; Panenka et al., 2013; Figure 1.2). Once released into the synapse, monoamines bind with postsynaptic monoamine receptors, which in turn activate dopaminergic, serotonergic and noradrenergic systems within the mesocorticolimbic pathway (Courtney & Ray, 2014; Cruickshank & Dyer, 2009; Goldstein & Volkow, 2011; Panenka et al., 2013). This potent activation of dopaminergic systems increases the feeling of reward, orientating behavioural output towards increased drug-seeking and drug-taking whilst simultaneously reducing the drive to seek naturally rewarding stimuli such as food, social interaction or sexual activity (Courtney & Ray, 2014; Goldstein & Volkow, 2011; Hart et al., 2001; O'Brien & Kalivas, 2008).

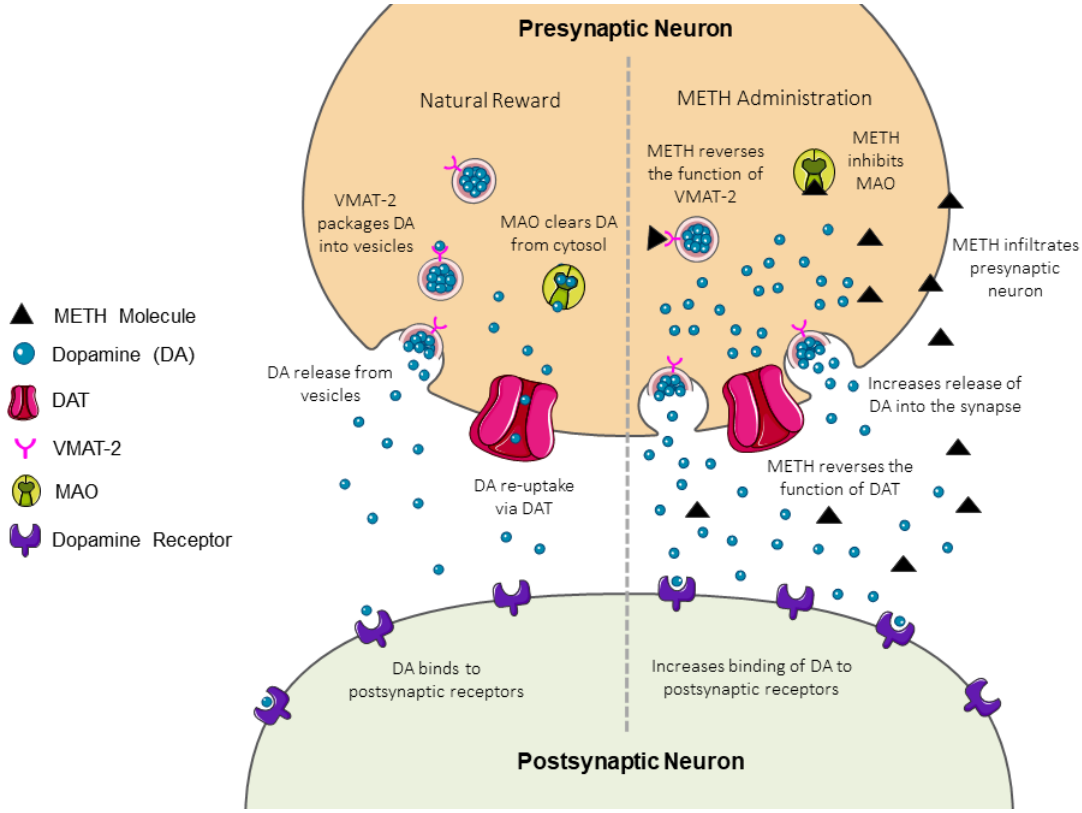

Figure 1.2. Changes to dopamine neurotransmission following METH administration. Figure created using resources from Servier Laboratories (Surenes, France).

The administration of METH can also inhibit monoamine oxidase, the primary enzyme responsible for the metabolism of monoamines, preventing clearance from the synapse and sustaining increased cytosolic and synaptic monoamine concentrations (Courtney & Ray, 2014; Cruickshank & Dyer, 2009; Panenka et al., 2013). Thus, administration of METH alters the natural monoamine regulation and synaptic clearance mechanisms, sustaining high concentration of monoamines and strengthening the associated feelings of reward (Courtney & Ray, 2014; Hart et al., 2001; O'Brien & Kalivas, 2008). It is hypothesized that these acute changes to monoamine neurotransmission following administration of addictive drugs are critical in driving the acute rewarding and reinforcing effects of drug use (Courtney & Ray, 2014; Everitt & Robbins, 2005; Goldstein & Volkow, 2011; Hart et al., 2001; Kalivas, 2009; Sarnyai & Kovács, 2014; Volkow & Morales, 2015; Yang, Qi, Han, Wang, & Wu, 2010) and could also explain many of the core

behavioural and cognitive sequelae associated with abuse of METH (Darke et al., 2008). However, the effects of METH administration can cause more prolonged pathological changes within the brain.

1.2.2 Long Term Drug-induced Changes to Reward Circuitry

Addiction to drugs of abuse, including METH, can cause functional changes to the mesocorticolimbic dopaminergic system that persist despite prolonged abstinence from drug taking (O'Brien & Kalivas, 2008; Robinson & Berridge, 1993; Sarnyai & Kovács, 2014; Volkow et al., 2012; Yang et al., 2010). Repeated or compulsive use of METH can also lead to depletion of presynaptic stores of monoamines, causing permanent pathological damage to reward circuitry in the brain (Courtney & Ray, 2014; Hart et al., 2001; O'Brien & Kalivas, 2008). Evidence also suggests METH can induce neurotoxic effects, including an accumulation of reactive oxygen species and oxidative stress within dopaminergic neurons (Berman, O'Neill, Fears, Bartzokis, & London, 2008; Courtney & Ray, 2014; De Vito & Wagner, 1989; Fricks-Gleason & Keefe, 2013; Krasnova & Cadet, 2009). Whilst typically antioxidant enzymes, such as monoamine oxidase, would act to scavenge reactive oxygen species within the brain, METH inhibits this antioxidant function, consequently enhancing neurotoxic effects (Krasnova & Cadet, 2009).

Repeated exposure to addictive drugs is also postulated to cause neural sensitisation and altered salience of drug-associated stimuli (Di Chiara, 2002; Kelley & Berridge, 2002; Robinson & Berridge, 1993). This theory of addiction, the incentive-sensitisation theory, attributes increased salience of drug-associated stimuli to the increased desire and motivation to obtain and consume drugs (Kelley & Berridge, 2002; Robinson & Berridge, 1993). These pathological

changes to brain circuits are long-lasting and drive the chronic, relapsing nature of addiction which in turn increases the difficulty of abstaining from drug-seeking and drug-taking behaviours (Di Chiara, 2002; Goldstein & Volkow, 2011; Kelley & Berridge, 2002; O'Brien & Kalivas, 2008). Drug addiction negatively impacts on many key substrates within the reward circuit, including the NAc and PFC.

1.3 The Role of the Nucleus Accumbens in Reward and Addiction

The NAc is anatomically situated within the ventral striatum and receives limbic information that may be converted to motivational actions via connections with the motor system (Koob, 1992; Koob & Volkow, 2010). The majority of striatal neurons are medium spiny projection neurons, however inhibitory tone is maintained in the striatum via GABAergic interneurons (Yager, Garcia, Wunsch, & Ferguson, 2015). The NAc also receives dopaminergic, glutamatergic and cholinergic input (Jackson & Moghaddam, 2001; Yager et al., 2015).

The primary functional role of the NAc is to respond to the emotional and motivational significance of a stimulus (Hyman & Malenka, 2001; Jackson & Moghaddam, 2001). The NAc can be subdivided into two subregions; the dorsolateral core and the medioventral shell (Usuda, Tanaka, & Chiba, 1998). The core and shell subregions have different projection patterns, with the shell portion projecting to the ventral pallidum, lateral hypothalamus, substantia nigra, amygdala and VTA, whilst the NAc core projects to the ventral pallidum, globus pallidus, substantia nigra and subthalamic nucleus (Usuda et al., 1998). The NAc is postulated to be critical for the establishment of drug-seeking behaviours (Di Chiara, 2002; Hyman et al., 2006). More specifically, the NA shell is thought to be more involved in the acute rewarding effects and

acquisition of drug self-administration, whereas responding to drug-associated cues is driven by the NAc core (Di Chiara, 2002; Hyman et al., 2006). Once both drug-seeking behaviour and drug-associated cues are consolidated, responding shifts from the NAc to the dorsal striatum (Hyman et al., 2006).

The NAc is highly interconnected with the PFC (Usuda et al., 1998), receiving glutamatergic efferent projections from the mPFC (Everitt & Robbins, 2005; Kalivas, 2008; Killcross & Coutureau, 2003; Scofield et al., 2016). Increased dopamine release in the NAc may act to increase glutamatergic activity within the VTA, PFC and hippocampus, triggering activation of many downstream brain regions (Hsieh, Stein, & Howells, 2014; Hyman & Malenka, 2001; Jackson & Moghaddam, 2001; Kelley & Berridge, 2002; Yager et al., 2015). It has been suggested that increased activity of glutamatergic PFC-NAc projections may drive drug-induced neuroadaptations and act to consolidate compulsive, drug-seeking behaviours (Hyman & Malenka, 2001; Kearns et al., 2018; McFarland, Lapish, & Kalivas, 2003; Scofield et al., 2016; Yager et al., 2015).

1.4 The Prefrontal Cortex

The PFC is structurally heterogeneous and is composed of predominantly excitatory glutamatergic pyramidal neurons, but also contains a small population of GABAergic interneurons (10-15%) which act to maintain balanced excitatory/inhibitory neuronal activity (Garcia, Nakata, & Ferguson, 2017). The PFC is densely interconnected with other downstream cortical and subcortical brain regions, including limbic, striatal, hypothalamic and autonomic nuclei (Del Arco & Mora, 2009; Garcia et al., 2017; Goldstein & Volkow, 2011; Jackson &

Moghaddam, 2001; Karreman & Moghaddam, 1996; Moorman, James, McGlinchey, & Aston-Jones, 2015; Ridderinkhof et al., 2004). The human PFC is comprised of many different subregions with discrete functional roles (Moorman et al., 2015). The rodent PFC can be subdivided into three distinct parts; the medial PFC (mPFC), orbitofrontal cortex (OFC) and the lateral PFC. Similarities have been noted across human and rodent subregions of the PFC, with the rodent mPFC and OFC considered to be analogous to the human anterior cingulate cortex and dorsolateral PFC and OFC respectively, allowing translation from animal studies (Hoover & Vertes, 2007; Moorman et al., 2015).

1.4.1 The Medial Prefrontal Cortex

In the rat, the mPFC can be furthered differentiated into the anterior cingulate cortex (Cg1), prelimbic cortex (PrL) and infralimbic cortex (IL). Each subregion of the mPFC has unique structural connectivity, with dense connections between Cg1 and PrL observed (Hoover & Vertes, 2007). The rodent mPFC receives dopaminergic input from the VTA and limbic regions and projects to the NAc (Moorman et al., 2015). The mPFC-NAc projections are topographically organized, with the PrL projecting primarily to the NAc core and the IL projecting primarily to the NAc shell (Usuda et al., 1998; Yager et al., 2015). The mPFC is a key region in the mesocorticolimbic system and is postulated to regulate drug-taking behaviour (Moorman et al., 2015).

1.4.2 The Orbitofrontal Cortex

The rodent OFC is anatomically situated lateral and ventral to the mPFC, and is highly interconnected with the mPFC, NAc, dorsal striatum and hypothalamus (Hyman et al., 2006).

The OFC is uniquely positioned to use associative information to guide decision making or determine expected outcomes (Schoenbaum, Roesch, & Stalnaker, 2006). The rodent OFC can be divided into smaller subregions which are named after their relative location; the medial orbitofrontal cortex (MO), ventral orbitofrontal cortex (VO) and lateral orbitofrontal cortex (LO). Subregions of the OFC are densely interconnected with subregions of the mPFC; the Cg1 is strongly connected with the MO, the PrL is strongly connected with the MO, VO and LO and the IL is strongly connected with the VO and LO (Hoover & Vertes, 2007). The OFC is highly heterogeneous and has been implicated in many functional roles (Stalnaker, Cooch, & Schoenbaum, 2015). However, further research is required to identify the specific functional role of each subregion within the OFC (Zimmermann, Li, Rainnie, Ressler, & Gourley, 2018). Recently, the LO and VO have been implicated in conditioning-related plasticity (Zimmermann et al., 2018), whilst the MO and LO have been implicated in attributing value (Lopatina et al., 2017).

1.4.3 The Functional Role of the Prefrontal Cortex

The PFC is a brain region fundamentally involved in an array of neuropsychological functions including cognition, emotion, motivation, decision-making and behaviour (Del Arco & Mora, 2009; Garcia et al., 2017; Goldstein & Volkow, 2011; Kalivas, 2009; Moorman et al., 2015; Ridderinkhof et al., 2004; Volkow & Morales, 2015). The PFC is hypothesised to coordinate cognitive processes via two distinct brain circuits; PFC-driven inhibitory control circuitry and corticostriatal habit circuitry (Jackson & Moghaddam, 2001; Kalivas, 2008; Karreman & Moghaddam, 1996; Killcross & Coutureau, 2003; Moorman et al., 2015).

Under normal conditions, the PFC will send information to other brain regions, such as the VTA, amygdala or NAc, modifying behavioural output to suit current processing demands (Jackson & Moghaddam, 2001; Kalivas, 2009; Ridderinkhof et al., 2004). The PFCs initial response to a stimulus is goal-directed and voluntarily controlled (Killcross & Coutureau, 2003). This PFC-driven adaptive, cognitive control system is essential for goal-directed behaviour, discrimination of contextually relevant information and optimisation of processing pathways (Everitt & Robbins, 2005; Hyman et al., 2006; Ridderinkhof et al., 2004). Once a specific behaviour is elicited, the appropriateness and performance of the behaviour is assessed and adjusted if required (Killcross & Coutureau, 2003; Ridderinkhof et al., 2004). However, the performance of voluntarily controlled behaviours comes at an evolutionary cost; energy is expended to continuously control and modify behaviour, reducing processing capacity for alternative information (Kalivas, 2008; Killcross & Coutureau, 2003).

In contrast, well-learned behaviours are executed without PFC involvement; these behaviours are no longer goal-directed or voluntarily controlled by the PFC, instead relying on neuronal circuits connecting the cortex, dorsal striatum and thalamus (Everitt & Robbins, 2005; Kalivas, 2008; Killcross & Coutureau, 2003; Smith & Laiks, 2018; Van den Oever et al., 2010). These behaviours can be described as habit behaviours and are continued despite reductions in the controlling influence on the goal (Everitt & Robbins, 2005; Ridderinkhof et al., 2004). For example, an individual may continue to seek a food reward (the habit behaviour) despite satiation or food poisoning, which acts to reduce the drive to seek food (the goal) (Everitt & Robbins, 2005). This reliance on striatal habit circuitry allows simple and efficient engagement,

enabling the PFC remains to integrate and process new information (Everitt & Robbins, 2005; Kalivas, 2008; Killcross & Coutureau, 2003; Smith & Laiks, 2018).

1.4.4 The Role of the Prefrontal Cortex in Addiction

Addiction research has predominately focused on the role of the NAc, however more recently the PFC has gained significant attention as many of the behaviours mediated by the PFC, such as impulse control and executive function, are disrupted in addiction (Hyman et al., 2006; Moorman et al., 2015; Volkow et al., 2012). It has been hypothesised that the transition from voluntary social drug use to compulsive, relapsing addiction is partially due to a decrease in PFC-driven inhibitory control over behaviour (Courtney & Ray, 2014; Everitt & Robbins, 2005; Goldstein & Volkow, 2011; Kalivas, 2008, 2009; Smith & Laiks, 2018; Volkow & Morales, 2015; Volkow et al., 2012). Following chronic exposure to drugs, the PFC is unable to modulate and suppress the rewarding and reinforcing effects of drug-taking behaviours, disrupting the normal hierarchy of behaviours and driving continuation of maladaptive habit behaviours (Everitt et al., 2018; Everitt & Robbins, 2005; Hyman et al., 2006; Kalivas, 2008, 2009; Karreman & Moghaddam, 1996; Ridderinkhof et al., 2004; Smith & Laiks, 2018; Van den Oever et al., 2010). Furthermore, this transition from voluntary drug use to compulsive, habitual behaviour could explain the inefficacy of current pharmacotherapies aimed at targeting addiction; current treatments may remove the reinforcing and rewarding effects, but do not reduce the motivational drive to seek drugs and relapse (Everitt & Robbins, 2005; Robinson & Berridge, 1993). Thus, it is imperative to enhance our knowledge of how neural circuitry may be altered following acute METH administration, prolonged or chronic METH use and during relapse to METH-taking behaviour.

1.4.5 Changes to Prefrontal Cortex Function and Circuitry in Addiction

Whilst there is published evidence to support the role of the PFC in drug-seeking behaviour, there is little research investigating how administration of METH may detrimentally impact functional connectivity between subregions of the PFC. In terms of the mPFC, activation of the PrL has been associated with increased-drug seeking or relapse behaviours and enhanced drug-craving (Miller & Marshall, 2004; Rocha & Kalivas, 2010), whilst activation of the IL has generally been associated with suppression or extinction of drug-related behaviours or abstinence (Moorman et al., 2015; Rocha & Kalivas, 2010). The Cg1 is relatively under investigated in addiction models, however this region may also be implicated (Goldstein et al., 2007).

Although the OFC is not directly involved in mediating the rewarding effects of administered drugs, this region has been implicated in addiction due to involvement in promoting behaviours based on expected outcomes (Schoenbaum et al., 2006; Schoenbaum & Shaham, 2008; Volkow et al., 2012). It is hypothesised that compulsive drug use and propensity to relapse is driven, in part, by drug-induced changes to OFC function (Schoenbaum et al., 2006; Schoenbaum & Shaham, 2008; Volkow et al., 2012). Although there is some research highlighting the role of the PFC in addiction, further research is required to identify specific drug-induced neuroadaptations or neurotoxic effects that may be disrupting the function of these regions.

1.4.6 Alterations to Prefrontal Cortex Neurotransmission in Addiction

Published literature has predominately focused on increases in dopamine and glutamate neurotransmission following drug exposure (Del Arco & Mora, 2009; Everitt et al., 2018;

Goldstein & Volkow, 2011; Kalivas, 2009; Shin et al., 2018; Van den Oever et al., 2010). It is hypothesised that drug-induced changes to dopamine or glutamate neurotransmission in the PFC could drive increased excitation of glutamatergic pyramidal neurons, in turn increasing dopaminergic and glutamatergic activity in reward substrates, including the NAc (Del Arco & Mora, 2009; Hyman et al., 2006; Karreman & Moghaddam, 1996; Qi et al., 2012; Rocha & Kalivas, 2010; Scofield et al., 2016; Yang et al., 2010).

Studies conducted in preclinical animal models and human addicts have demonstrated increased neuronal activity in the PFC following exposure to drugs or drug-associated cues, as evidenced by increased cerebral flow (Goldstein & Volkow, 2011; Kalivas, 2009) or increased immediate early gene expression (Franklin & Druhan, 2000; Miller & Marshall, 2004; Morshedi & Meredith, 2007; Van den Oever et al., 2010). Despite substantial evidence suggesting increased neuronal activity in the PFC following drug exposure, it is unknown which neuronal subtypes exhibit increased activity (Van den Oever et al., 2010) or the relationship between immediate early gene expression and patterns of neuronal firing (Miller & Marshall, 2004). Furthermore, it remains unknown how discrete subregions interact following drug exposure and what impact increased activation in one subregion may have on overall output and functional connectivity.

It is plausible that abuse of METH could also disrupt the release of γ-amino-butyric acid (GABA), within the PFC (Qi et al., 2012; Yang et al., 2010). Reductions in the inhibitory action of GABA in the PFC could contribute to increased neuronal activation, disrupt the excitatory/inhibitory balance and disinhibit efferent projections from the PFC, resulting in

increased glutamate or dopamine release within reward circuitry (Hsieh et al., 2014; Karreman & Moghaddam, 1996; Miller & Marshall, 2004; Morshedi & Meredith, 2007; Qi et al., 2012).

1.5 GABA

GABA, the most ubiquitous inhibitory neurotransmitter within the central nervous system (Koob, 1992), is synthesised by the rate-limiting enzyme glutamate-decarboxylase (GAD; (Uematsu et al., 2008). Following synthesis, GABA is packaged into vesicles and stored in neuronal terminals ready for extracellular release (Uematsu et al., 2008). The GABAergic system within the mammalian brain consists of GABA-releasing neurons and receptors that bind with GABA molecules (Brickley & Mody, 2012). Both mechanisms act to inhibit circuit or region output (Brickley & Mody, 2012). Receptors that bind with GABA are highly diverse, with 19 different subunit clusters, and are present on most neurons within the brain (Brickley & Mody, 2012).

Cortical networks within the brain are modulated by local GABA-releasing interneurons, which regulate the activity of glutamatergic pyramidal neurons (Brickley & Mody, 2012; Tremblay, Lee, & Rudy, 2016). Although GABAergic interneurons only represent approximately 10-30% of the total neuronal population (Markram et al., 2004; Rudy, Fishell, Lee, & Hjerling-Leffler, 2011; Tremblay et al., 2016), emerging evidence suggests GABAergic interneurons are critical in controlling temporal precision of pyramidal cell firing and modulating the excitatory/inhibitory balance within the brain (Brickley & Mody, 2012; Rudy et al., 2011; Tremblay et al., 2016). For these reasons, the present thesis will primarily focus on GABAergic interneurons.

1.5.1 Subpopulations of GABA Interneurons

GABAergic interneurons are highly heterogeneous and can synapse with a diverse range of surface features including somata, axons and dendritic shafts (Kawaguchi & Kondo, 2002; Markram et al., 2004). Differences in morphology and cellular organisation facilitate variations in functional output and physiology across interneuron subpopulations (Garcia et al., 2017; Kawaguchi & Kondo, 2002; Kawaguchi & Kubota, 1997; Tremblay et al., 2016). GABAergic interneuron subtypes provide distinct responses to neurotransmitters, altering the function of neuronal circuits (Markram et al., 2004; Rudy et al., 2011; Tremblay et al., 2016). GABAergic interneurons can be characterized into nine broad subpopulations based on morphology, functional activity and expression of proteins and neuromodulators (Table 1).

Despite significant increases in our understanding of how different GABAergic interneuron subpopulations may contribute to specific functions in specific cortical areas, our understanding of how interneuron subtype activity contributes to underlying behaviour is currently limited (Tremblay et al., 2016). In the context of METH addiction, two subpopulations of GABAergic interneurons are of particular interest; neuronal nitric oxide synthase-expressing interneurons, which are involved in the production of nitric oxide and may contribute to METH-induced neurotoxicity (Fricks-Gleason & Keefe, 2013; Gabbott & Bacon, 1995; Le Roux, Amar, Moreau, & Fossier, 2009); and parvalbumin-expressing interneurons, which are known to synapse directly onto glutamatergic pyramidal cells, facilitating temporal control (Ferguson & Gao, 2018).

Table 1

Summary of GABAergic interneuron subpopulations.

Expresses	Subpopulation	Proportion	Cortical Distribution	Morphological Classification	Functional Classification
Calcium binding protein	Parvalbumin	~ 40%	Layers II - VI	Basket cell – perisomatic targeting	Fast spiking
	Calbindin	Highly co-expressed	Layers II - VI	Chandelier cell – axon targeting	Prolonged burst/slow spiking
	Calretinin	~ 30%	Layers I - VI	Chandelier cell – axon targeting	Irregular-spiking
Enzyme	Neuronal nitric oxide synthase	< 10%	Layers I, V-VI	Bipolar cell - long, thin axons	Prolonged burst/slow spiking
Hormone	Somatostatin	~30%	Layers II - VI	Martinotti cell - dendrite targeting	Prolonged burst/slow spiking
	Cholecystokinin	Highly co-expressed	Layers II - VI	Basket cell - perisomatic targeting	Prolonged burst/slow spiking
	Corticotropin-Releasing Hormone	Highly co-expressed	Layers II - V	Chandelier cell – axon targeting	Irregular-spiking
Peptide	Vasointestinal Peptide	Highly co-expressed	Layers I - V	Double bouquet cell – dendrite targeting	Irregular-spiking
	Neuropeptide Y	Highly co-expressed	Layers II –III, VI	Bipolar cell - long, thin axons	Fast or irregular spiking

1.5.1.1 Neuronal Nitric Oxide Synthase-expressing Interneurons.

Nitric oxide synthase (NOS), a signaling molecule found within many organs including the brain, is responsible for the synthesis and release of nitric oxide (NO) (Hardingham, Dachtler, & Fox, 2013). Whilst there are three known isoforms of NOS, neuronal NOS (nNOS) is the most ubiquitous isoform within the central nervous system and synthesizes approximately 95% of NO within the cerebral cortex (Hardingham et al., 2013). nNOS is expressed within the cytoplasm of a small population of GABAergic interneurons located within the cortex and hippocampus (Gabbott & Bacon, 1995; Hardingham et al., 2013; Taniguchi et al., 2011; Tremblay et al., 2016).

Morphologically, nNOS interneurons are characterised by their long, fine axons (Taniguchi et al., 2011), which ramify throughout the cortex, aiding the spread of NO across large distances (Hardingham et al., 2013). Anatomically, nNOS interneurons have been identified in close proximity to GABAergic synapses, suggesting functional interactions with other nNOS interneuron subtypes (Hardingham et al., 2013). Functionally, nNOS interneurons are thought to regulate non-synaptic GABA release (Le Roux et al., 2009), stimulating long-lasting hyperpolarisation and inactivation of local circuits (Taniguchi et al., 2011). Experiments conducted by Le Roux et al. (2009) revealed increased excitatory signaling in the visual cortex following increased concentration of NO. Thus, it is plausible that increased activation of nNOS interneurons within the mPFC or NAc could enhance the overall production of NO and alter the communication of neurotransmitter systems, such as glutamate, dopamine and GABA, within the mesocorticolimbic system (Fricks-Gleason & Keefe, 2013; Gabbott & Bacon, 1995; Hardingham et al., 2013).

The role of nNOS-expressing GABAergic interneurons in METH-related behaviours is currently unknown, however, findings by Sammut and West (2008) and Nasif et al (2011) have revealed treatment with an nNOS inhibitor prevented the effects of acute cocaine and the development of cocaine sensitisation, respectively. This suggests nNOS activation in the mesocorticolimbic system may be involved in cocaine-induced neuroadaptations and could also be altered following relapse to METH. Recently, Smith et al. (2017) hypothesised glutamate spillover within the NAc may be activating metabotropic glutamate receptors located on nNOS interneurons in the NAc. The authors demonstrated chemogenetic activation of nNOS interneurons in the NAc was sufficient to reinstate prior cocaine-seeking behaviour and increase NO production. Furthermore, Fricks-Gleason and Keefe (2013) hypothesise that NO production and METH-induced dopamine neurotoxicity arises from activation of nNOS interneurons in the striatum. Collectively, these findings implicate nNOS interneurons in both relapse to drug-seeking, activation of the nitrergic system and drug-induced neurotoxicity (Fricks-Gleason & Keefe, 2013; Smith et al., 2017). In light of these findings, enhancing our knowledge of the activity of nNOS interneurons following METH exposure may reveal new insights into treatment avenues for reducing METH abuse.

1.5.1.2 Parvalbumin-expressing Interneurons.

Parvalbumin-expressing interneurons (PV) are the largest population of interneurons within the neocortex (Rudy et al., 2011; Tremblay et al., 2016). Morphologically, PV interneurons are found throughout cortical layers II-VI (Kawaguchi & Kubota, 1997) and are characterised by their basket or chandelier appearance (Markram et al., 2004; Tremblay et al., 2016). PV interneurons are strongly interconnected with neighbouring cells, innervating the

perisomatic region of target cells (Ferguson & Gao, 2018; Hu, Gan, & Jonas, 2014; Kvitsiani et al., 2013).

The structural organisation and dense interconnectivity of PV interneurons evidence their functional role; PV interneurons are responsible for generating network oscillations and modulating the activity of pyramidal cells and inhibitory subtypes via feedback and feed-forward mechanisms (Ferguson & Gao, 2018; Hu et al., 2014). Furthermore, PV interneurons are hypothesised to play a critical role in maintaining the excitatory/inhibitory balance within the PFC by gating the generation and timing of pyramidal cell spiking (Ferguson & Gao, 2018). This ensures appropriate information is relayed to downstream brain regions, facilitating the appropriate execution of behaviours (Ferguson & Gao, 2018).

Previous literature provides contradictory evidence of drug-induced changes to PV interneurons; some studies have evidenced upregulation of PV expression (Mohila & Onn, 2005; Wearne, Parker, Franklin, Goodchild, & Cornish, 2017), whilst other studies have suggested deficits to or loss of PV expression (Morshedi & Meredith, 2007; Veerasakul, Thanoi, Reynolds, & Nudmamud-Thanoi, 2016), which may alter functionality. Although it remains unclear what impact alterations to PV function may have on overall function of the PFC, diminished function of PV interneurons has been implicated in an array of neuropsychological sequelae including autism spectrum disorder, Tourette's syndrome and schizophrenia (Bernacer, Prensa, & Gimenez-Amaya, 2012; Enwright et al., 2016; Ferguson & Gao, 2018; Filice, Vorckel, Sungur, Wohr, & Schwaller, 2016; Lewis, Curley, Glausier, & Volk, 2012; Wohr et al., 2015). Currently,

there is a distinct lack of research investigating the functional role of PV interneurons in the development of addiction and relapse to drug-taking.

1.5.2 GABA and Addiction

The broad consensus within current published literature is that relapse to drug-taking behaviour is driven by increased extracellular glutamate in the PrL, which in turn drives increased concentrations of glutamate and dopamine within the NAc (McFarland et al., 2003; Scofield et al., 2016; Van den Oever et al., 2010). However other neurotransmitters, such as GABA, may also be implicated in the pathogenesis of addiction (Qi et al., 2012).

Currently, there is a lack of research examining the role of GABA systems in addictive behaviours and the impact of prolonged drug exposure on GABA signaling. Hsieh et al. (2014) hypothesise that excessive release of glutamate and dopamine within the PFC may damage GABAergic interneurons, disrupting temporal control of pyramidal cell firing and contributing to enhanced glutamate outflow. However, Miller and Marshall (2004) found increased activation of GABAergic interneurons in the PrL of rats undergoing METH conditioned place preference. It is plausible that METH may alter GABA systems within the PFC and NAc, altering the overall balance of excitation and inhibition, in turn driving maladaptive drug-seeking behaviours. Thus it is imperative to enhance understanding of the function of GABA systems during drug-seeking and relapse behaviours, as current treatment strategies involving administration of non-selective GABA agonists, are of limited efficacy (Morley et al., 2017).

Recently, direct administration of oxytocin has been shown to increase GABAergic activity in the PrL and elicit anxiolytic effects (Sabihi, Dong, Maurer, Post, & Leuner, 2017). This finding suggests oxytocin may selectively interact with GABA systems. Therefore, oxytocin may act to restore the excitatory/inhibitory balance and reduce METH-induced neuroadaptations in the PrL, indicating promising potential for this neuropeptide as an efficacious pharmacotherapy.

1.6 Oxytocin

1.6.1 Systems and Pharmacology

Oxytocin is an endogenous mammalian nonapeptide synthesised within, transported in and secreted from oxytocinergic neurons located within hypothalamic accessory, supraoptic and paraventricular nuclei (PVN) of the brain (Althammer & Grinevich, 2018; Gimpl & Fahrenholz, 2001; Sarnyai & Kovács, 2014). Magnocellular oxytocinergic neurons project to the posterior pituitary, where oxytocin is released into the blood stream and acts as a neurohormone on peripheral targets (Althammer & Grinevich, 2018; Gimpl & Fahrenholz, 2001; Sarnyai & Kovács, 2014). Magnocellular oxytocinergic neurons of the PVN also ascend and bifurcate, facilitating infiltration and local dendritic release of oxytocin in forebrain, limbic and midbrain regions (Althammer & Grinevich, 2018; Sarnyai & Kovács, 2014). In contrast, parvocellular oxytocinergic neurons are not implicated in neuroendocrine functions within the hypothalamus (Althammer & Grinevich, 2018). Instead, parvocellular oxytocinergic neurons descend to regions within the brainstem and spinal cord, acting to modulate autonomic functions such as breathing and feeding (Althammer & Grinevich, 2018; Gimpl & Fahrenholz, 2001; Quintana, Kemp, Alvares, & Guastella, 2013). Oxytocin is capable of acting as a neurotransmitter or

neuromodulator, interacting with other endogenous neurotransmitters, such as dopamine, GABA and glutamate (Baracz & Cornish, 2016; Gimpl & Fahrenholz, 2001; McGregor & Bowen, 2012; Ninan, 2011; Sarnyai & Kovács, 2014).

Oxytocin has been implicated in a wide range of behavioural and endocrine functions including maternal care, social behaviours, stress, memory and learning (Althammer & Grinevich, 2018; Gimpl & Fahrenholz, 2001; Quintana et al., 2013; Sarnyai & Kovács, 2014). Due to its functional role in learning and memory, it has been postulated that administration of exogenous oxytocin may attenuate the maladaptive memory and learning processes that drive drug addiction (Baracz & Cornish, 2016; Gimpl & Fahrenholz, 2001; McGregor & Bowen, 2012; Sarnyai & Kovács, 2014; Yang et al., 2010).

1.6.2 The Effects of Peripheral and Central Oxytocin Administration in Drug-related Behaviours

Oxytocin receptors (OTRs) have been identified in many cortical and limbic brain regions (Gimpl & Fahrenholz, 2001). Oxytocin is hypothesised to bind with receptors located in corticolimbic brain regions, acting to inhibit the effects of addictive drugs (Baracz, Everett, McGregor, & Cornish, 2014; Baskerville & Douglas, 2010; Kovacs, Sarnyai, Barbarczi, Szabo, & Telegdy, 1990; Sarnyai, 2011; Yang et al., 2010). Oxytocin is also postulated to inhibit excessive release of glutamate, decrease dopamine release and dopamine receptor binding in the mesolimbic dopaminergic pathway, which in turn acts to inhibit drug reward and drug-seeking behaviours (Baskerville & Douglas, 2010; Kovacs et al., 1990; Sarnyai, 2011; Yang et al., 2010).

Exogenous administration of oxytocin has been shown to modulate drug-seeking behaviours in experimental animals. Peripheral or systemic injection of oxytocin has yielded reductions in cocaine (Sarnyai & Kovacs, 1994), alcohol (Bowen et al., 2015), and methamphetamine self-administration in rodent models (Cox, Young, See, & Reichel, 2013; Everett, McGregor, Baracz, & Cornish, 2018; Hicks, Cornish, Baracz, Suraev, & McGregor, 2016). However, the efficacy of systemic oxytocin administration may be limited, as the penetrance of oxytocin across the blood brain barrier remains debated (Gimpl & Fahrenholz, 2001; Quintana et al., 2013). In addition, central administration of oxytocin into mesolimbic brain regions or cerebral ventricles has yielded reductions in drug-induced behaviours including decreased METH-induced hyperlocomotion (Qi et al., 2008), decreased acquisition of METH-induced conditioned place preference (Baracz et al., 2012; Qi et al., 2009) and METH-induced reinstatement (Baracz, Everett, & Cornish, 2015; Baracz et al., 2014; Cox et al., 2017).

Evidence of attenuated drug-seeking behaviours following treatment with oxytocin has also been shown in human clinical trials which revealed reductions in alcohol dependence (Pedersen et al., 2013), marijuana dependence (McRae-Clark, Baker, Maria, & Brady, 2013), cocaine use (Lee et al., 2014) and heroin use (Buisman-Pijlman et al., 2014). Currently there are no published studies examining the role of oxytocin in reducing METH abuse in humans. Despite substantial experimental evidence demonstrating oxytocin-induced attenuation of drug-seeking behaviour, the neural mechanisms by which oxytocin modulates drug-seeking behaviour are not well understood (Baracz & Cornish, 2016; Qi et al., 2012).

Exogenous administration of oxytocin has also been shown to interact with other endogenous neurotransmitters, including dopamine, glutamate and GABA systems (Gimpl & Fahrenholz, 2001; Ninan, 2011; Sarnyai & Kovács, 2014). Whilst the PFC is not known to contain magno- or parvocellular nuclei, the PFC is reported to contain oxytocin-sensitive neurons (Ninan, 2011), express OTRs (Marlin, Mitre, D'amour, Chao, & Froemke, 2015; Ninan, 2011), and receive long range axonal projections from hypothalamic oxytocinergic cells (Sabihi, Durosko, Dong, & Leuner, 2014). Furthermore, experiments conducted by Carson et al. (2010) revealed treatment with systemic oxytocin reduced METH-induced Fos expression in the PrL of male rats. More recently, direct administration of oxytocin into the PrL has been shown to increase GABAergic activity (Sabihi, Dong, Maurer, Post, & Leuner, 2017). Collectively, these findings suggest a functional role for oxytocin in the PFC and indicate oxytocin may be interacting with GABA systems in the PrL.

1.7 Designer Receptors Exclusively Activated by Designer Drugs

In the past decade, chemogenetic strategies such as designer receptors exclusively activated by designer drugs (DREADDs), have enabled researchers to remotely target and manipulate neuronal activity via synthetically modified G-protein coupled receptors (Armbruster, Li, Pausch, Herlitze, & Roth, 2007; Roth, 2016). This approach enables identification of cellular mechanisms, neuronal populations and circuits that modulate and drive behavioural output *in vivo* (Campbell & Marchant, 2018; Roth, 2016). DREADDs were first developed from human muscarinic receptors and can be excitatory (hM3Dq), triggering depolarisation, or inhibitory (hM4Di), inducing hyperpolarisation and strong inhibition of neurotransmitter release (Armbruster et al., 2007; Roth, 2016). DREADDs are transiently

activated via administration of the agonist clozapine-N-oxide (CNO), a synthetic ligand with high bioavailability in rodents and humans (Armbruster et al., 2007; Roth, 2016).

Currently, DREADDs are the most widely used chemogenetic tool and are particularly useful for behavioural experiments as the technique is non-restrictive and relatively non-invasive (Campbell & Marchant, 2018; Roth, 2016). DREADD approaches can be used with viral vectors and genetically modified animals to selectively target specific neuronal populations (Campbell & Marchant, 2018; Roth, 2016). Recently, DREADDs have yielded new insights relating to the circuitry involved in cocaine reinstatement (Mahler et al., 2018; Mahler et al., 2014; Smith et al., 2017; Yager et al., 2015) and may prove useful for examining an interaction between GABA systems and oxytocin during reinstatement of METH-seeking behaviour.

1.8 Behavioural Models of Addiction

The field of addiction aims to enhance our understanding of the behavioural, environmental and neurochemical changes contributing to the addiction processes, and develop effective treatments to prevent relapse to addictive drugs (Epstein et al., 2006; Everitt et al., 2018; Van den Oever et al., 2010). Whilst many experiments are conducted on humans, studies of human addiction are limited by ethical concerns and confounding factors including comorbid neuropsychological disorders, poly drug use, environmental and genetic influences (Hall, Carter, & Morley, 2004). Animal models of addiction are a useful tool for studying drug-induced changes in physiology, behaviour and brain neurochemistry under controlled laboratory conditions (Panlilio & Goldberg, 2007). For further review of preclinical models of addiction, see Appendix 1.

The present thesis will utilise an intravenous drug self-administration paradigm, where experimental animals are required to perform a trained operant response (lever pressing) in order to receive delivery of an addictive drug (Kalivas, 2008; Panlilio & Goldberg, 2007). Drug-self administration is a form of operant conditioning as drug administration acts as a reinforcement, increasing the likelihood of repeating the response which triggered drug delivery (Kalivas, 2009; Panlilio & Goldberg, 2007). Furthermore, drug self-administration paradigms often incorporate environmental cues such as lights and/or tones which act to predict the availability of drug, utilising classical conditioning principles to strengthen the association between the performed response and drug reward (Panlilio & Goldberg, 2007). Drug self-administration paradigms exhibit a strong correlation with human drug administration (Epstein et al., 2006; Panlilio & Goldberg, 2007), including a similar incidence of addiction-like behaviours in a drug-using population (Deroche-Gamonet et al., 2004).

The reinstatement model of drug-seeking is widely used to emulate human relapse behaviours following a period of behavioural extinction or abstinence (Panlilio & Goldberg, 2007; Shaham et al., 2003). Reinstatement of drug-seeking behaviour is initiated via presentation with one of three stimuli; a non-contingent drug injection, drug-associated cue or an acute stressor (Epstein et al., 2006; Kalivas, 2008). Once presented with this stimulus, drug-seeking behaviour will dominate over extinction-induced inhibition of responding, causing the animal to initiate previously learnt behaviours associated with drug administration (Kalivas, 2009; Shaham et al., 2003). Reinstatement models of addiction enable investigation of the neural mechanisms driving relapse to drug-taking behaviour and assist in the development of effective

pharmacotherapies which may reduce relapse in human addicts (Epstein et al., 2006; Everitt et al., 2018; Van den Oever et al., 2010).

1.9 Aims and Hypotheses

There is considerable published evidence suggesting exposure to addictive drugs or drug-associated cues can elicit increased neuronal activation in reward circuitry, specifically in the PFC and NAc (Del Arco & Mora, 2009; Franklin & Druhan, 2000; Liu et al., 2014; Miller & Marshall, 2004; Morshedi & Meredith, 2007; Thomas, Arroyo, & Everitt, 2003). However, it remains unknown precisely which neuronal populations are active and what effect this may have on interconnected brain regions. Similarly, existing literature suggests GABA systems may be altered following METH exposure (Miller & Marshall, 2004; Veerasakul et al., 2016; Wearne et al., 2015; Wearne et al., 2016, 2017). Thus, it is critical to investigate how GABA systems, specifically GABAergic interneurons, may be affected. Increased or decreased activity of GABA systems could lead to aberrant hyperactivity in reward circuitry. Identification of METH-induced changes to GABA systems may enable the development of more targeted pharmacotherapies that aim to restore the excitatory/inhibitory balance and reduce the loss of inhibitory control over drug-related behaviours.

Chapter 2 will investigate changes to neuronal activity in subregions of the mPFC, OFC and NAc following acute METH exposure, chronic METH and relapse to METH-seeking. It is hypothesised that:

a) Following a period of behavioural extinction, animals will reinstate prior METH-seeking behaviour (responding on the active lever) following administration of a non-contingent METH-prime.
b) Acute exposure to METH will alter neuronal activity within subregions of the mPFC, OFC and NAc.
c) Chronic exposure to METH will alter the activation or number of nNOS and PV immunoreactive neurons within the mPFC, OFC and NAc.

Furthermore, there is a growing body of literature to support a mechanistic interaction between the neuromodulator oxytocin and GABA systems. However, the mechanism by which systemic administration of oxytocin interacts with GABA systems within the brain remains to be elucidated. Chapter 3 will employ a chemogenetic approach to explore a potential interaction between systemic oxytocin and GABAergic neurons within the PrL during reinstatement of METH-seeking behaviour. It is hypothesised:

a) Animals will reinstate to prior-METH seeking behaviour following presentation of a drug-associated cue and non-contingent METH prime.
b) Systemic administration of oxytocin will significantly attenuate reinstatement of METH-seeking behaviour and METH-induced locomotor activity.
c) Chemogenetic inactivation of GABAergic neurons within the PrL will blunt the efficacy of systemic oxytocin treatment, facilitating robust reinstatement of METH-seeking behaviours.

References

Althammer, F., & Grinevich, V. (2018). Diversity of oxytocin neurones: Beyond magno- and parvocellular cell types? *Journal of Neuroendocrinology, 30*(8), e12549. doi:doi:10.1111/jne.12549

Armbruster, B. N., Li, X., Pausch, M. H., Herlitze, S., & Roth, B. L. (2007). Evolving the lock to fit the key to create a family of G protein-coupled receptors potently activated by an inert ligand. *Proc Natl Acad Sci U S A, 104*(12), 5163-5168. doi:10.1073/pnas.0700293104

American Psychological Association (2013). *Diagnostic and Statistical Manual of Mental Disorders (DSM-5)*. Washington DC: American Psychiatric Association.

Australian Institute of Health and Welfare (2017) National Drug Strategy Household Survey Detailed Report 2016.

Baracz, S., & Cornish, J. (2016). The neurocircuitry involved in oxytocin modulation of methamphetamine addiction. *Frontiers in Neuroendocrinology, 43*, 1-18.

Baracz, S. J., Everett, N. A., & Cornish, J. L. (2015). The involvement of oxytocin in the subthalamic nucleus on relapse to methamphetamine-seeking behaviour. *PLOS One, 10*(8), e0136132. doi:doi:10.1371/ journal.pone.0136132

Baracz, S. J., Everett, N. A., McGregor, I. S., & Cornish, J. L. (2014). Oxytocin in the nucleus accumbens core reduces reinstatement of methamphetamine-seeking behaviour in rats. *Addiction Biology, 21*, 316-325.

Baracz, S. J., Rourke, P. I., Pardey, M. C., Hunt, G. E., McGregor, I. S., & Cornish, J. L. (2012). Oxytocin directly administered into the nucleus accumbens core or subthalamic nucleus attenuates methamphetamine-induced conditioned place preference. *Behav Brain Res, 228*(1), 185-193. doi:10.1016/j.bbr.2011.11.038

Baskerville, T. A., & Douglas, A. J. (2010). Dopamine and oxytocin interactions underlying behaviors: potential contributions to behavioral disorders. *CNS Neurosci Ther, 16*(3), e92-123. doi:10.1111/j.1755-5949.2010.00154.x

Berman, S., O'Neill, J., Fears, S., Bartzokis, G., & London, E. D. (2008). Abuse of amphetamines and structural abnormalities in the brain. *Ann N Y Acad Sci, 1141*, 195-220. doi:10.1196/annals.1441.031

Bernacer, J., Prensa, L., & Gimenez-Amaya, J. M. (2012). Distribution of GABAergic interneurons and dopaminergic cells in the functional territories of the human striatum. *PLOS One, 7*(1), e30504. doi:10.1371/journal.pone.0030504

Bowen, M. T., Peters, S. T., Absalom, N., Chebib, M., Neumann, I. D., & McGregor, I. S. (2015). Oxytocin prevents ethanol actions at δ subunit-containing GABA_A receptors and attenuates ethanol-induced motor impairment in rats. *Proceedings of the National Academy of Sciences, 112*, 3104-3109.

Brickley, S. G., & Mody, I. (2012). Extrasynaptic GABA(A) receptors: their function in the CNS and implications for disease. *Neuron, 73*(1), 23-34. doi:10.1016/j.neuron.2011.12.012

Buisman-Pijlman, F. T. A., Sumracki, N. M., Gordan, J. J., Hull, P. R., Carter, C. S., & Tops, M. (2014). Individual differences underlying susceptibility to addiction: role for the endogenous oxytocin system. *Pharmacology, Biochemistry and Behaviour, 119*, 22-38.

Campbell, E. J., & Marchant, N. J. (2018). The use of chemogenetics in behavioural neuroscience: receptor variants, targeting approaches and caveats. *Br J Pharmacol, 175*(7), 994-1003. doi:10.1111/bph.14146

Carson, D. S., Hunt, G. E., Guastella, A. J., Barber, L., Cornish, J. L., Arnold, J. C., . . . McGregor, I. S. (2010). Systemically administered oxytocin decreases methamphetamine activation of the subthalamic nucleus and accumbens core and stimulates oxytocinergic neurons in the hypothalamus. *Addiction Biology, 15*, 448-463.

Courtney, K. E., & Ray, L. A. (2014). Methamphetamine: an update on epidemiology, pharmacology, clinical phenomenology and treatment literature. *Drug Alcohol Dependence, 143*, 11-21.

Cox, B. M., Bentzley, B. S., Regen-Tuero, H., See, R. E., Reichel, C. M., & Aston-Jones, G. (2017). Oxytocin acts in Nucleus Accumbens to attenuate methamphetamine seeking and demand. *Biological Psychiatry, 81*, 949-958.

Cox, B. M., Young, A. B., See, R. E., & Reichel, C. M. (2013). Sex differences in methamphetamine seeking in rats: impact of oxytocin. *Psychoneuroendocrinology, 38*(10), 2343-2353. doi:10.1016/j.psyneuen.2013.05.005

Cruickshank, C. C., & Dyer, K. R. (2009). A review of the clinical pharmacology of methamphetamine. *Addiction, 104*(7), 1085-1099. doi:10.1111/j.1360-0443.2009.02564.x

Darke, S., Kaye, S., & Duflou, J. (2017). Rates, characteristics and circumstances of methamphetamine-related death in Australia: a national 7-year study. *Addiction, 112*(12), 2191-2201. doi:doi:10.1111/add.13897

Darke, S., Kaye, S., McKetin, R., & Duflou, J. (2008). Major physical and psychological harms of methamphetamine use. *Drug Alcohol Rev, 27*(3), 253-262. doi:10.1080/09595230801923702

De Vito, M. J., & Wagner, G. C. (1989). Methamphetamine-induced neuronal damage: a possible role for free radicals. *Neuropharmacology, 28*(10), 1145-1150.

Degenhardt, L., Sara, G., McKetin, R., Roxburgh, A., Dobbins, T., Farrell, M., . . . Hall, W. D. (2017). Crystalline methamphetamine use and methamphetamine-related harms in Australia. *Drug Alcohol Rev, 36*(2), 160-170. doi:10.1111/dar.12426

Del Arco, A., & Mora, F. (2009). Neurotransmitters and prefrontal cortex-limbic system interactions: implications for plasticity and psychiatric disorders. *J Neural Transm (Vienna), 116*(8), 941-952. doi:10.1007/s00702-009-0243-8

Deroche-Gamonet, V., Belin, D., & Piazza, P. V. (2004). Evidence for addiction-like behavior in the rat. *Science, 305*(5686), 1014-1017. doi:10.1126/science.1099020

Di Chiara, G. (2002). Nucleus accumbens shell and core dopamine: differential role in behavior and addiction. *Behav Brain Res, 137*(1), 75-114. doi:https://doi.org/10.1016/S0166-4328(02)00286-3

Enwright, J. F., Sanapala, S., Foglio, A., Berry, R., Fish, K. N., & Lewis, D. A. (2016). Reduced Labeling of Parvalbumin Neurons and Perineuronal Nets in the Dorsolateral Prefrontal Cortex of Subjects with Schizophrenia. *Neuropsychopharmacology, 41*(9), 2206-2214. doi:10.1038/npp.2016.24

Epstein, D. H., Preston, K. L., Stewart, J., & Shaham, Y. (2006). Toward a model of drug relapse: an assessment of the validity of the reinstatement procedure. *Psychopharmacology (Berl), 189*(1), 1-16. doi:10.1007/s00213-006-0529-6

Everett, N. A., McGregor, I. S., Baracz, S. J., & Cornish, J. L. (2018). The role of the vasopressin V1A receptor in oxytocin modulation of methamphetamine primed reinstatement. *Neuropharmacology, 133*, 1-11. doi:https://doi.org/10.1016/j.neuropharm.2017.12.036

Everitt, B. J., Giuliano, C., & Belin, D. (2018). Addictive behaviour in experimental animals: prospects for translation. *Philos Trans R Soc Lond B Biol Sci, 373*(1742). doi:10.1098/rstb.2017.0027

Everitt, B. J., & Robbins, T. W. (2005). Neural systems of reinforcement for drug addiction: from actions to habits to compulsion. *Nat Neurosci, 8*(11), 1481-1489. doi:10.1038/nn1579

Ferguson, B. R., & Gao, W. J. (2018). PV Interneurons: Critical Regulators of E/I Balance for Prefrontal Cortex-Dependent Behavior and Psychiatric Disorders. *Front Neural Circuits, 12*, 37. doi:10.3389/fncir.2018.00037

Filice, F., Vorckel, K. J., Sungur, A. O., Wohr, M., & Schwaller, B. (2016). Reduction in parvalbumin expression not loss of the parvalbumin-expressing GABA interneuron subpopulation in genetic parvalbumin and shank mouse models of autism. *Mol Brain, 9*, 10. doi:10.1186/s13041-016-0192-8

Franklin, T. R., & Druhan, J. P. (2000). Expression of Fos-related antigens in the nucleus accumbens and associated regions following exposure to a cocaine-paired environment. *Eur J Neurosci, 12*(6), 2097-2106.

Fricks-Gleason, A. N., & Keefe, K. A. (2013). Evaluating the role of neuronal nitric oxide synthase-containing striatal interneurons in methamphetamine-induced dopamine neurotoxicity. *Neurotoxicity Research, 24*(2), 288-297. doi:10.1007/s12640-013-9391-6

Gabbott, P. L., & Bacon, S. J. (1995). Co-localisation of NADPH diaphorase activity and GABA immunoreactivity in local circuit neurones in the medial prefrontal cortex (mPFC) of the rat. *Brain Res, 699*(2), 321-328.

Garcia, A. F., Nakata, K. G., & Ferguson, S. M. (2017). Viral strategies for targeting cortical circuits that control cocaine-taking and cocaine-seeking in rodents. *Pharmacol Biochem Behav*. doi:10.1016/j.pbb.2017.05.009

Gimpl, G., & Fahrenholz, F. (2001). The oxytocin receptor system: structure, function, and regulation. *Physiol Rev, 81*(2), 629-683. doi:10.1152/physrev.2001.81.2.629

Goldstein, R. Z., Tomasi, D., Rajaram, S., Cottone, L. A., Zhang, L., Maloney, T., . . . Volkow, N. D. (2007). Role of the anterior cingulate and medial orbitofrontal cortex in processing drug cues in cocaine addiction. *Neuroscience, 144*(4), 1153-1159. doi:10.1016/j.neuroscience.2006.11.024

Goldstein, R. Z., & Volkow, N. D. (2011). Dysfunction of the prefrontal cortex in addiction: neuroimaging findings and clinical implications. *Nat Rev Neurosci, 12*(11), 652-669. doi:10.1038/nrn3119

Hall, W., Carter, L., & Morley, K. (2004). Neuroscience research on the addictions: a prospectus for future ethical and policy analysis. *Addictive Behaviours, 29*, 1481-1495.

Hardingham, N., Dachtler, J., & Fox, K. (2013). The role of nitric oxide in pre-synaptic plasticity and homeostasis. *Frontiers in Cellular Neuroscience, 7*(190). doi:10.3389/fncel.2013.00190

Hart, C. L., Ward, A. S., Haney, M., Foltin, R. W., & Fischman, M. W. (2001). Methamphetamine self-administration by humans. *Psychopharmacology (Berl), 157*(1), 75-81.

Hicks, C., Cornish, J. L., Baracz, S. J., Suraev, A., & McGregor, I. S. (2016). Adolescent pre-treatment with oxytocin protects against adult methamphetamine-seeking behaviour in female rats. *Addiction Biology, 21*, 304-315.

Hoover, W. B., & Vertes, R. P. (2007). Anatomical analysis of afferent projections to the medial prefrontal cortex in the rat. *Brain Struct Funct, 212*(2), 149-179. doi:10.1007/s00429-007-0150-4

Hsieh, J. H., Stein, D. J., & Howells, F. M. (2014). The neurobiology of methamphetamine induced psychosis. *Frontiers in Human Neuroscience, 8*, 537-548. doi:doi: 10.3389/fnhum.2014.00537

Hu, H., Gan, J., & Jonas, P. (2014). Interneurons. Fast-spiking, parvalbumin(+) GABAergic interneurons: from cellular design to microcircuit function. *Science, 345*(6196), 1255263. doi:10.1126/science.1255263

Hyman, S. E., & Malenka, R. C. (2001). Addiction and the brain: the neurobiology of compulsion and its persistence. *Nat Rev Neurosci, 2*(10), 695-703. doi:10.1038/35094560

Hyman, S. E., Malenka, R. C., & Nestler, E. J. (2006). Neural mechanisms of addiction: the role of reward-related learning and memory. *Annu Rev Neurosci, 29*, 565-598. doi:10.1146/annurev.neuro.29.051605.113009

Ikemoto, S., & Bonci, A. (2014). Neurocircuitry of drug reward. *Neuropharmacology, 76 Pt B*, 329-341. doi:10.1016/j.neuropharm.2013.04.031

Jackson, M. E., & Moghaddam, B. (2001). Amygdala regulation of nucleus accumbens dopamine output is governed by the prefrontal cortex. *J Neurosci, 21*(2), 676-681.

Kalivas, P. W. (2008). Addiction as a pathology in prefrontal cortical regulation of corticostriatal habit circuitry. *Neurotoxicity Research, 14*(2), 185-189. doi:10.1007/bf03033809

Kalivas, P. W. (2009). The glutamate homeostasis hypothesis of addiction. *Nature Reviews Neuroscience, 10*, 561. doi:10.1038/nrn2515

Kaneko, Y., Pappas, C., Tajiri, N., & Borlongan, C. V. (2016). Oxytocin modulates GABAAR subunits to confer neuroprotection in stroke in vitro. *Scientific Reports, 6*, 35659. doi:10.1038/srep35659

Karreman, M., & Moghaddam, B. (1996). The prefrontal cortex regulates the basal release of dopamine in the limbic striatum: an effect mediated by ventral tegmental area. *J Neurochem, 66*(2), 589-598.

Kawaguchi, Y., & Kondo, S. (2002). Parvalbumin, somatostatin and cholecystokinin as chemical markers for specific GABAergic interneuron types in the rat frontal cortex. *J Neurocytol, 31*(3-5), 277-287.

Kawaguchi, Y., & Kubota, Y. (1997). GABAergic cell subtypes and their synaptic connections in rat frontal cortex. *Cereb Cortex, 7*(6), 476-486.

Kearns, A., Weber, R. A., Carter, S., Cox, S., Peters, J., & Reichel, C. M. (2018). Inhibition of the prelimbic to nucleus accumbens core pathway decreases methamphetamine cued reinstatement. *Society for Neuroscience*, Washington DC, USA, 3-7 November.

Kelley, A. E., & Berridge, K. C. (2002). The neuroscience of natural rewards: relevance to addictive drugs. *J Neurosci, 22*(9), 3306-3311. doi:20026361

Killcross, S., & Coutureau, E. (2003). Coordination of Actions and Habits in the Medial Prefrontal Cortex of Rats. *Cerebral Cortex, 13*(4), 400-408. doi:10.1093/cercor/13.4.400

Koob, G. F. (1992). Drugs of abuse: anatomy, pharmacology and function of reward pathways. *Trends Pharmacol Sci, 13*(5), 177-184.

Koob, G. F., & Volkow, N. D. (2010). Neurocircuitry of Addiction. *Neuropsychopharmacology, 35*(1), 217-238. doi:10.1038/npp.2009.110

Kovacs, G. L., Sarnyai, Z., Barbarczi, E., Szabo, G., & Telegdy, G. (1990). The role of oxytocin-dopamine interactions in cocaine-induced locomotor hyperactivity. *Neuropharmacology, 29*(4), 365-368.

Krasnova, I. N., & Cadet, J. L. (2009). Methamphetamine toxicity and messengers of death. *Brain Research Reviews, 60*(2), 379-407. doi:https://doi.org/10.1016/j.brainresrev.2009.03.002

Kvitsiani, D., Ranade, S., Hangya, B., Taniguchi, H., Huang, J. Z., & Kepecs, A. (2013). Distinct behavioural and network correlates of two interneuron types in prefrontal cortex. *Nature, 498*(7454), 363-366. doi:10.1038/nature12176

Le Roux, N., Amar, M., Moreau, A. W., & Fossier, P. (2009). Roles of nitric oxide in the homeostatic control of the excitation–inhibition balance in rat visual cortical networks. *Neuroscience, 163*(3), 942-951. doi:https://doi.org/10.1016/j.neuroscience.2009.07.010

Lee, M. R., Glassman, M., King-Casas, B., Kelly, D. L., Stein, E. A., Schroeder, J., & Salmeron, B. J. (2014). Complexity of oxytocin's effects in a chronic cocaine dependent population. *European Neuropsychopharmacology, 24*, 1483-1391.

Leshner, A. I. (1997). Addiction is a brain disease, and it matters. *Science, 278*(5335), 45-47.

Lewis, D. A., Curley, A. A., Glausier, J. R., & Volk, D. W. (2012). Cortical parvalbumin interneurons and cognitive dysfunction in schizophrenia. *Trends Neurosci, 35*(1), 57-67. doi:10.1016/j.tins.2011.10.004

Liu, Q.-R., Rubio, F. J., Bossert, J. M., Marchant, N. J., Fanous, S., Hou, X., . . . Hope, B. T. (2014). Detection of molecular alterations in methamphetamine-activated Fos-expressing neurons from a single rat dorsal striatum using fluorescence-activated cell sorting (FACS). *J Neurochem, 128*(1), 173-185. doi:10.1111/jnc.12381

Mahler, S. V., Brodnik, Z. D., Cox, B. M., Buchta, W. C., Bentzley, B. S., Cope, Z. A., . . . Aston-Jones, G. (2018). Chemogenetic Manipulations of Ventral Tegmental Area Dopamine Neurons Reveal Multifaceted Roles in Cocaine Abuse. *bioRxiv*. doi:10.1101/246595

Mahler, S. V., Vazey, E. M., Beckley, J. T., Keistler, C. R., McGlinchey, E. M., Kaufling, J., . . . Aston-Jones, G. (2014). Designer receptors show role for ventral pallidum input to ventral tegmental area in cocaine seeking. *Nat Neurosci, 17*(4), 577-585. doi:10.1038/nn.3664

Markram, H., Toledo-Rodriguez, M., Wang, Y., Gupta, A., Silberberg, G., & Wu, C. (2004). Interneurons of the neocortical inhibitory system. *Nat Rev Neurosci, 5*(10), 793-807. doi:10.1038/nrn1519

Marlin, B. J., Mitre, M., D'amour, J. A., Chao, M. V., & Froemke, R. C. (2015). Oxytocin enables maternal behaviour by balancing cortical inhibition. *Nature, 520*, 499. doi:10.1038/nature14402 https://www.nature.com/articles/nature14402 - supplementary-information

McFarland, K., Lapish, C. C., & Kalivas, P. W. (2003). Prefrontal glutamate release into the core of the nucleus accumbens mediates cocaine-induced reinstatement of drug-seeking behavior. *J Neurosci, 23*(8), 3531-3537.

McGregor, I. S., & Bowen, M. T. (2012). Breaking the loop: oxytocin as a potential treatment for drug addiction. *Horm Behav, 61*(3), 331-339. doi:10.1016/j.yhbeh.2011.12.001

McRae-Clark, A. L., Baker, N. L., Maria, M. M., & Brady, K. T. (2013). Effect of oxytocin on craving and stress response in marijuana-dependent individuals: a pilot study. *Psychopharmacology, 228*, 623-631.

Miller, C. A., & Marshall, J. F. (2004). Altered prelimbic cortex output during cue-elicited drug seeking. *J Neurosci, 24*(31), 6889-6897. doi:10.1523/jneurosci.1685-04.2004

Mohila, C. A., & Onn, S. P. (2005). Increases in the density of parvalbumin-immunoreactive neurons in anterior cingulate cortex of amphetamine-withdrawn rats: evidence for corticotropin-releasing factor in sustained elevation. *Cereb Cortex, 15*(3), 262-274. doi:10.1093/cercor/bhh128

Moorman, D. E., James, M. H., McGlinchey, E. M., & Aston-Jones, G. (2015). Differential roles of medial prefrontal subregions in the regulation of drug seeking. *Brain Res, 1628*(Pt A), 130-146. doi:10.1016/j.brainres.2014.12.024

Morley, K. C., Cornish, J. L., Faingold, A., Wood, K., & Haber, P. S. (2017). Pharmacotherapeutic agents in the treatment of methamphetamine dependence. *Expert Opin Investig Drugs, 26*(5), 563-578. doi:10.1080/13543784.2017.1313229

Morshedi, M. M., & Meredith, G. E. (2007). Differential laminar effects of amphetamine on prefrontal parvalbumin interneurons. *Neuroscience, 149*(3), 617-624. doi:10.1016/j.neuroscience.2007.07.047

Nasif, F. J., Hu, X. T., Ramirez, O. A., & Perez, M. F. (2011). Inhibition of neuronal nitric oxide synthase prevents alterations in medial prefrontal cortex excitability induced by repeated cocaine administration. *Psychopharmacology (Berl), 218*(2), 323-330. doi:10.1007/s00213-010-2105-3

Ninan, I. (2011). Oxytocin suppresses basal glutamatergic transmission but facilitates activity-dependent synaptic potentiation in the medial prefrontal cortex. *J Neurochem, 119*(2), 324-331. doi:10.1111/j.1471-4159.2011.07430.x

O'Brien, C., & Kalivas, P. (2008). Drug addiction as a pathology of staged neuroplasticity. *Neuropsychopharmacology, 33*, 166-180.

Panenka, W. J., Procyshyn, R. M., Lecomte, T., MacEwan, G. W., Flynn, S. W., Honer, W. G., & Barr, A. M. (2013). Methamphetamine use: a comprehensive review of molecular, preclinical and clinical findings. *Drug Alcohol Depend, 129*(3), 167-179. doi:10.1016/j.drugalcdep.2012.11.016

Panlilio, L., & Goldberg, A. (2007). Self-administration of drugs in animals and humans as a model and an investigative tool. *Addiction, 102*, 1863-1870.

Pedersen, C. A., Smedley, K. L., Leserman, J., Jarskog, L. F., Rau, S. W., Kampov-Polevoi, A., & Garbutt, J. C. (2013). Intranasal oxytocin blocks alcohol withdrawal in human subjects. *Alcoholism: Clinical and Experimental Research, 37*(3), 484-489.

Qi, J., Han, W., Yang, J., Wang, L., Dong, Y., Wang, F., . . . Wu, C. (2012). Oxytocin regulates changes in extracellular glutamate and GABA levels induced by methamphetamine in the mouse brain. *Addiction Biology, 17*, 758-769.

Qi, J., Yang, J. Y., Song, M., Li, Y., Wang, F., & Wu, C. F. (2008). Inhibition by oxytocin of methamphetamine-induced hyperactivity related to dopamine turnover in the mesolimbic region in mice. *Naunyn Schmiedebergs Arch Pharmacol, 376*(6), 441-448. doi:10.1007/s00210-007-0245-8

Qi, J., Yang, J. Y., Wang, F., Zhao, Y. N., Song, M., & Wu, C. F. (2009). Effects of oxytocin on methamphetamine-induced conditioned place preference and the possible role of glutamatergic neurotransmission in the medial prefrontal cortex of mice in reinstatement. *Neuropharmacology, 56*(5), 856-865. doi:10.1016/j.neuropharm.2009.01.010

Quintana, D., Kemp, A., Alvares, G., & Guastella, A. (2013). A role for autonomic cardiac control in the effects of oxytocin on social behavior and psychiatric illness. *Frontiers in Neuroscience, 7*(48). doi:10.3389/fnins.2013.00048

Ridderinkhof, K. R., van den Wildenberg, W. P., Segalowitz, S. J., & Carter, C. S. (2004). Neurocognitive mechanisms of cognitive control: the role of prefrontal cortex in action selection, response inhibition, performance monitoring, and reward-based learning. *Brain Cogn, 56*(2), 129-140. doi:10.1016/j.bandc.2004.09.016

Robinson, T. E., & Berridge, K. C. (1993). The neural basis of drug craving: an incentive-sensitization theory of addiction. *Brain Res Brain Res Rev, 18*(3), 247-291.

Rocha, A., & Kalivas, P. W. (2010). Role of the prefrontal cortex and nucleus accumbens in reinstating methamphetamine seeking. *Eur J Neurosci, 31*(5), 903-909. doi:10.1111/j.1460-9568.2010.07134.x

Roth, B. L. (2016). DREADDs for Neuroscientists. *Neuron, 89*(4), 683-694. doi:10.1016/j.neuron.2016.01.040

Rudy, B., Fishell, G., Lee, S., & Hjerling-Leffler, J. (2011). Three groups of interneurons account for nearly 100% of neocortical GABAergic neurons. *Dev Neurobiol, 71*(1), 45-61. doi:10.1002/dneu.20853

Sabihi, S., Dong, S. M., Maurer, S. D., Post, C., & Leuner, B. (2017). Oxytocin in the medial prefrontal cortex attenuates anxiety: Anatomical and receptor specificity and mechanism of action. *Neuropharmacology, 125*, 1-12. doi:https://doi.org/10.1016/j.neuropharm.2017.06.024

Sabihi, S., Durosko, N. E., Dong, S. M., & Leuner, B. (2014). Oxytocin in the prelimbic medial prefrontal cortex reduces anxiety-like behavior in female and male rats. *Psychoneuroendocrinology, 45*, 31-42. doi:10.1016/j.psyneuen.2014.03.009

Sammut, S., & West, A. R. (2008). Acute cocaine administration increases NO efflux in the rat prefrontal cortex via a neuronal NOS-dependent mechanism. *Synapse, 62*(9), 710-713. doi:10.1002/syn.20537

Sarnyai, Z. (2011). Oxytocin as a potential mediator and modulator of drug addiction. *Addict Biol, 16*(2), 199-201. doi:10.1111/j.1369-1600.2011.00332.x

Sarnyai, Z., & Kovacs, G. L. (1994). Role of oxytocin in the neuroadaptation to drugs of abuse. *Psychoneuroendocrinology, 19*(1), 85-117.

Sarnyai, Z., & Kovács, G. L. (2014). Oxytocin in learning and addiction: From early discoveries to the present. *Pharmacology Biochemistry and Behavior, 119*, 3-9. doi:https://doi.org/10.1016/j.pbb.2013.11.019

Schoenbaum, G., Roesch, M. R., & Stalnaker, T. A. (2006). Orbitofrontal cortex, decision-making and drug addiction. *Trends in neurosciences, 29*(2), 116-124. doi:10.1016/j.tins.2005.12.006

Schoenbaum, G., & Shaham, Y. (2008). The role of orbitofrontal cortex in drug addiction: a review of preclinical studies. *Biological Psychiatry, 63*(3), 256-262. doi:10.1016/j.biopsych.2007.06.003

Scofield, M. D., Heinsbroek, J. A., Gipson, C. D., Kupchik, Y. M., Spencer, S., Smith, A. C., . . . Kalivas, P. W. (2016). The Nucleus Accumbens: Mechanisms of Addiction across Drug Classes Reflect the Importance of Glutamate Homeostasis. *Pharmacol Rev, 68*(3), 816-871. doi:10.1124/pr.116.012484

Shaham, Y., Shalev, U., Lu, L., de Wit, H., & Stewart, J. (2003). The reinstatement model of drug relapse: history, methodology and major findings. *Psychopharmacology (Berl), 168*(1-2), 3-20. doi:10.1007/s00213-002-1224-x

Shin, C. B., Templeton, T. J., Chiu, A. S., Kim, J., Gable, E. S., Vieira, P. A., . . . Szumlinski, K. K. (2018). Endogenous glutamate within the prelimbic and infralimbic cortices regulates the incubation of cocaine-seeking in rats. *Neuropharmacology, 128*, 293-300. doi:10.1016/j.neuropharm.2017.10.024

Smith, A. C. W., Scofield, M. D., Heinsbroek, J. A., Gipson, C. D., Neuhofer, D., Roberts-Wolfe, D. J., . . . Kalivas, P. W. (2017). Accumbens nNOS Interneurons Regulate Cocaine Relapse. *The Journal of Neuroscience, 37*(4), 742-756. doi:10.1523/JNEUROSCI.2673-16.2016

Smith, R. J., & Laiks, L. S. (2018). Behavioral and neural mechanisms underlying habitual and compulsive drug seeking. *Prog Neuropsychopharmacol Biol Psychiatry, 87*(Pt A), 11-21. doi:10.1016/j.pnpbp.2017.09.003

Stafford, J., Breen, C., & Burns, L. (2016). Australian Drug Trends 2016: Findings from the Illicit Drug Reporting System (IDRS). Australian Drug Trends Conference, Sydney. National Drug and Alcohol Research Centre University of New South Wales, Australia.

Stalnaker, T. A., Cooch, N. K., & Schoenbaum, G. (2015). What the orbitofrontal cortex does not do. *Nat Neurosci, 18*, 620. doi:10.1038/nn.3982

Taniguchi, H., He, M., Wu, P., Kim, S., Paik, R., Sugino, K., . . . Huang, Z. J. (2011). A resource of Cre driver lines for genetic targeting of GABAergic neurons in cerebral cortex. *Neuron, 71*(6), 995-1013. doi:10.1016/j.neuron.2011.07.026

Thomas, K. L., Arroyo, M., & Everitt, B. J. (2003). Induction of the learning and plasticity-associated gene Zif268 following exposure to a discrete cocaine-associated stimulus. *Eur J Neurosci, 17*(9), 1964-1972.

Tremblay, R., Lee, S., & Rudy, B. (2016). GABAergic Interneurons in the Neocortex: From Cellular Properties to Circuits. *Neuron, 91*(2), 260-292. doi:10.1016/j.neuron.2016.06.033

Uematsu, M., Hirai, Y., Karube, F., Ebihara, S., Kato, M., Abe, K., . . . Kawaguchi, Y. (2008). Quantitative chemical composition of cortical GABAergic neurons revealed in transgenic venus-expressing rats. *Cereb Cortex, 18*(2), 315-330. doi:10.1093/cercor/bhm056

United Nations Office on Drugs and Crime, World Drug Report 2018 (United Nations publication, Sales No. E.18.XI.9).

Usuda, I., Tanaka, K., & Chiba, T. (1998). Efferent projections of the nucleus accumbens in the rat with special reference to subdivision of the nucleus: biotinylated dextran amine study. *Brain Res, 797*(1), 73-93.

Van den Oever, M. C., Spijker, S., Smit, A. B., & De Vries, T. J. (2010). Prefrontal cortex plasticity mechanisms in drug seeking and relapse. *Neuroscience & Biobehavioral Reviews, 35*(2), 276-284. doi:https://doi.org/10.1016/j.neubiorev.2009.11.016

Veerasakul, S., Thanoi, S., Reynolds, G. P., & Nudmamud-Thanoi, S. (2016). Effect of Methamphetamine Exposure on Expression of Calcium Binding Proteins in Rat Frontal Cortex and Hippocampus. *Neurotox Res, 30*(3), 427-433. doi:10.1007/s12640-016-9628-2

Volkow, Nora D., & Morales, M. (2015). The Brain on Drugs: From Reward to Addiction. *Cell, 162*(4), 712-725. doi:https://doi.org/10.1016/j.cell.2015.07.046

Volkow, N. D., Wang, G.-J., Fowler, J. S., & Tomasi, D. (2012). Addiction Circuitry in the Human Brain. *Annual review of pharmacology and toxicology, 52*, 321-336. doi:10.1146/annurev-pharmtox-010611-134625

Wearne, T. A., Mirzaei, M., Franklin, J. L., Goodchild, A. K., Haynes, P. A., & Cornish, J. L. (2015). Methamphetamine-Induced Sensitization Is Associated with Alterations to the Proteome of the Prefrontal Cortex: Implications for the Maintenance of Psychotic Disorders. *Journal of Proteome Research, 14*(1), 397-410. doi:10.1021/pr500719f

Wearne, T. A., Parker, L. M., Franklin, J. L., Goodchild, A. K., & Cornish, J. L. (2016). GABAergic mRNA expression is differentially expressed across the prelimbic and orbitofrontal cortices of rats sensitized to methamphetamine: Relevance to psychosis. *Neuropharmacology, 111*, 107-118. doi:https://doi.org/10.1016/j.neuropharm.2016.08.038

Wearne, T. A., Parker, L. M., Franklin, J. L., Goodchild, A. K., & Cornish, J. L. (2017). Behavioral sensitization to methamphetamine induces specific interneuronal mRNA pathology across the prelimbic and orbitofrontal cortices. *Progress in Neuro-Psychopharmacology and Biological Psychiatry, 77*, 42-48. doi:https://doi.org/10.1016/j.pnpbp.2017.03.018

Wohr, M., Orduz, D., Gregory, P., Moreno, H., Khan, U., Vorckel, K. J., . . . Schwaller, B. (2015). Lack of parvalbumin in mice leads to behavioral deficits relevant to all human autism core symptoms and related neural morphofunctional abnormalities. *Transl Psychiatry, 5*, e525. doi:10.1038/tp.2015.19

Yager, L. M., Garcia, A. F., Wunsch, A. M., & Ferguson, S. M. (2015). The ins and outs of the striatum: role in drug addiction. *Neuroscience, 301*, 529-541. doi:10.1016/j.neuroscience.2015.06.033

Yang, J.-y., Qi, J., Han, W.-y., Wang, F., & Wu, C.-f. (2010). Inhibitory role of oxytocin in psychostimulant-induced psychological dependence and its effects on dopaminergic and glutaminergic transmission. *Acta Pharmacologica Sinica, 31*(9), 1071-1074. doi:10.1038/aps.2010.140

Young, K. A., Liu, Y., Gobrogge, K. L., Wang, H., & Wang, Z. (2014). Oxytocin Reverses Amphetamine-Induced Deficits in Social Bonding: Evidence for an Interaction with Nucleus Accumbens Dopamine. *The Journal of Neuroscience, 34*(25), 8499-8506. doi:10.1523/JNEUROSCI.4275-13.2014

Zimmermann, K. S., Li, C. C., Rainnie, D. G., Ressler, K. J., & Gourley, S. L. (2018). Memory Retention Involves the Ventrolateral Orbitofrontal Cortex: Comparison with the Basolateral Amygdala. *Neuropsychopharmacology, 43*(2), 373-383. doi:10.1038/npp.2017.139

Chapter 2: Methamphetamine-Induced Changes to Neuronal Activity and GABAergic Systems within the Prefrontal Cortex, Orbitofrontal Cortex, and Nucleus Accumbens

2.1 Introduction

Methamphetamine (METH) is a highly potent psychostimulant drug and is considered one of the most harmful illicit drugs, detrimentally impacting on individual drug users and society more broadly (Courtney & Ray, 2014; Morley, Cornish, Faingold, Wood, & Haber, 2017; Panenka et al., 2013). Unfortunately, treatments for METH abuse, including cognitive behavioural therapy and pharmacotherapies, have been ineffective in reducing drug use or the incidence of relapse (Morley et al., 2017).

Administration of METH has been shown to perturb neurotransmitter systems within the brain (Cruickshank & Dyer, 2009). However, our understanding of the neurobiological mechanisms that lead to METH addiction remain limited (Van den Oever, Spijker, Smit, & De Vries, 2010). It is postulated that the functional output of key substrates within reward circuitry, such as the prefrontal cortex (PFC) and nucleus accumbens (NAc), may be altered following exposure to addictive drugs (Garcia, Nakata, & Ferguson, 2017; Moorman, James, McGlinchey, & Aston-Jones, 2015). Additionally, dysfunction of the orbitofrontal cortex (OFC), a component of the PFC, has been implicated as disruption of OFC-driven behaviours, including decision-making and outcome expectancy, are characteristic of addiction (Lucantonio, Stalnaker, Shaham, Niv, & Schoenbaum, 2012; Schoenbaum, Roesch, & Stalnaker, 2006; Schoenbaum & Shaham, 2008; Volkow & Fowler, 2000).

Exposure to psychostimulants or drug-associated cues have been shown to increase neuronal activity (Franklin & Druhan, 2000; Goldstein et al., 2007; Miller & Marshall, 2004; Morshedi & Meredith, 2007; Thomas, Arroyo, & Everitt, 2003) within in the NAc, mPFC and

OFC. Whilst, alterations to NAc, mPFC and OFC function are associated with compulsive repetition of maladaptive behaviours, it is unknown which subregions are most impacted or if functional connectivity is altered (Garcia et al., 2017; Moorman et al., 2015; Panenka et al., 2013; Van den Oever et al., 2010). Furthermore, it is unclear how METH acts on specific neuronal subtypes to manipulate functional activity.

Previous literature has predominately focused on alterations to dopamine and glutamate neurotransmission, however recently dysfunction of GABAergic interneurons has also been implicated (Hsieh, Stein, & Howells, 2014; Karreman & Moghaddam, 1996; Miller & Marshall, 2004; Morshedi & Meredith, 2007; Qi et al., 2012). GABAergic interneurons function within the brain to regulate glutamatergic pyramidal cell output and the excitatory/inhibitory balance (Tremblay, Lee, & Rudy, 2016). Thus, if functional activity of GABAergic interneurons was altered, downstream brain regions could be detrimentally impacted (Moorman et al., 2015).

Two key GABAergic interneuron subtypes are neuronal nitric oxide synthase-expressing (nNOS) and parvalbumin-expressing (PV) GABAergic interneurons. It has been suggested increased activation of nNOS interneurons within the mPFC and NAc may lead to increased production of nitric oxide, leading to psychostimulant-induced neurotoxic effects (Gabbott & Bacon, 1995; Hardingham, Dachtler, & Fox, 2013). Furthermore, previous research has revealed both downregulation and upregulation of PV expression in the PFC following exposure to psychostimulants (Mohila & Onn, 2005; Todtenkopf et al., 2004; Veerasakul et al., 2016; Wearne et al., 2015; Wearne et al., 2017). Thus, it is possible that changes to the number or activation of

nNOS or PV interneurons may alter the excitatory/inhibitory balance within cortical networks, contributing to the pathogenesis of addiction.

The aim of this study was to investigate if neuronal activation was altered within the NAc, mPFC and OFC following METH exposure. A secondary aim was to investigate how METH exposure may be altering the number or function of nNOS and PV interneurons. Enhanced knowledge of the neurobiological mechanisms underlying addiction, particularly how disruption to GABA systems may change overall circuit function, may yield new insights into potential treatment strategies aimed at reducing METH abuse and incidence of relapse.

2.2 Materials and Methods

2.2.1 Animals

All experimental procedures were conducted in accordance with the Australian Code of Practice for the Care and Use of Animals for Scientific Purposes (8th Edition, 2013) and were approved by the Macquarie University Animal Ethics Committee (Animal Research Authority: 2017/043, Appendix 2).

Thirty-two male Long Evans rats (weighing 250-290g upon arrival) were obtained from the Australian Resources Centre (Perth, WA). Rats were pair-housed (cage size: 40 x 27 x 16cm) for the entirety of the experiment excluding two days of individual housing post-surgery. Wooden blocks, straws, sunflower seeds and shredded paper were provided in home cages for environmental enrichment. Rats were maintained in a temperature and light-controlled room (21 $\pm$1^{o} C, 12-hour light/dark cycle) and all experiments were conducted during the light cycle. Food

and water were available *ad libitum* in home cages and not during experimental sessions. Rats were acclimated to the facility for seven days and were handled daily by the experimenter for an additional five days prior to surgery.

2.2.2 Surgery

Rats underwent surgery to implant chronic indwelling catheters into the right jugular vein. Rats were anaesthetised with 3% isoflurane (2-chloro-2-1, 1, 1-trifluoroethyl difluoro-ethane) in oxygen (2L/min). Once anaesthetised, animals were treated with a subcutaneous (SC) injection of non-steroidal anti-inflammatory analgesic carprofen (Cenvet, Kings Park, NSW, 5mg/kg) and were hydrated with 0.9% saline (2mL, SC). The fur along the upper back and front of the neck was shaved and the area was sterilised with 70% alcohol and betadine in preparation for jugular intravenous (IV) catheter implantation. Instructions for catheter construction can be found in Appendix 3.

The depth of anaesthesia and breathing rate were routinely monitored throughout the surgery. Catheters were implanted into the right external jugular vein using an aseptic surgical technique and were flushed with 0.2mL of antibiotic cephazolin sodium (20mg/mL) immediately following implantation. All surgical tools and implants were autoclaved or sterilised in chlorhexidine with 70% alcohol.

2.2.3 Post-Operative Care

For post-operative care, rats were placed into a heated recovery chamber (27^{o} C) for 45 minutes following surgery and monitored until ambulatory. After recovery, rats were returned to

individual housing for two days post operation, where carprofen (5mg/kg, SC) was administered and catheters were flushed daily with 0.2mL of cephazolin sodium (IV). The post-operative weight and behaviour of the animal were monitored and recorded daily. For the remaining duration of the experiment, catheter patency was maintained via daily flushing with 0.1mL of heparinised saline (100UI/mL) prior to intravenous self-administration (IVSA) and 0.2mL of cephazolin sodium in heparinised saline (300IU/mL) post IVSA.

2.2.4 Drugs

Methamphetamine hydrochloride (METH, 99% purity) powder was purchased from Australian Government Analytical Laboratories (Pymble, NSW, Australia). METH was dissolved in 0.9% isotonic saline for treatment administration. Vehicle administration consisted of 0.9% isotonic saline solution. METH was filtered via a syringe filter (0.22μm) for IV administration. For METH IVSA experiments, animals were administered 0.1mg/kg/infusion of METH or vehicle. For drug-primed reinstatement experiments, rats were intraperitoneally injected (IP) with 1mg/kg of METH or vehicle at a volume of 1mL/kg.

2.2.5 Self-Administration Apparatus

Behavioural testing was conducted in 16 standard operant response chambers (32 x 25 x 34cm; Med Associates, St Albans, VT, USA). Operant response chambers were housed in sound-attenuating boxes (41 x 56 x 56cm) equipped with a fan for ventilation. Each chamber was equipped with two retractable levers, two cue lights and a house light. Chambers also contained a metal arm and a spring connector attached to a swivel. Polyethylene tubing was passed through the spring connector and attached to a 10mL syringe, driven by an infusion pump (Med

Associates) located on top of the standard operant response chamber, inside the sound attenuating chamber. Four infrared detectors, located on the side wall of each operant chamber, were used to measure locomotor activity during test sessions. Active and inactive lever presses, number of infusions and locomotor activity was recorded using MED-PC software (Med Associates).

2.2.6 Self-Administration Paradigm

Rats underwent experimentation as two separate cohorts and were allocated to one of two IVSA groups (Figure 2.1). A total of 22 rats were randomly assigned to lever press for METH. Of these 22 METH IVSA animals, 10 rats were assigned yoked partners who would receive vehicle IV. The remaining METH IVSA rats were not paired to yoked control animals.

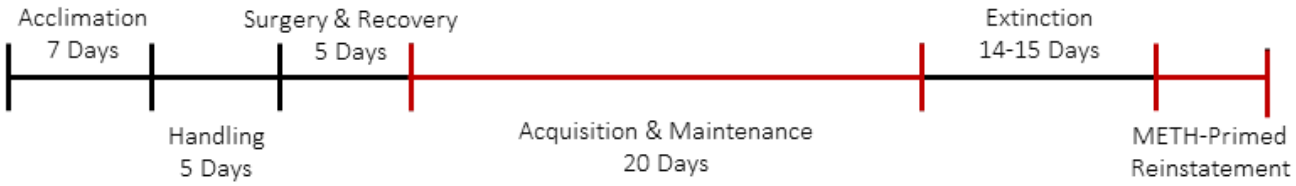

Figure 2.1. Schematic diagram displaying experimental timeline. Animals were culled 90 minutes after reinstatement injection.

2.2.6.1 Acquisition and Maintenance of METH Self-Administration

Rats were allowed to acquire self-administration during 3-hour fixed ratio 1 (FR1) schedule sessions conducted five days a week. Levers were allocated as active or inactive, where the location of active lever was counterbalanced across chambers and treatment groups.

Prior to the commencement of each IVSA session, polyethylene tubing lines were flushed with 1mL of 70% ethanol followed by METH or saline solution. Catheters were then flushed with 0.1mL of heparinised saline (10IU/mL) and a polyethylene infusion line was threaded onto

the animal's back via a back mount (Bioscientific, Kirawee, NSW). Rats were then placed inside the operant chamber and parameters, such as lever extension and house light illumination, indicated the initiation of the IVSA session.

Depression of the active lever resulted in a 3-second 0.05mL infusion of METH or vehicle, which was signaled by 3-second illumination of the cue light positioned directly above the active lever. During infusion, the house light was eliminated and a 20-second time out period occurred, during which depression of the levers was recorded without consequence. Once the 20-second time out period had elapsed, the house light was again illuminated signaling drug availability. Depression of the inactive lever had no consequences and thus was not directly relevant to METH-taking or METH-seeking behaviour, however this measure was used to determine if rats specifically acquired drug-paired responding.

To avoid drug overdose, rats were limited to a maximum of 100 infusions per 3-hour session (10mg/kg of METH, IV). The session ended when 180 minutes had elapsed or the rat had received the maximum number of infusions. Completion of the session was indicated via retraction of the levers and elimination of the house light. At the end of the session, rats were disconnected from infusion lines and catheters were flushed with 0.2mL of cephazolin sodium in heparinised saline solution before placement in their home cage. METH self-administration was undertaken for a total of 20 days.

2.2.6.2 Extinction of METH Self-administration

Following the final day of IVSA, rats were exposed to daily extinction sessions that were progressively decreased from 180 to 90 minutes in length (Day 1-3: 180mins, Day 4: 140mins, Day 5-7: 120mins, Day 8-14: 90mins). Parameters and cues were maintained throughout extinction training. That is, depression of the active lever triggered 3-second illumination of the cue light and a time-out period, as signaled by elimination of the house light (20-seconds), however no infusion was delivered. On the final day of extinction, rats were administered 1mL/kg of vehicle IP to habituate to drug-primed reinstatement injections. Strict criteria were employed to ensure rats had extinguished drug-paired responses before commencement of reinstatement testing. The extinction period extended for 14-15 days until responding on the active lever was less than 30% of the number of active lever presses on the final day of IVSA for two consecutive days (Yan, Nitta, Mizoguchi, Yamada, & Nabeshima, 2006).

2.2.6.3 Reinstatement of METH Self-administration

Rats underwent one reinstatement test and a between-subjects design was employed (2x2), meaning rats were allocated to one of four reinstatement groups; vehicle IVSA and vehicle prime (Veh/Veh; n=5), vehicle IVSA and METH-prime (Veh/METH; n=5), METH IVSA and vehicle prime (METH/Veh; n = 8) and METH IVSA and METH-prime (METH/METH; n = 8). Factors such as total METH intake, number of active lever presses during IVSA, number of active lever presses during extinction and number of inactive lever presses during extinction were considered to ensure even allocation across both METH/Veh and METH/METH groups.

Reinstatement testing was conducted over two test days for each cohort of animals. Animals were injected with either vehicle (1mL/kg) or METH (1mg/kg, IP) then placed into operant response chambers for a total of 90 minutes. Reinstatement parameters were identical to extinction parameters. The number of non-reinforced active lever presses was used as a measure of reinstatement of METH-seeking behaviour.

2.2.7 Euthanasia and Histology

Upon the completion of the reinstatement session, rats underwent intracardiac perfusion fixation. Rats were heavily anaesthetised via an injection of sodium pentobarbitone (135mg/2mL, IP). Depth of anaesthesia was determined using a firm pinch of the hind paw and tail. Once motor responses to hind paw or tail pinches were absent, the chest cavity was opened using surgical scissors and the heart was exposed. A blunt 18G needle was inserted into the aorta and the animal was perfused with ice cold Dulbecco's Modified Eagle's Medium/Nutrient Mixture F-12 Ham (DMEM; 200mL/8 minutes) followed by 4% paraformaldehyde (PFA; 200mL/8 minutes). Brains were carefully removed from the skull and post-fixed in 4% PFA overnight at 4ºC. Brains were then placed into graded sucrose solutions (10% sucrose for 24 hours, 20% sucrose for 24 hours and 30% sucrose for 48 hours). Brains were preserved in cryoprotectant solution (30% ethylene glycol, 30% sucrose and 2% polyvinylpyrolidone dissolved in 0.1M phosphate buffered saline [PBS]) and stored at -20 ºC until sectioning.

Brains were coronally blocked rostral to the hypothalamus with the assistance of a 1mm graticule and mounted caudal surface down. Brains were sectioned coronally (40μm thick, 1:5 serial sections) using a vibrating microtome (VTS1200S; Leica Microsystems).

2.2.8 Immunohistochemistry

Immunohistochemistry was used to examine Fos, a marker of neuronal activity (Dragunow & Faull, 1989), PV and nNOS immunoreactivity in five brains from each of the four reinstatement conditions (n = 20). For the Veh/Veh and Veh/METH conditions, the brains from all animals were analysed. For the METH/Veh condition, five animals were randomly selected. Lastly, the animals with highest number of active lever presses during reinstatement were selected from the METH/METH group, as these animals are mostly likely to evidence relapse-induced neurochemical changes. Free floating sections were stained with primary antibodies (Appendix 4) for a total of 68 hours, followed by secondary antibodies (see Appendix 5 for detailed protocol). Sections were mounted onto glass slides and coverslipped with Dako fluorescence mounting media (Agilent, Mulgrave, Victoria, Australia).

2.2.9 Image Analysis and Quantification

One hemisphere from each animal was examined for Fos, PV and nNOS immunoreactivity. A total of seven tissue sections (ranging from +1.7 to + 4.7mm from Bregma; Figure 2.2) were imaged under epifluorescence (Zeiss AxioImager Z2 microscope 10x/0.30M27 objective lens running ZEN 2011) at consistent exposure times. Tiled images of each coronal section were captured at 10x magnification, stitched and adjusted for brightness and contrast in an identical manner using Zen software (Zeiss, Gottingen, Germany). The total number of positive immunoreactive neurons within each region of interest (ROI) was counted by an experimenter blind to treatment conditions using the ImageJ plugin Fiji (Schindelin et al., 2012).

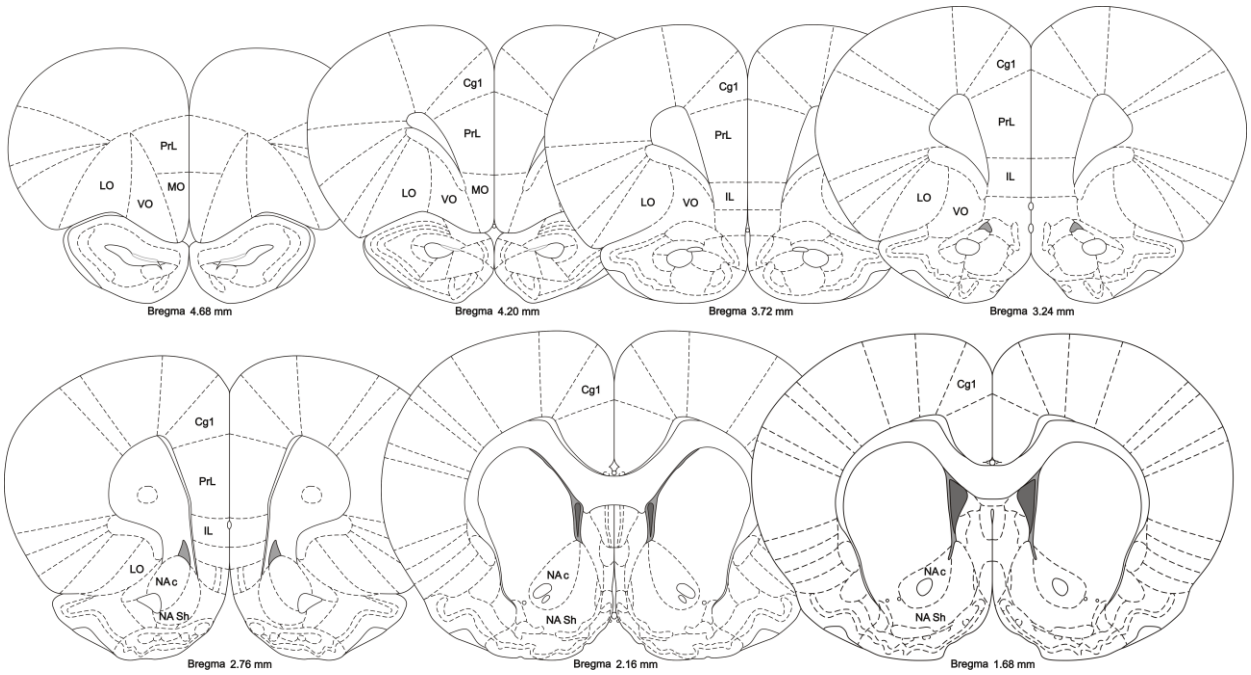

Figure 2.2. Anatomical coronal diagrams depicting each the brain region of interest and the coordinates (mm from Bregma) at which the regions were analysed. Adapted from the Rat Brain Atlas (Paxinos and Watson, 2007).

2.2.10 Correlational Analysis and Description of Activated Brain Circuits

Indications of potential functional connections were gained by correlating Fos immunoreactivity across each ROI. Correlations were first performed using data from the entire cohort of analysed brains (n = 20) then broken down into treatment groups (n = 4-5) to facilitate examination of how correlated activity may be changing with METH exposure. This analysis approach has previously been employed to examine the functional brain circuits underlying many behavioural processes (Castilla-Ortega et al., 2016; Castilla-Ortega et al., 2014; Siette et al., 2013). This approach was also used to analyse the relationship between Fos/nNOS/PV immunoreactivity and total METH-intake and Fos/nNOS/PV immunoreactivity and active lever presses during reinstatement.

2.2.11 Statistical Analyses

To determine if rats had acquired METH self-administration, the mean number of active and inactive lever presses, drug infusions and locomotor activity counts were compared across the IVSA period using a repeated measures ANOVA, with the first and final day directly compared. In order to ensure METH IVSA rats had learnt to differentiate between the active and inactive lever, the number of active and inactive lever presses on the final day of IVSA were directly compared using a paired t-test. Rats that failed to acquire a preference for the METH-paired lever were excluded from the final analyses.

In order to assess if the preference for the drug-paired lever had been extinguished in METH IVSA animals, the mean number of active lever presses on the final three days of extinction was compared to the mean number of active lever presses during the final three days of IVSA using a paired t-test. To ensure similar levels of METH exposure and METH-seeking behaviour across METH/Veh and METH/METH animals, paired t-tests were used to compare METH intake (mg/kg), active lever pressing during the final three days of IVSA and active lever pressing during the final three days of extinction.

To determine if METH/METH treated rats had reinstated to previous METH-paired lever pressing, the total number of active lever presses during reinstatement was compared across all reinstatement conditions and to the extinction day prior using a one-way ANOVA. To ensure active lever pressing was not due to METH-induced hyperlocomotion, the number of active lever and inactive lever presses were directly compared within METH/METH group using a paired t-

test. Total locomotor activity was also compared across all reinstatement conditions using a one-way ANOVA.

Total number of neurons immunoreactive for Fos, nNOS and PV were analysed using a 2x2 ANOVA (Factor 1: IVSA treatment - vehicle or METH; Factor 2: priming treatment - vehicle or METH). Pearson's correlation coefficients were used to investigate any relationship between METH intake, active lever pressing during reinstatement and total number of immunoreactive neurons. For correlational analysis, both p and q values were calculated to control for a 5% false discovery rate (Storey, 2002). All statistical analyses were performed using SPSS Version 20 for PC (SPSS Incorporated, Chicago, IL, USA) Data are presented as mean ± SEM. Differences were considered significant when $p < 0.05$.

2.3 Results

2.3.1 Excluded Animals

Of the original 32 animals that underwent intravenous catheter implantation, the data from seven animals was removed from the final analyses due to: failure to acquire METH IVSA (n = 2), failure to extinguish drug-paired responding on the active lever (n = 4) and abnormal Fos immunoreactivity (2 SD $\pm$ the mean; n = 1 belonging to METH/Veh group).

2.3.2 Intravenous METH Self-Administration

Rats acquired intravenous METH self-administration, as evidenced by a significant increase in the number of delivered infusions from Day 1 to Day 20 ($F(1, 17) = 30.706$, $p = 0.000$; Figure 2.3A). The number of responses on the active lever also significantly increased

across the IVSA period ($F(1, 17) = 5.476$, $p = 0.032$), whilst the number of inactive lever responses did not significantly differ ($F(1, 17) = 2.906$, $p = 0.106$; Figure 2.3B). Active and inactive lever presses were directly compared in METH IVSA animals, with rats displaying a distinct preference for the drug-paired lever on Day 20 ($t(16) = 8.642$; $p = 0.000$). Locomotor activity was also significantly increased from Day 1 to Day 20 ($F(1, 16) = 29.401$, $p = 0.000$; Figure 2.3C).

2.3.3 Behavioural Extinction

Active lever pressing in METH IVSA animals was had significantly reduced from the final three days of IVSA to the final three days of extinction ($t(29) = -5.630$; $p = 0.000$). The end of the extinction period was signaled by a reduction in active lever pressing (< 30% of pressing on the final three days of FR1) across two consecutive days (Yan et al., 2006). No statistically significant differences in METH intake were found between METH/Veh and METH/METH

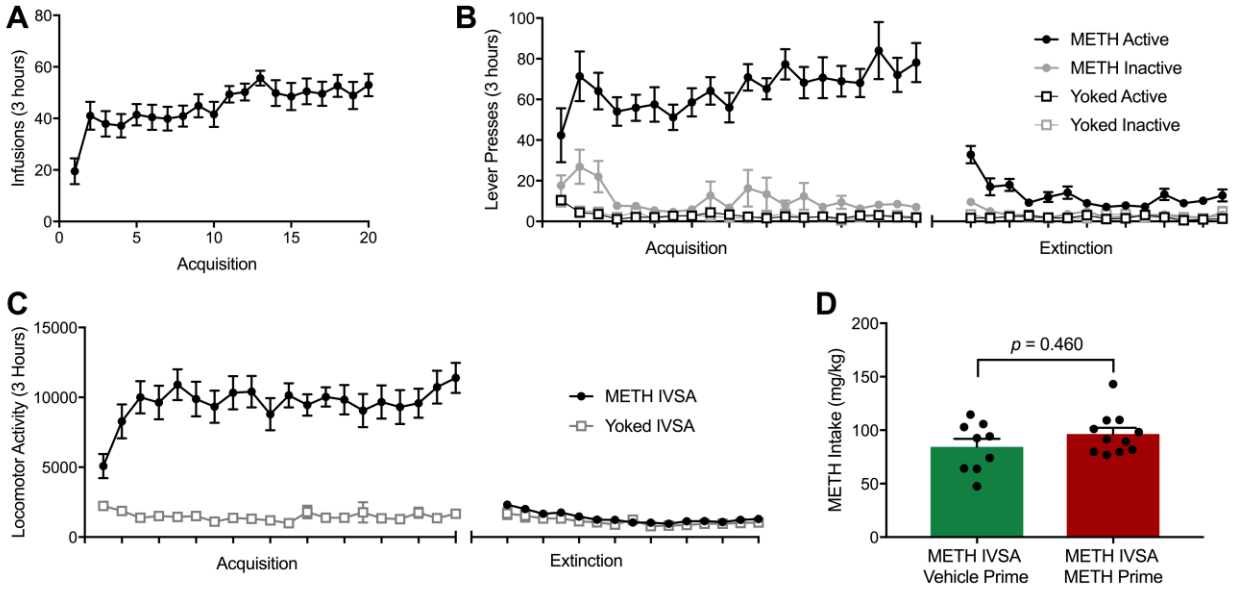

Figure 2.3. Mean number of delivered infusions (A), active and inactive lever presses (B) and locomotor activity counts (C) during IVSA and extinction in METH IVSA and yoked controls. Total METH intake (mg/kg) did not significantly differ across animals designated to the vehicle prime and METH prime reinstatement groups (D). All data presented as mean + SEM. Data presented as n= 22 METH IVSA rats, n = 10 yoked controls.

groups ($t(9) = -0.772$; $p = 0.460$; Figure 2.3D). There were also no statistically significant differences in the mean number of active lever presses across the final three days of IVSA ($t(9) = -1.127$; $p = 0.289$) or the number of active lever presses during extinction ($t(9) = -0.664$; $p = 0.523$) between METH/Veh and METH/METH groups, suggesting both groups had a similar METH IVSA experience and any differences can be attributed to METH-primed reinstatement.

2.3.4 METH-Primed Reinstatement

Administration of a non-contingent METH-prime produced robust reinstatement of active lever pressing in the METH/METH group ($F(1, 16) = 30.964$, $p = 0.000$). The number of active lever presses was significantly increased when compared to the extinction day prior ($t(3) = 4.680$, $p = 0.001$; Figure 2.4A). Active lever pressing was also significantly increased in the METH/METH group when compared to inactive lever presses ($t(9) = 5.469$, $p = 0.000$; Figure 2.4B), suggesting increased active lever pressing was not due METH-induced hyperlocomotion or increase generalised lever pressing. Locomotor activity was also significantly increased in the METH/METH group when compared to other treatment conditions ($F(1, 16) = 37.9502$, $p = 0.000$) and the extinction day prior ($t(3) = -3.632$, $p = 0.036$; Figure 2.4C).

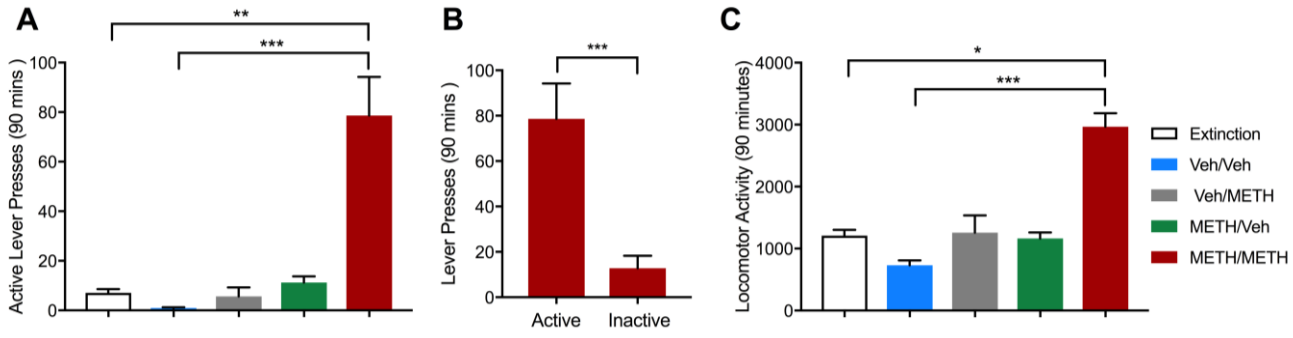

*Figure 2.4. Effects of a non-contingent vehicle or METH-prime (1mg/kg) on active lever pressing (A), active versus inactive lever pressing in METH/METH group (B) and locomotor activity (C). *represent p = 0.036, ** represents p = 0.001 and *** represents p = 0.000. Data presented as mean + SEM. Data presented as n = 5 in Veh/Veh and Veh/METH groups, n = 10 in METH/Veh and METH/METH groups.*

2.3.5 Administration of METH Increases Neuronal Activity

There was a significant main effect of priming treatment, with rats that received a non-contingent injection of METH displaying increased Fos immunoreactivity in the NAc core, mPFC and OFC [NAc core $F(1, 15) = 20.022$, $p = 0.000$; NAc shell $F(1, 15) = 10.670$, $p = 0.005$; Cg1 $F(1, 15) = 12.923$, $p = 0.003$; PrL $F(1, 15) = 5.785$, $p = 0.030$; LO $F(1, 15) = 13.714$, $p = 0.002$; MO $F(1, 15) = 5.058$, $p = 0.040$; Figure 2.5A-C]. There was no effect of priming treatment on Fos immunoreactivity in the infralimbic and ventral orbitofrontal cortices [IL; $F(1, 15) = 1.336$, $p = 0.266$; VO $F(1, 15) = 0.136$, $p = 0.718$]. Animals treated with a vehicle prime exhibited low numbers of neurons immunoreactive for Fos, likely reflecting basal levels of neuronal activation. Overall there was a no significant effect of IVSA treatment on Fos immunoreactivity in METH/Veh rats, suggesting prior METH experience did not increase neuronal activity in absence of METH.

Interestingly, there was significant interaction between IVSA and priming treatment in the NAc core [$F(1, 15) = 8.614$, $p = 0.010$]. Further analysis revealed a statistically significant increase in Fos immunoreactivity in METH/METH animals when directly compared to Veh/METH animals ($t(8) = -2.896$, $p = 0.020$). This finding is also supported by the presence of a strong correlation between the number of active lever presses during reinstatement testing and the total number of Fos immunoreactive neurons within the NAc core ($r = 0.822$, $p = 0.000$; Figure 2.5D). This suggests whilst acute METH administration increases neuronal activity in the NAc core, this effect is more pronounced during relapse.

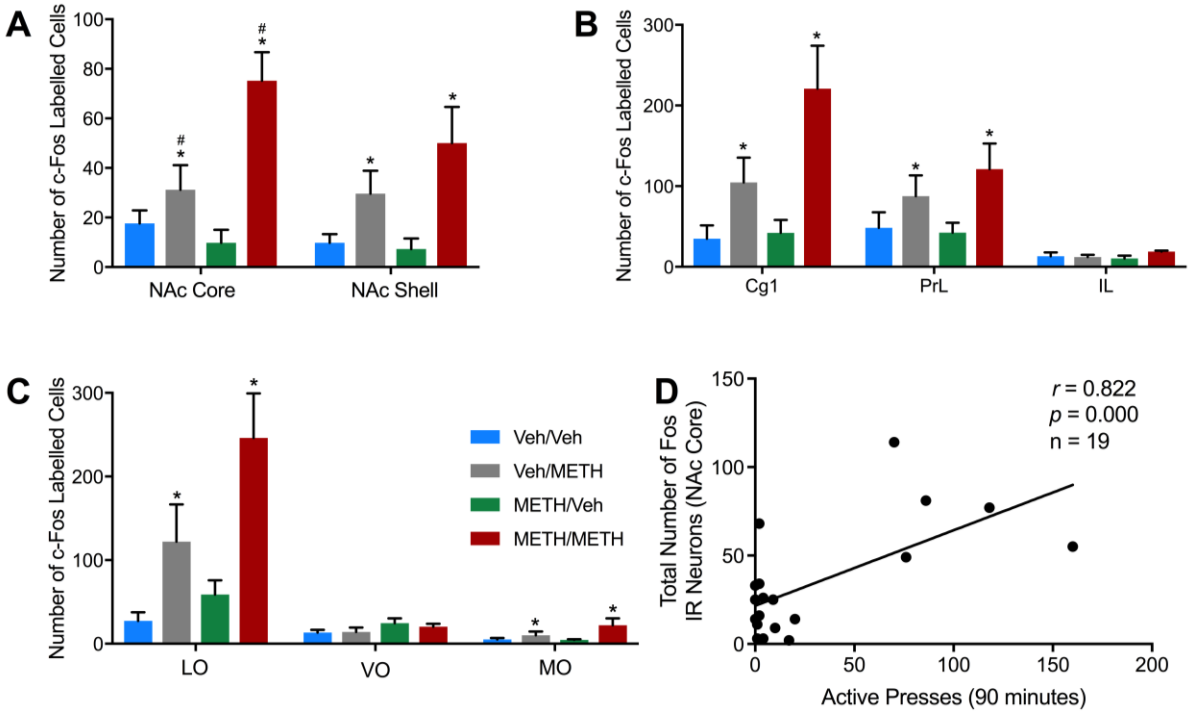

Figure 2.5. Treatment groups which received a non-contingent injection of METH (1mg/kg) during relapse testing displayed significantly increased Fos immunoreactivity when compared to groups treated with vehicle ($p < 0.05$; A-C). NAc core Fos immunoreactivity was also significantly increased in METH/METH animals when compared to Veh/METH animals (# $p = 0.020$). The total number of Fos immunoreactive neurons in the NAc core was positively correlated with active presses during reinstatement (D). Data presented as mean +SEM. Data presented as n = 4 in METH/Veh group, n = 5 in all other groups.*

Results of Pearson's correlation analysis revealed a total of 16 statistically significant correlations, of which 15 met *q* criteria (Figure 2.6). Analyses were then performed within groups to examine how functional connectivity may be altered. Animals in the Veh/Veh condition displayed a total of 11 statistically significant correlations linking functional activity between seven of the eight examined brain regions. Correlated activity was decreased in all METH-experienced conditions, with Veh/METH and METH/METH animals displaying four significant correlations, whilst METH/Veh animals displayed three significant correlations (Figure 2.7). However, many of the within-group correlations did not meet *q* criteria, suggesting these correlations had a high probability of being false positives (>5 %) and should be interpreted with caution (Storey, 2002).

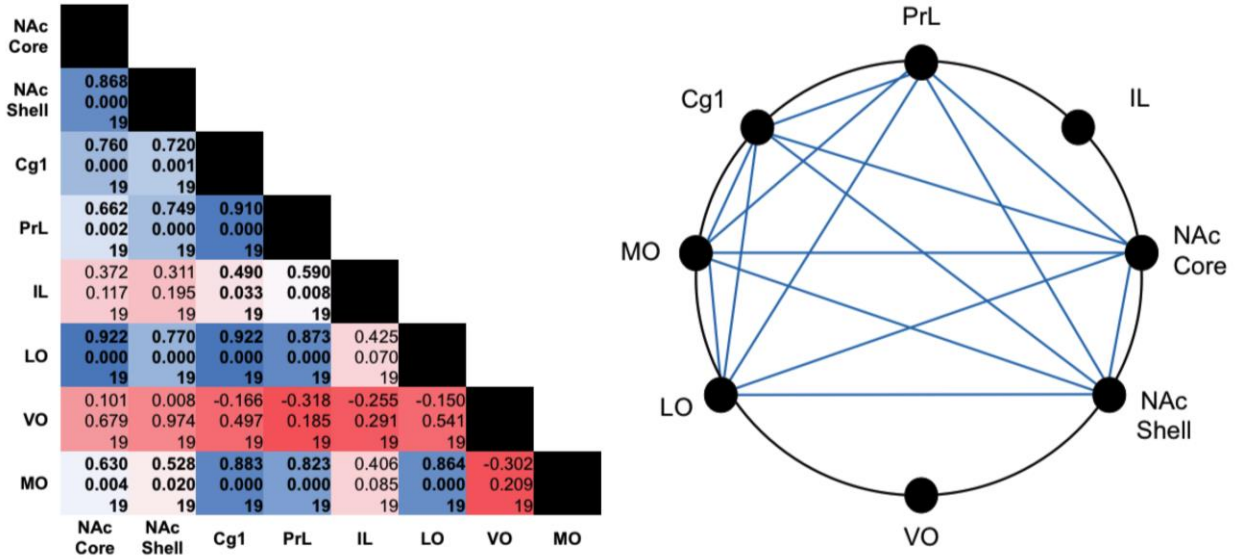

Figure 2.6. Correlative analysis revealed functional correlations between subregions of the mPFC, OFC and NAc. Blue was been used to depict positive Pearson's correlation coefficients, whilst red has been used to depict negative coefficients. The strength of the correlation is depicted by the shade, with weak correlations presented in lighter shades and stronger correlations presented in darker shades. Statistically significant correlations are shown in bold. Data presented as n = 4 in METH/Veh group, n = 5 in all other groups.

Under Veh/Veh conditions, it appears neuronal activation in the IL is correlated with activity in the Cg1, PrL, LO and MO. Markedly, in all other conditions, the IL does not appear to be functionally correlated with any other examined brain region. Furthermore, under vehicle priming conditions, Veh/Veh or METH/Veh rats, the activity of NAc core and NAc shell is highly correlated. Conversely, Veh/METH and METH/METH rats exhibited a lack of correlated activity between subregions of the NAc. Interestingly, activation in the MO and LO was correlated in all treatment conditions except METH/METH animals.

2.3.6 Administration of METH Affected Immunoreactivity of GABA Markers

Fos immunoreactivity was analysed for colocalisation with nNOS and PV immunoreactivity (Appendix 6). Analysis of colocalisation revealed only a small proportion of

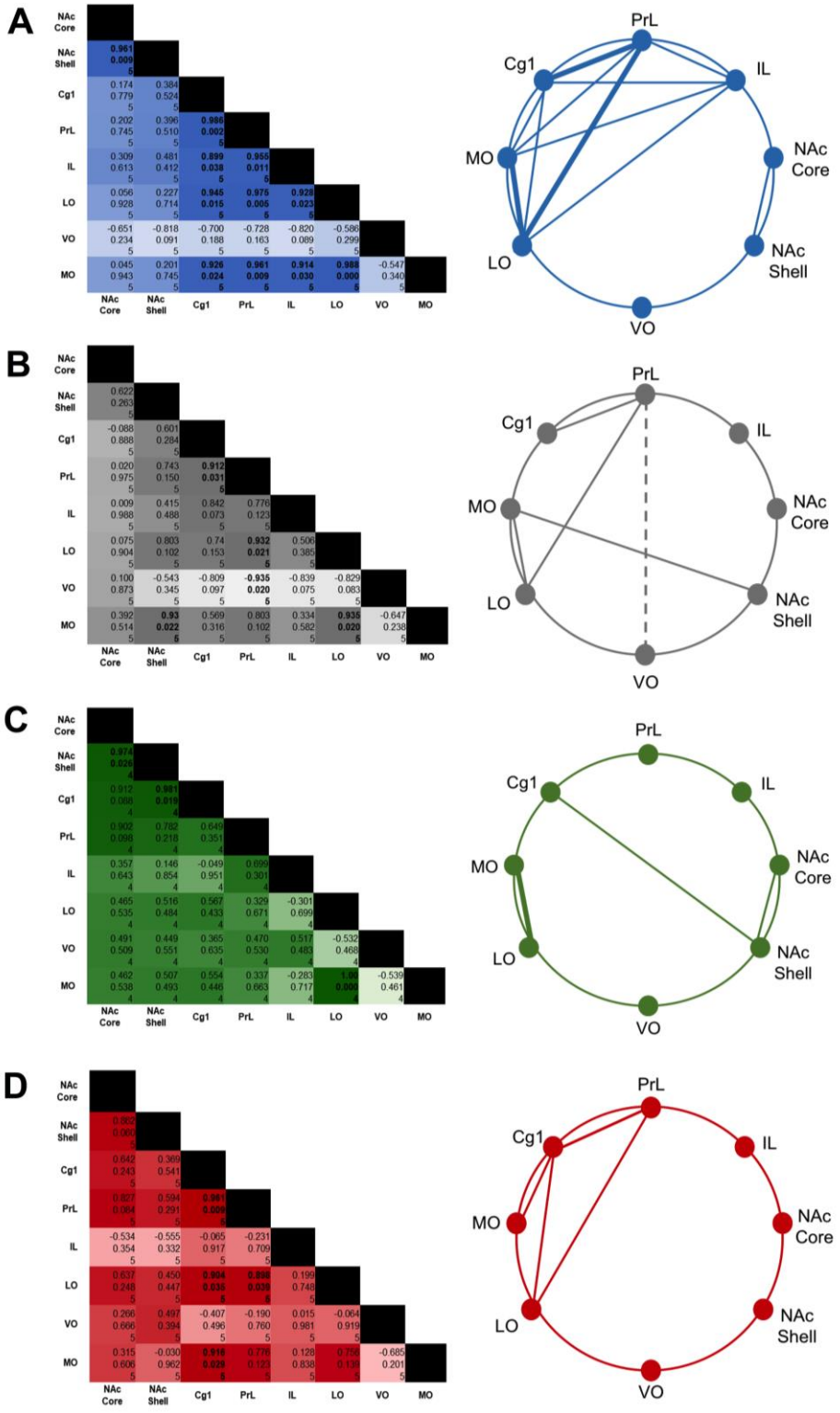

Figure 2.7. Pearson's correlation coefficients and connectivity diagrams for Veh/Veh (A), Veh/METH (B), METH/Veh (C) and METH/METH (D) treated animals. LHS: Matrices describing the Pearson's correlation coefficient, p-value and n value. The strength of the correlation is depicted by the shade, with weak correlations presented in lighter shades and stronger correlations presented in darker shades. Statistically significant correlations are presented in bold. RHS: Diagrams displaying possible functional connectivity between examined brain regions. Solid lines represent positive correlations which were statistically significant. Dotted lines present a negative correlation which was statistically significant. Bold lines represent significant positive correlations which met q criteria.

immunoreactivity was colocalised with nNOS or PV in the NAc, mPFC and OFC. Furthermore, there were no differences in activation of nNOS or PV immunoreactive interneurons across treatment groups. Thus, to determine if METH exposure was triggering loss of neurons, the total number of neurons immunoreactive for nNOS or PV was compared across treatment groups.

2.3.6.1 Prolonged METH Exposure Induced Increased nNOS Immunoreactivity

METH exposure yielded a non-significant effect on nNOS immunoreactivity in the NAc core [IVSA treatment: $F(1, 16) = 0.301$, $p = 0.591$; priming treatment: $F(1, 16) = 0.157$, $p = 0.697$; IVSA treatment x priming treatment: $F(1, 16) = 0.604$, $p = 0.448$; Figure 2.8A]. Interestingly, when a specific coordinate (+ 2.2mm from Bregma) of the NAc core was analysed, nNOS immunoreactivity was positively correlated with Fos immunoreactivity ($r = 0.569$, $p = 0.011$; n = 19; Figure 2.8B).

Upon analysis of a discrete coordinate of the PrL (+3.2mm from Bregma), METH self-administration significantly increased nNOS immunoreactivity [IVSA treatment: $F(1, 16) =$

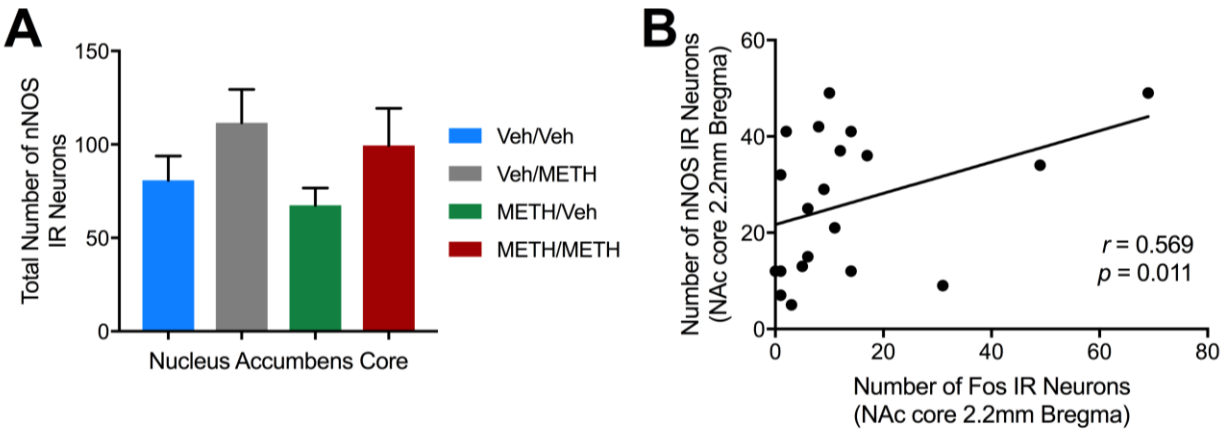

Figure 2.8. There were no significant differences across treatment groups in the number of nNOS-expressing neurons (A), however correlational analysis revealed significant correlations between nNOS immunoreactivity in the nucleus accumbens core and Fos immunoreactivity in the nucleus accumbens core (B). Data presented as n = 5 per group or n = 20 for correlation analysis.

4.893, $p = 0.042$; Figure 2.9A-C]. This effect appears to be specific to prolonged METH exposure, as there was no effect of priming treatment [$F(1, 16) = 0.007$, $p = 0.936$] or interaction effects [IVSA treatment x priming treatment: $F(1, 16) = 0.168$, $p = 0.688$]. This finding is further supported by analysis which revealed a positive correlation between the total number of nNOS immunoreactive neurons in the PrL and METH intake, which was trending towards significance ($r = 0.620$, $p = 0.056$; Figure 2.9E). However, when PrL coordinates were combined to enable examination nNOS immunoreactivity across the entire PrL, there was a no effect of METH exposure on nNOS immunoreactivity [$F(1, 16) = 0.642$, $p = 0.435$; Figure 2.9D], following trends observed in the NAc core. Analysis of nNOS immunoreactivity in subregions of the OFC yielded no significant differences across experimental groups at the total regional level or at specific coordinates.

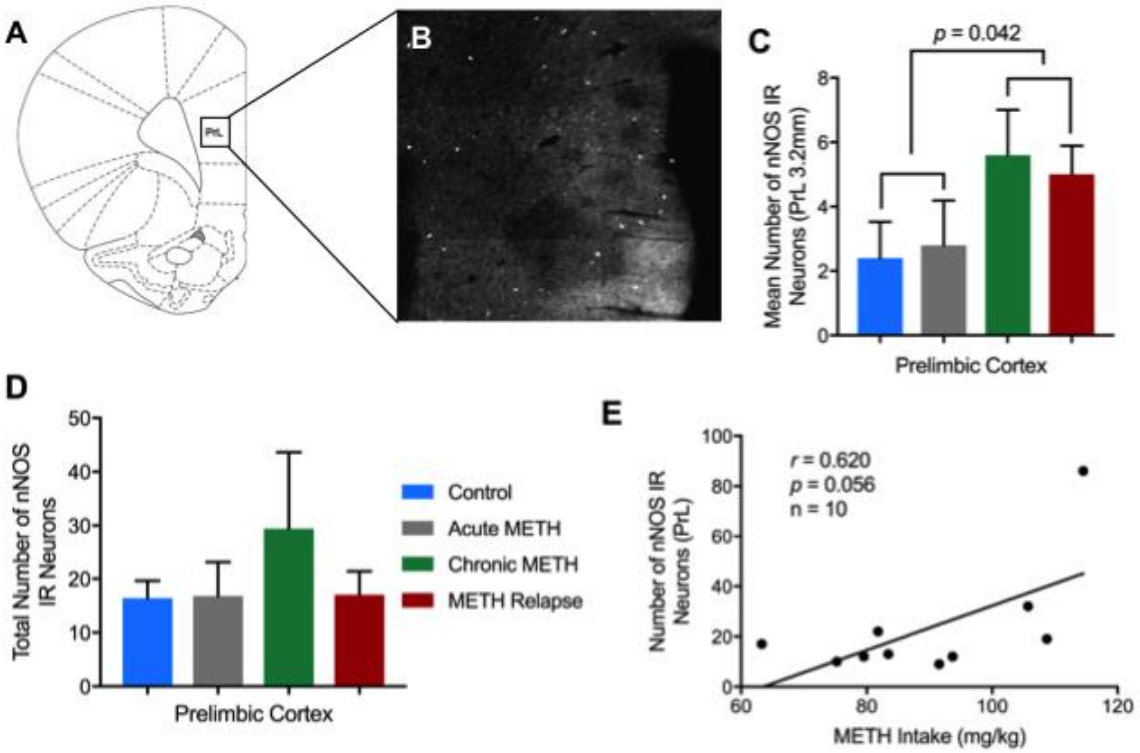

Figure 2.9. Examination of nNOS reactivity in the PrL (+ 3.2mm from Bregma) revealed a significant effect of METH IVSA (A-C), however this effect was not observed when the PrL was examined as an entire subregion (D). Correlation analysis revealed a positive correlation between nNOS immunoreactivity in the PrL and METH intake, which trended towards significance (E). All data presented as mean + SEM. Data presented as n = 5.

Colocalisation of Fos with nNOS immunoreactivity was also examined to determine what proportions of nNOS immunoreactive neurons were activated. Only a small proportion of nNOS immunoreactive neurons co-expressed Fos in the NAc core and PrL, suggesting minimal activation of nNOS interneurons in these brain regions (Figure 2.10A). Overall, there was a non-significant effect of priming treatment on nNOS activation, however in the prelimbic cortex IVSA treatment was trending towards significance [$F(1, 16) = 0.3.229$, $p = 0.092$]. In contrast, there was a statistically significant correlation between the number of total number of activated nNOS neurons in the NAc core and the number of active presses during reinstatement session $r = 0.579$, $p = 0.007$; Figure 2.10B).

2.3.6.2 Parvalbumin Immunoreactivity is Decreased in Caudal Coordinates of the Nucleus Accumbens Core and Prelimbic Cortex following METH Self-Administration

Analysis of discrete caudal coordinates of the NAc core revealed a significant reduction in PV immunoreactivity following METH IVSA [NAc core +1.7mm: $F(1, 16) = 4.563$, $p = 0.048$; Figure 2.11A], with no differences found in more rostral coordinates [+2.2mm $F(1, 16) = 0.908$, $p = 0.355$; +2.7mm $F(1, 15) = 2.664$, $p = 0.123$]. Interestingly, this trend is also observed

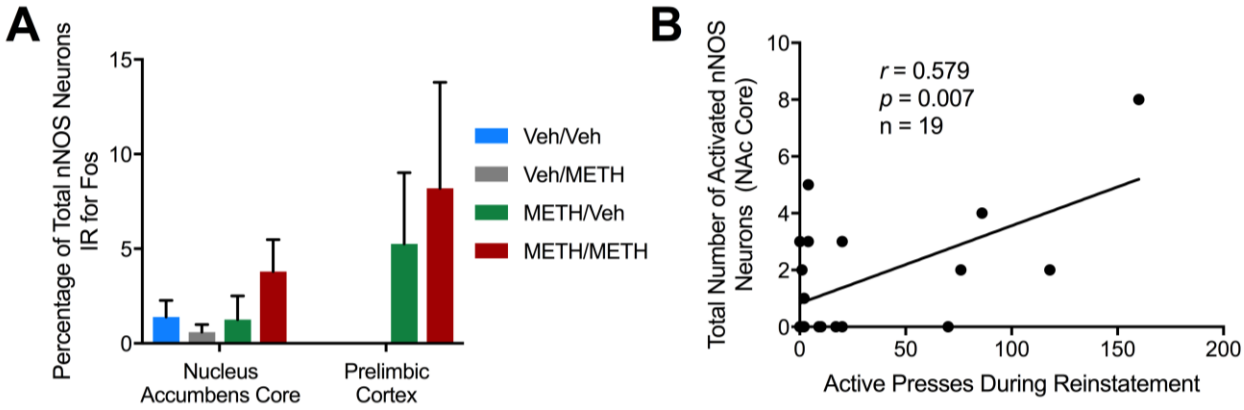

Figure 2.10. Analysis of the proportion of nNOS neurons which were activated revealed increases in METH IVSA animals which trended towards significance (A). There was also a positive correlation, which was statistically significant, between total number of activated nNOS neurons and the number of active presses during reinstatement (B). Data presented as mean + SEM. Data presented as n = 4 in METH/Veh group, n = 5 in all other groups.

in discrete regions of the PrL, where caudal coordinates show a trend towards decreased PV immunoreactivity in METH IVSA groups [+2.7mm: $F(1, 16) = 4.100$, $p = 0.061$; Figure 2.11B], which is not evident in rostral coordinates of the PrL [+3.2mm: $F(1, 16) = 0.358$, $p = 0.558$; +3.7mm: $F(1, 16) = 0.772$, $p = 0.394$]. Analysis of other subregions within the NAc, mPFC and OFC revealed no difference in PV immunoreactivity across treatment groups.

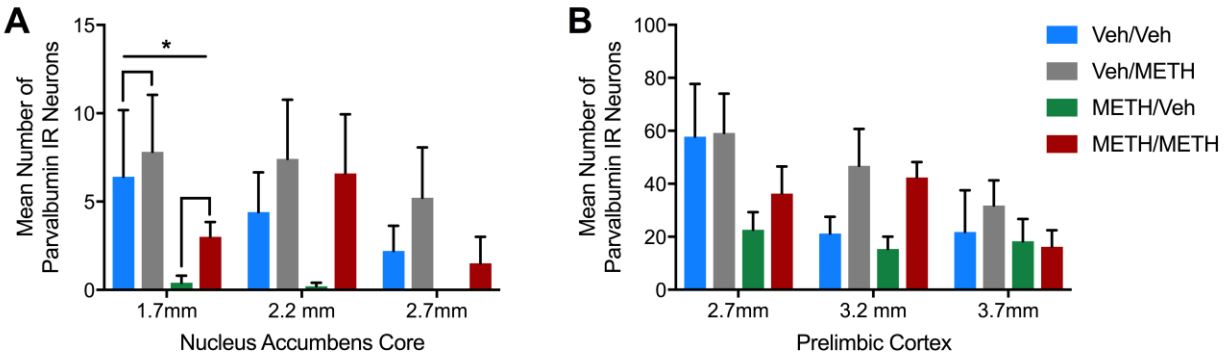

*Figure 2.11. There were significant reductions in parvalbumin immunoreactivity in caudal coordinates of the nucleus accumbens core (A). Caudal coordinates of the prelimbic cortex also trended towards decreased PV immunoreactivity (B), however no differences across groups were observed in rostral coordinates. Data presented as mean + SEM. Coordinates presented are rostral of Bregma. *represent p = 0.048. Data presented as n = 5 per group.*

2.4 Discussion

The aim of this experiment was to investigate if neuronal activation was altered within the mPFC, OFC and NAc following various levels of exposure to METH. Furthermore, measures of neuronal activity were correlated across ROIs, providing an indication of direct or indirect functional connectivity. A secondary aim was to investigate if METH exposure alters the function of GABA systems, particularly nNOS and PV interneurons. Previous published literature suggested GABA systems may be altered following prolonged METH exposure (Veerasakul et al., 2016; Wearne et al., 2015), thus it is possible that changes to neuronal activity

and functional connectivity may be influenced by METH-induced changes to GABA function. It was hypothesised that METH exposure would increase neuronal activity in reward-associated brain regions, leading to decreases in correlated neuronal activity across brain regions. Furthermore, GABA systems, specifically nNOS and PV immunoreactivity, would also be altered within the mPFC, OFC and NAc.

2.4.1 Main Findings

2.4.1.1 Administration of METH Alters the Pattern of Neuronal Activity

Analysis of total regional Fos immunoreactivity revealed increased neuronal activation in the NAc core, NAc shell, Cg1, PrL, LO and MO following METH-priming treatment. These findings align with existing literature demonstrating increased neuronal activation in the NAc and OFC following acute administration of drugs or drug-associated cues (Breiter et al., 1997; Franklin & Druhan, 2000; Kufahl et al., 2005; Miller & Marshall, 2004; Morshedi & Meredith, 2007; Thomas et al., 2003; Volkow et al., 2012). Nevertheless, contradictory evidence is present in the literature with functional magnetic resonance imaging of cocaine-dependent humans revealing decreased blood-oxygenation signals following intravenous cocaine administration (Kufahl et al., 2005). The findings of Kufahl et al. (2005) are consistently refuted, with most evidence suggesting increased activation of the NAc following drug administration (Breiter et al., 1997; Franklin & Druhan, 2000; Scofield et al., 2016).

Furthermore, no changes to neuronal activation were observed in the IL or VO cortices of any treatment group. This finding is surprising, as the IL has previously been implicated in extinction of drug-seeking behaviours; hence increased neuronal activity in the IL may have been

expected in METH/Veh animals. It is possible IL activation may be more pronounced during earlier stages of the extinction period. Moreover, recent findings by Zimmermann, Li, Rainnie, Ressler, and Gourley (2018) have suggested the function of the rodent ventrolateral OFC may be closely linked with the function of the IL.

2.4.1.2 METH-induced Changes to Neuronal Activity are Not Driven by Increased activity of PV or nNOS Neurons

Previous literature has evidenced drug-induced changes to neuronal activation, however it remains unknown which neuronal populations are activated as neuroimaging techniques and expression of immediate early genes, such as *c-Fos*, are limited in their ability to differentiate neuronal populations (Dragunow & Faull, 1989; Van den Oever et al., 2010). The present study investigated colocalisation of Fos with two GABAergic interneuron populations; nNOS and PV. Only a small proportion of the activated neurons were colocalised with either nNOS or PV, suggesting the activated neurons were mostly likely other neuronal populations. It is likely activated neurons are glutamatergic, as previous evidence has suggested exposure to drugs or drug-associated cues increases glutamate-mediated firing in reward-associated brain regions (Cruz, Javier Rubio, & Hope, 2015; Scofield et al., 2016).

Interestingly, the findings from the present study suggest neuronal activity is increased to a greater extent in the NAc core following relapse to METH-seeking when compared with acute administration of METH (Figure 2.5). Scofield et al. (2016) hypothesise that relapse to drug-seeking behaviour, and the resulting increases in NAc core neuronal activity, may be driven by drug-induced plasticity of PrL-NAc core glutamatergic projections. Indeed, evidence suggests

activation of glutamatergic PrL-NAc projections is critical for reinstatement of cocaine seeking (McFarland, Davidge, Lapish, & Kalivas, 2004; McFarland, Lapish, & Kalivas, 2003; Scofield et al., 2016), as inhibition of this pathway has been shown to attenuate reinstatement of drug-seeking behaviour (Cornish & Kalivas, 2000; McFarland et al., 2003; Stefanik et al., 2013). More recently, chemogenetic inhibition of PrL-NAc core projections has been shown to decrease reinstatement of METH-seeking behaviour (Kearns et al., 2018). Whilst the findings of the present study do not directly investigate the role of glutamatergic PrL-NAc core projections in driving relapse, the minimal activation of nNOS and PV interneurons following METH-primed relapse supports the activation of other neuronal types, likely to be glutamatergic efferents, in mediating relapse.

2.4.1.3 METH Exposure Alters Functional Connectivity of Reward Circuits

The analysis of Fos immunoreactivity has revealed critical insights, however the examination of isolated brain regions is of limited utility. Hence, measures of neuronal activity were correlated across subregions of the NAc, mPFC and OFC, allowing interpretation of how reduced correlated neuronal activity could indicate reductions in functional connectivity on a broader circuitry scale. Neuroimaging studies conducted on cocaine and amphetamine addicts have highlighted disrupted functional relationships between mPFC, OFC and NAc (Breiter et al., 1997; Ersche et al., 2005; Goldstein et al., 2007; Koob & Volkow, 2010; Kufahl et al., 2005), however, there is a distinct lack of research examining how METH exposure may alter functional connectivity. In the current study, correlational analysis was performed on each treatment group, allowing changes to correlated activity to be contrasted across acute METH exposure, prolonged exposure and relapse to METH-seeking.

Control animals displayed a large number of statistically significant correlations between IL and PrL, Cg1, LO and MO subregions; yet the IL was not correlated with any other examined region in any METH-exposed groups. This finding is not surprising, as neuroimaging studies conducted on human cocaine addicts have revealed a negatively correlated activity between the IL and OFC and IL and Cg1 (Volkow et al., 2012). A distinct lack of positive or negative correlated activity in the IL following METH exposure suggests that the IL may be differentially affected by cocaine exposure.

Strong correlated activity was observed between the PrL and LO in Veh/Veh, Veh/METH and METH/METH groups. Whilst this might suggest this pathway is acting similarly across treatment groups, when interpreted alongside Fos immunoreactivity data, it is clear the PrL and LO are exhibiting basal levels of activity in the Veh/Veh group, whilst activation is significantly increased in both the Veh/METH and METH/METH groups. Similar trends were observed between the PrL and Cg1. These findings indicate direct or indirect functional connectivity between the PrL and Cg1 and PrL and LO, both of which are activated by METH.

In animals treated with a vehicle prime, neuronal activation in the LO and MO subregions was correlated. Furthermore, in Veh/METH treated animals, neuronal activity was increased but positively correlated in the LO and MO. In contrast, neuronal activity was increased in these regions in METH/METH animals, however there is a lack of correlated activity. This indicates whilst neuronal activity is increased the LO and MO during reinstatement of METH-seeking, this activity is not correlated, indicating a lack of functional connectivity. Under normal conditions, the LO and MO subregions are densely interconnected and are

postulated to work together to determine perceived value and expected outcomes (Lopatina et al., 2017). Recently, Lopatina et al. (2017) used electrophysiology to investigate how neurons within the rodent LO and MO represent information relating to the perceived value of a behavioural task. The authors postulate that the LO utilises contextual information about tasks and behaviours, i.e. behaviour X is required to achieve Y reward, whilst the MO acts to group behavioural tasks by type, using episodic memory to place a perceived value (Lopatina et al., 2017). Hence, it is possible disrupted functional connectivity between the LO and MO may lead to dysfunctional encoding of the value of a behavioural task, consequently causing stimuli, tasks or behaviours to be overvalued. In the context of METH addiction, disrupted functional connectivity between the LO and MO may explain the compulsive drive to seek addictive drugs at the expense of other stimuli or behaviours

2.4.1.4 The Effect of METH Exposure on GABA Systems

Analysis of nNOS immunoreactivity and activation patterns revealed some non-significant effects of METH-exposure, conflicting with previous published literature implicating activation of nNOS interneurons in cocaine-associated behaviours (Nasif, Hu, Ramirez, & Perez, 2011; Sammut & West, 2008; Smith et al., 2017). However, analysis of nNOS immunoreactivity at one discrete coordinate of the PrL did reveal a significant increase in nNOS immunoreactivity following METH self-administration. Additionally, nNOS immunoreactivity in the PrL was also positively correlated with METH-intake. Collectively, these findings suggest METH exposure may induce a subtle effect on nNOS interneurons or that these effects may be discretely localised. Hence, crude analysis of large areas or brain regions may dilute significant effects. Additionally, analysis of a specific coordinate of the NAc core revealed strong positive

correlations between nNOS immunoreactivity and Fos immunoreactivity, and the number of activated nNOS neurons and active presses during reinstatement, both of which were statistically significant. These findings are consistent with the findings of Smith et al. (2017) which demonstrated activation of NAc core nNOS-expressing interneurons following cue-induced reinstatement of cocaine-seeking. When considered together, these findings suggest increased activation of the nitrergic system within the NAc core may contribute to METH-relapse behaviours and/or neurotoxic effects including excessive production of NO, oxidative stress and apoptosis, leading to altered neuronal signaling in this brain region (Berman, O'Neill, Fears, Bartzokis, & London, 2008; Courtney & Ray, 2014; De Vito & Wagner, 1989; Krasnova & Cadet, 2009).

Initially, it was hypothesised that PV interneurons may be altered following exposure to METH, contributing to disruptions to the excitatory/inhibitory balance and aberrant pyramidal cell spiking (Ferguson & Gao, 2018). Whilst drug addiction is characterised by deficits to inhibitory control mechanisms, suggesting reduced functionality of GABA systems, previous literature has revealed drug-induced upregulation of PV expression in the mPFC (Mohila & Onn, 2005; Wearne, Parker, Franklin, Goodchild, & Cornish, 2016); hence, the expected direction of change was unclear as existing literature presents contradictory findings (Veerasakul et al., 2016; Wearne et al., 2016). The results from this study fail to shed light, revealing a non-significant effect of METH IVSA on immunoreactivity or activation of PV interneurons. However, at one specific coordinate in the NAc core (+ 1.7mm from Bregma) there was a statistically significant reduction in PV immunoreactivity in animals that were experienced in METH IVSA, aligning

more closely with the findings of Veerasakul et al. (2016). Further investigation is required to validate changes to PV interneurons following chronic METH intake.

2.4.2 Limitations, Methodological Considerations and Future Directions.

The present study was exploratory in terms of using IVSA methodology to investigate METH-induced changes to correlated neuronal activity across subregions of the NAc and PFC, as neuroadaptations in these key substrates is hypothesized to underlie drug-relapse (Hyman et al., 2006). However, there are many other reward-associated brain regions implicated in the pathogenesis of addiction that were not examined in this study, including the VTA and dorsal striatum. Therefore, the value of this research could be enhanced by incorporating investigation of correlated neuronal activation in additional reward-associated brain regions.

The present study utilised Fos, the protein product of the immediate early gene *c-Fos*, as an inexpensive and rapid readout of functional activity (Dragunow & Faull, 1989; Kovacs, 1998). However, immediate early genes are limited in that they can only provide information about the activity of neuronal circuits 90-120min prior to euthanasia (Dragunow & Faull, 1989; Kovacs, 1998). Fibre photometry, a technique which enables real-time recording of neuronal calcium transients, can be used to quantify neuronal activity in multiple brain regions simultaneously (Kim et al., 2016). In addition, fibre photometry can be performed in behaving animals, meaning recordings can also be obtained over multiple test sessions, facilitating within animal analysis (Kim et al., 2016). Future experiments could adopt fibre photometry to record neuronal activity in brain regions of interest, such as the PrL, Cg1, LO and NAc, following different METH administration regimes. This approach would provide critical temporal

information relating to how connectivity may be changed along the timecourse of repeated METH use, allowing further elucidation of the neurobiological mechanisms driving addiction.

The secondary aim of this study was to examine GABA systems, specifically nNOS and PV immunoreactivity, within each brain ROI. Some trends towards altered nNOS and PV immunoreactivity were noted, however overall minimal differences were found across treatment groups. Any reduction in the total number of GABA-releasing neurons could alter tonic inhibition; additionally, alterations to expression of the PV protein or nNOS enzyme could also impact on functionality (Morshedi & Meredith, 2007; Todtenkopf et al., 2004). The present study did not examine the intensity of cytoplasmic immunofluorescent signals, which could have indicated the relative amount of protein or enzyme expression. Previous published studies examining PV immunoreactivity following exposure to psychostimulants revealed no changes to the total number of neurons, yet found changes to expression of the PV protein (Mohila & Onn, 2005; Morshedi & Meredith, 2007; Todtenkopf et al., 2004; Veerasakul et al., 2016; Wearne et al., 2015; Wearne et al., 2017). Thus, examination of the intensity of immunoreactivity may reveal more significant findings in the future and align more closely with the findings of Veerasakul et al. (2016) and Wearne et al (2015, 2017).

Many factors influence the neurobiological neuroadaptations induced by drug exposure, including the amount of drug consumed, contingency of drug administration and withdrawal influences (Yager, Garcia, Wunsch, & Ferguson, 2015). Therefore, it is plausible that more pronounced effects would be observed following increased METH exposure. Experiments by Schwendt et al. (2009) revealed more pronounced cognitive deficits and increased evidence of

METH-induced neurotoxicity in animals that were provided extended access to METH (6-hour sessions) compared with animals that were provided limited access (2-hour sessions). As the animals in the present study experienced 20 x 3-hour METH IVSA sessions, it is possible extending IVSA sessions or increasing the number of IVSA days may also yield more significant findings.

The brain regions investigated in the current study are highly heterogeneous and express multiple subpopulations of GABAergic interneurons. Here, only nNOS and PV interneurons were investigated due to their functional role in maintaining the excitatory/inhibitory balance and controlling the output of neuronal circuits. It is possible that while the impact of METH exposure was minimal on nNOS and PV interneurons, other GABAergic subpopulations may be more affected. Immunohistochemical approaches enable investigation of a limited number of markers on individual brain sections. Alternatively, more innovative approaches, such as spatially-resolved transcript amplicon readout mapping (STARmap), could be used to investigate all subpopulations of GABAergic interneurons in one tissue specimen (Wang et al., 2018). Recently, Wang et al. (2018) used STARmapping to investigate the functional activity of 15 distinct cell types in the mPFC following an acute cocaine injection. In the future, this approach could be used to investigate the activation of excitatory and inhibitory neuronal subpopulations following acute METH and relapse to METH-seeking behaviours.

In summary, this study presented the first comparison of correlated neuronal activity following acute exposure to METH, prolonged exposure and relapse to METH-seeking. The results indicate exposure to METH may evoke aberrant activity of excitatory neurons,

consequently altering neuronal activity within the mPFC, OFC and NAc. Thus, whilst the present study does not directly investigate the role of glutamatergic PrL-NAc core projections in driving relapse to drug-seeking behaviour, the minimal activation of nNOS and PV interneurons PFC following METH-primed relapse suggests a more prominent role of other neuronal types, such as glutamatergic projection neurons, in mediating relapse (Kearns et al., 2018; McFarland et al., 2004; McFarland et al., 2003; Scofield et al., 2016; Stefanik et al., 2013). The present thesis yields new insights into altered neuronal activity, importantly identifying possible impairment to LO-MO connections in METH-relapse animals. In this instance, the present study failed to shed light on METH-induced changes to PV immunoreactivity, yet some subtle impacts on nNOS immunoreactivity and the nitrergic system within the PrL and NAc core were observed. Further research is required to identify how other GABAergic subpopulations may be affected by METH and if dysfunction of GABA systems is a cause or consequence of altered neuronal activity. It is imperative to continue to enhance knowledge of the neurobiological mechanisms driving METH addiction, as further identification of METH-induced neuroadapatations may lead to the development of more effective pharmacotherapies for METH addiction and associated disorders.

References

Berman, S., O'Neill, J., Fears, S., Bartzokis, G., & London, E. D. (2008). Abuse of amphetamines and structural abnormalities in the brain. *Ann N Y Acad Sci, 1141*, 195-220. doi:10.1196/annals.1441.031

Breiter, H. C., Gollub, R. L., Weisskoff, R. M., Kennedy, D. N., Makris, N., Berke, J. D., . . . Hyman, S. E. (1997). Acute effects of cocaine on human brain activity and emotion. *Neuron, 19*(3), 591-611.

Castilla-Ortega, E., Blanco, E., Serrano, A., Ladron de Guevara-Miranda, D., Pedraz, M., Estivill-Torrus, G., . . . Santin, L. J. (2016). Pharmacological reduction of adult hippocampal neurogenesis modifies functional brain circuits in mice exposed to a cocaine conditioned place preference paradigm. *Addict Biol, 21*(3), 575-588. doi:10.1111/adb.12248

Castilla-Ortega, E., Rosell-Valle, C., Pedraza, C., Rodriguez de Fonseca, F., Estivill-Torrus, G., & Santin, L. J. (2014). Voluntary exercise followed by chronic stress strikingly increases mature adult-born hippocampal neurons and prevents stress-induced deficits in 'what-when-where' memory. *Neurobiol Learn Mem, 109*, 62-73. doi:10.1016/j.nlm.2013.12.001

Cornish, J. L., & Kalivas, P. W. (2000). Glutamate transmission in the nucleus accumbens mediates relapse in cocaine addiction. *J Neurosci, 20*(15), Rc89.

Courtney, K. E., & Ray, L. A. (2014). Methamphetamine: an update on epidemiology, pharmacology, clinical phenomenology and treatment literature. *Drug Alcohol Dependence, 143*, 11-21.

Cruickshank, C. C., & Dyer, K. R. (2009). A review of the clinical pharmacology of methamphetamine. *Addiction, 104*(7), 1085-1099. doi:10.1111/j.1360-0443.2009.02564.x

Cruz, F. C., Javier Rubio, F., & Hope, B. T. (2015). Using c-fos to study neuronal ensembles in corticostriatal circuitry of addiction. *Brain Res, 1628*(Pt A), 157-173. doi:10.1016/j.brainres.2014.11.005

De Vito, M. J., & Wagner, G. C. (1989). Methamphetamine-induced neuronal damage: a possible role for free radicals. *Neuropharmacology, 28*(10), 1145-1150.

Dragunow, M., & Faull, R. (1989). The use of c-fos as a metabolic marker in neuronal pathway tracing. *Journal of Neuroscience Methods, 29*(3), 261-265. doi:https://doi.org/10.1016/0165-0270(89)90150-7

Enwright, J. F., Sanapala, S., Foglio, A., Berry, R., Fish, K. N., & Lewis, D. A. (2016). Reduced Labeling of Parvalbumin Neurons and Perineuronal Nets in the Dorsolateral Prefrontal Cortex of Subjects with Schizophrenia. *Neuropsychopharmacology, 41*(9), 2206-2214. doi:10.1038/npp.2016.24

Ersche, K. D., Fletcher, P. C., Lewis, S. J., Clark, L., Stocks-Gee, G., London, M., . . . Sahakian, B. J. (2005). Abnormal frontal activations related to decision-making in current and former amphetamine and opiate dependent individuals. *Psychopharmacology (Berl), 180*(4), 612-623. doi:10.1007/s00213-005-2205-7

Ferguson, B. R., & Gao, W. J. (2018). PV Interneurons: Critical Regulators of E/I Balance for Prefrontal Cortex-Dependent Behavior and Psychiatric Disorders. *Front Neural Circuits, 12*, 37. doi:10.3389/fncir.2018.00037

Franklin, T. R., & Druhan, J. P. (2000). Expression of Fos-related antigens in the nucleus accumbens and associated regions following exposure to a cocaine-paired environment. *Eur J Neurosci, 12*(6), 2097-2106.

Gabbott, P. L., & Bacon, S. J. (1995). Co-localisation of NADPH diaphorase activity and GABA immunoreactivity in local circuit neurones in the medial prefrontal cortex (mPFC) of the rat. *Brain Res, 699*(2), 321-328.

Garcia, A. F., Nakata, K. G., & Ferguson, S. M. (2017). Viral strategies for targeting cortical circuits that control cocaine-taking and cocaine-seeking in rodents. *Pharmacol Biochem Behav*. doi:10.1016/j.pbb.2017.05.009

Goldstein, R. Z., Tomasi, D., Rajaram, S., Cottone, L. A., Zhang, L., Maloney, T., . . . Volkow, N. D. (2007). Role of the anterior cingulate and medial orbitofrontal cortex in processing drug cues in cocaine addiction. *Neuroscience, 144*(4), 1153-1159. doi:10.1016/j.neuroscience.2006.11.024

Hardingham, N., Dachtler, J., & Fox, K. (2013). The role of nitric oxide in pre-synaptic plasticity and homeostasis. *Frontiers in Cellular Neuroscience, 7*(190). doi:10.3389/fncel.2013.00190

Hsieh, J. H., Stein, D. J., & Howells, F. M. (2014). The neurobiology of methamphetamine induced psychosis. *Frontiers in Human Neuroscience, 8*, 537-548. doi:doi: 10.3389/fnhum.2014.00537

Hyman, S. E., Malenka, R. C., & Nestler, E. J. (2006). Neural mechanisms of addiction: the role of reward-related learning and memory. *Annu Rev Neurosci, 29*, 565-598. doi:10.1146/annurev.neuro.29.051605.113009

Karreman, M., & Moghaddam, B. (1996). The prefrontal cortex regulates the basal release of dopamine in the limbic striatum: an effect mediated by ventral tegmental area. *J Neurochem, 66*(2), 589-598.

Kearns, A., Weber, R. A., Carter, S., Cox, S., Peters, J., & Reichel, C. M. (2018). Inhibition of the prelimbic to nucleus accumbens core pathway decreases methamphetamine cued reinstatement. *Society for Neuroscience*, Washington DC, USA, 3-7 November.

Kim, C. K., Yang, S. J., Pichamoorthy, N., Young, N. P., Kauvar, I., Jennings, J. H., . . . Deisseroth, K. (2016). Simultaneous fast measurement of circuit dynamics at multiple sites across the mammalian brain. *Nat Methods, 13*(4), 325-328. doi:10.1038/nmeth.3770

Koob, G. F., & Volkow, N. D. (2010). Neurocircuitry of Addiction. *Neuropsychopharmacology, 35*(1), 217-238. doi:10.1038/npp.2009.110

Kovacs, K. J. (1998). c-Fos as a transcription factor: a stressful (re)view from a functional map. *Neurochem Int, 33*(4), 287-297.

Krasnova, I. N., & Cadet, J. L. (2009). Methamphetamine toxicity and messengers of death. *Brain Research Reviews, 60*(2), 379-407. doi:https://doi.org/10.1016/j.brainresrev.2009.03.002

Kufahl, P. R., Li, Z., Risinger, R. C., Rainey, C. J., Wu, G., Bloom, A. S., & Li, S. J. (2005). Neural responses to acute cocaine administration in the human brain detected by fMRI. *Neuroimage, 28*(4), 904-914. doi:10.1016/j.neuroimage.2005.06.039

Lewis, D. A., Curley, A. A., Glausier, J. R., & Volk, D. W. (2012). Cortical parvalbumin interneurons and cognitive dysfunction in schizophrenia. *Trends Neurosci, 35*(1), 57-67. doi:10.1016/j.tins.2011.10.004

Lopatina, N., Sadacca, B. F., McDannald, M. A., Styer, C. V., Peterson, J. F., Cheer, J. F., & Schoenbaum, G. (2017). Ensembles in medial and lateral orbitofrontal cortex construct cognitive maps emphasizing different features of the behavioral landscape. *Behav Neurosci, 131*(3), 201-212. doi:10.1037/bne0000195

Lucantonio, F., Stalnaker, T. A., Shaham, Y., Niv, Y., & Schoenbaum, G. (2012). The impact of orbitofrontal dysfunction on cocaine addiction. *Nat Neurosci, 15*(3), 358-366. doi:10.1038/nn.3014

McFarland, K., Davidge, S. B., Lapish, C. C., & Kalivas, P. W. (2004). Limbic and motor circuitry underlying footshock-induced reinstatement of cocaine-seeking behavior. *J Neurosci, 24*(7), 1551-1560. doi:10.1523/jneurosci.4177-03.2004

McFarland, K., Lapish, C. C., & Kalivas, P. W. (2003). Prefrontal glutamate release into the core of the nucleus accumbens mediates cocaine-induced reinstatement of drug-seeking behavior. *J Neurosci, 23*(8), 3531-3537.

Miller, C. A., & Marshall, J. F. (2004). Altered prelimbic cortex output during cue-elicited drug seeking. *J Neurosci, 24*(31), 6889-6897. doi:10.1523/jneurosci.1685-04.2004

Mohila, C. A., & Onn, S. P. (2005). Increases in the density of parvalbumin-immunoreactive neurons in anterior cingulate cortex of amphetamine-withdrawn rats: evidence for corticotropin-releasing factor in sustained elevation. *Cereb Cortex, 15*(3), 262-274. doi:10.1093/cercor/bhh128

Moorman, D. E., James, M. H., McGlinchey, E. M., & Aston-Jones, G. (2015). Differential roles of medial prefrontal subregions in the regulation of drug seeking. *Brain Res, 1628*(Pt A), 130-146. doi:10.1016/j.brainres.2014.12.024

Morley, K. C., Cornish, J. L., Faingold, A., Wood, K., & Haber, P. S. (2017). Pharmacotherapeutic agents in the treatment of methamphetamine dependence. *Expert Opin Investig Drugs, 26*(5), 563-578. doi:10.1080/13543784.2017.1313229

Morshedi, M. M., & Meredith, G. E. (2007). Differential laminar effects of amphetamine on prefrontal parvalbumin interneurons. *Neuroscience, 149*(3), 617-624. doi:10.1016/j.neuroscience.2007.07.047

Nasif, F. J., Hu, X. T., Ramirez, O. A., & Perez, M. F. (2011). Inhibition of neuronal nitric oxide synthase prevents alterations in medial prefrontal cortex excitability induced by repeated cocaine administration. *Psychopharmacology (Berl), 218*(2), 323-330. doi:10.1007/s00213-010-2105-3

Panenka, W. J., Procyshyn, R. M., Lecomte, T., MacEwan, G. W., Flynn, S. W., Honer, W. G., & Barr, A. M. (2013). Methamphetamine use: a comprehensive review of molecular, preclinical and clinical findings. *Drug Alcohol Depend, 129*(3), 167-179. doi:10.1016/j.drugalcdep.2012.11.016

Paxinos, G., & Watson, C. (2007). The Rat Brain in Stereotaxic Coordinates *123Library* (6 ed.): Academic Press.

Qi, J., Han, W., Yang, J., Wang, L., Dong, Y., Wang, F., . . . Wu, C. (2012). Oxytocin regulates changes in extracellular glutamate and GABA levels induced by methamphetamine in the mouse brain. *Addiction Biology, 17*, 758-769.

Ridderinkhof, K. R., van den Wildenberg, W. P., Segalowitz, S. J., & Carter, C. S. (2004). Neurocognitive mechanisms of cognitive control: the role of prefrontal cortex in action selection, response inhibition, performance monitoring, and reward-based learning. *Brain Cogn, 56*(2), 129-140. doi:10.1016/j.bandc.2004.09.016

Sammut, S., & West, A. R. (2008). Acute cocaine administration increases NO efflux in the rat prefrontal cortex via a neuronal NOS-dependent mechanism. *Synapse, 62*(9), 710-713. doi:10.1002/syn.20537

Schindelin, J., Arganda-Carreras, I., Frise, E., Kaynig, V., Longair, M., Pietzsch, T., . . . Cardona, A. (2012). Fiji: an open-source platform for biological-image analysis. *Nature Methods,*

9, 676. doi:10.1038/nmeth.2019 https://www.nature.com/articles/nmeth.2019 - supplementary-information

Schoenbaum, G., Roesch, M. R., & Stalnaker, T. A. (2006). Orbitofrontal cortex, decision-making and drug addiction. *Trends in neurosciences, 29*(2), 116-124. doi:10.1016/j.tins.2005.12.006

Schoenbaum, G., & Shaham, Y. (2008). The role of orbitofrontal cortex in drug addiction: a review of preclinical studies. *Biological Psychiatry, 63*(3), 256-262. doi:10.1016/j.biopsych.2007.06.003

Schwendt, M., Rocha, A., See, R. E., Pacchioni, A. M., McGinty, J. F., & Kalivas, P. W. (2009). Extended methamphetamine self-administration in rats results in a selective reduction of dopamine transporter levels in the prefrontal cortex and dorsal striatum not accompanied by marked monoaminergic depletion. *J Pharmacol Exp Ther, 331*(2), 555-562. doi:10.1124/jpet.109.155770

Scofield, M. D., Heinsbroek, J. A., Gipson, C. D., Kupchik, Y. M., Spencer, S., Smith, A. C., . . . Kalivas, P. W. (2016). The Nucleus Accumbens: Mechanisms of Addiction across Drug Classes Reflect the Importance of Glutamate Homeostasis. *Pharmacol Rev, 68*(3), 816-871. doi:10.1124/pr.116.012484

Siette, J., Westbrook, R. F., Cotman, C., Sidhu, K., Zhu, W., Sachdev, P., & Valenzuela, M. J. (2013). Age-specific effects of voluntary exercise on memory and the older brain. *Biol Psychiatry, 73*(5), 435-442. doi:10.1016/j.biopsych.2012.05.034

Smith, A. C. W., Scofield, M. D., Heinsbroek, J. A., Gipson, C. D., Neuhofer, D., Roberts-Wolfe, D. J., . . . Kalivas, P. W. (2017). Accumbens nNOS Interneurons Regulate Cocaine Relapse. *The Journal of Neuroscience, 37*(4), 742-756. doi:10.1523/JNEUROSCI.2673-16.2016

Smith, R. J., & Laiks, L. S. (2018). Behavioral and neural mechanisms underlying habitual and compulsive drug seeking. *Prog Neuropsychopharmacol Biol Psychiatry, 87*(Pt A), 11-21. doi:10.1016/j.pnpbp.2017.09.003

Stefanik, M. T., Moussawi, K., Kupchik, Y. M., Smith, K. C., Miller, R. L., Huff, M. L., . . . LaLumiere, R. T. (2013). Optogenetic inhibition of cocaine seeking in rats. *Addict Biol, 18*(1), 50-53. doi:10.1111/j.1369-1600.2012.00479.x

Storey, J. D. (2002). A Direct Approach to False Discovery Rates. *Journal of the Royal Statistical Society. Series B (Statistical Methodology), 64*(3), 479-498.

Thomas, K. L., Arroyo, M., & Everitt, B. J. (2003). Induction of the learning and plasticity-associated gene Zif268 following exposure to a discrete cocaine-associated stimulus. *Eur J Neurosci, 17*(9), 1964-1972.

Todtenkopf, M. S., Stellar, J. R., Williams, E. A., & Zahm, D. S. (2004). Differential distribution of parvalbumin immunoreactive neurons in the striatum of cocaine sensitized rats. *Neuroscience, 127*(1), 35-42. doi:10.1016/j.neuroscience.2004.04.054

Tremblay, R., Lee, S., & Rudy, B. (2016). GABAergic Interneurons in the Neocortex: From Cellular Properties to Circuits. *Neuron, 91*(2), 260-292. doi:10.1016/j.neuron.2016.06.033

Van den Oever, M. C., Spijker, S., Smit, A. B., & De Vries, T. J. (2010). Prefrontal cortex plasticity mechanisms in drug seeking and relapse. *Neuroscience & Biobehavioral Reviews, 35*(2), 276-284. doi:https://doi.org/10.1016/j.neubiorev.2009.11.016

Veerasakul, S., Thanoi, S., Reynolds, G. P., & Nudmamud-Thanoi, S. (2016). Effect of Methamphetamine Exposure on Expression of Calcium Binding Proteins in Rat Frontal

Cortex and Hippocampus. *Neurotox Res, 30*(3), 427-433. doi:10.1007/s12640-016-9628-2

Volkow, N. D., & Fowler, J. S. (2000). Addiction, a disease of compulsion and drive: involvement of the orbitofrontal cortex. *Cereb Cortex, 10*(3), 318-325.

Volkow, N. D., Wang, G.-J., Fowler, J. S., & Tomasi, D. (2012). Addiction Circuitry in the Human Brain. *Annual review of pharmacology and toxicology, 52*, 321-336. doi:10.1146/annurev-pharmtox-010611-134625

Wang, X., Allen, W. E., Wright, M. A., Sylwestrak, E. L., Samusik, N., Vesuna, S., . . . Deisseroth, K. (2018). Three-dimensional intact-tissue sequencing of single-cell transcriptional states. *Science*. doi:10.1126/science.aat5691

Wearne, T. A., Mirzaei, M., Franklin, J. L., Goodchild, A. K., Haynes, P. A., & Cornish, J. L. (2015). Methamphetamine-Induced Sensitization Is Associated with Alterations to the Proteome of the Prefrontal Cortex: Implications for the Maintenance of Psychotic Disorders. *Journal of Proteome Research, 14*(1), 397-410. doi:10.1021/pr500719f

Wearne, T. A., Parker, L. M., Franklin, J. L., Goodchild, A. K., & Cornish, J. L. (2016). GABAergic mRNA expression is differentially expressed across the prelimbic and orbitofrontal cortices of rats sensitized to methamphetamine: Relevance to psychosis. *Neuropharmacology, 111*, 107-118. doi:https://doi.org/10.1016/j.neuropharm.2016.08.038

Wearne, T. A., Parker, L. M., Franklin, J. L., Goodchild, A. K., & Cornish, J. L. (2017). Behavioral sensitization to methamphetamine induces specific interneuronal mRNA pathology across the prelimbic and orbitofrontal cortices. *Progress in Neuro-Psychopharmacology and Biological Psychiatry, 77*, 42-48. doi:https://doi.org/10.1016/j.pnpbp.2017.03.018

Yager, L. M., Garcia, A. F., Wunsch, A. M., & Ferguson, S. M. (2015). The ins and outs of the striatum: role in drug addiction. *Neuroscience, 301*, 529-541. doi:10.1016/j.neuroscience.2015.06.033

Yan, Y., Nitta, A., Mizoguchi, H., Yamada, K., & Nabeshima, T. (2006). Relapse of methamphetamine-seeking behavior in C57BL/6J mice demonstrated by a reinstatement procedure involving intravenous self-administration. *Behav Brain Res, 168*(1), 137-143. doi:https://doi.org/10.1016/j.bbr.2005.11.030

Zimmermann, K. S., Li, C. C., Rainnie, D. G., Ressler, K. J., & Gourley, S. L. (2018). Memory Retention Involves the Ventrolateral Orbitofrontal Cortex: Comparison with the Basolateral Amygdala. *Neuropsychopharmacology, 43*(2), 373-383. doi:10.1038/npp.2017.139

Chapter 3: Is Systemic Oxytocin Acting via GABAergic Neurons in the Prelimbic Cortex to Attenuate Methamphetamine-Relapse Behaviours?

3.1 Introduction

Administration of methamphetamine (METH), a powerful psychostimulant, acts to increase dopaminergic and glutamatergic signaling in substrates involved in reward and addiction (Courtney & Ray, 2014; Cruickshank & Dyer, 2009; Goldstein & Volkow, 2011; Panenka et al., 2013). Current treatment strategies aim to reduce the rewarding and reinforcing effects of the drug (Everitt & Robbins, 2005; Robinson & Berridge, 1993), but fail to act on the neuroadaptations that underlie addiction (Everitt, Giuliano, & Belin, 2018). Hence, pharmacotherapies that target METH-induced increases in neurotransmission may be more effective than currently available treatments.

Experiments conducted by Rocha and Kalivas (2010) revealed bilateral microinjection of GABA agonists muscimol and baclofen into the prelimbic cortex (PrL) or nucleus accumbens (NAc) core abolished cue-induced and METH-primed reinstatement. Additionally, optogenetic inhibition of the PrL reduced reinstatement in animals that frequently and compulsively self-administered cocaine (Martín-García et al., 2014). Whilst these findings suggest transient inhibition of the PrL may be effective in reducing relapse (Martín-García et al., 2014; Rocha & Kalivas, 2010), this approach does not act on drug-induced neuroadaptations or restore the excitatory/inhibitory balance within the brain. Therefore, it may be more beneficial to develop a pharmacotherapy that acts to increase GABAergic activity in a more selective manner, such as increasing the activity of GABA-releasing neurons or through specific activation of GABA receptor subtypes.

The endogenous neuropeptide oxytocin is postulated to modulate neurotransmitter release within the brain and has evidenced promising therapeutic potential in preclinical models of

METH addiction (Baracz, Everett, & Cornish, 2015; Baracz, Everett, McGregor, & Cornish, 2014; Bowen et al., 2015; Cox, Young, See, & Reichel, 2013; Everett, McGregor, Baracz, & Cornish, 2018; Hicks, Cornish, Baracz, Suraev, & McGregor, 2016; Sarnyai & Kovacs, 1994) Microdialysis experiments conducted by Qi et al. (2012) indicate whilst systemic (intracerebroventricular) administration of oxytocin had no effect on basal concentrations of glutamate, oxytocin acted to increase basal levels of GABA in the mPFC. Furthermore, co-administration of oxytocin with METH demonstrated significant attenuation of METH-induced increases in glutamate in the mPFC, whilst simultaneously increasing extracellular levels of GABA. This suggests oxytocin may interact with GABA systems to reduce METH-induced glutamate release.

There is a distinct lack of literature examining the interaction between oxytocin and GABA in models of addiction, however GABA-oxytocin interactions have been thoroughly investigated in neuropsychological disorders, including anxiety (Sabihi, Dong, Maurer, Post, & Leuner, 2017; Sabihi, Durosko, Dong, & Leuner, 2014) and autism spectrum disorder (Ninan, 2011; Owen et al., 2013). Recently, Owen et al. (2013) demonstrated decreased pyramidal cell firing, increased activity of PV interneurons and increased inhibitory tone in the hippocampus following administration with an oxytocin receptor (OTR) agonist. Owen et al. (2013) provide the first mechanistic explanation of how oxytocin may be interacting with GABA systems, hypothesising oxytocin can restore the excitatory/inhibitory balance by increasing the activity of GABAergic neurons. Furthermore, experiments by Sabihi et al. (2017) revealed increased activation of GABAergic neurons following direct administration of oxytocin into the PrL, but not the Cg1 or IL, which was dependent upon access to OTRs and $GABA_A$ receptors ($GABA_A$Rs). Accompanying this oxytocin-induced increase to local GABA activity, there was a

decrease in anxiety-like behavior, and a decrease in neuronal activity in the basolateral amygdala, a downstream target from PrL glutamatergic neurons. These findings suggest that oxytocin is acting specifically within the PrL to increase GABAergic activity, which reduced anxiety-induced glutamate output (Sabihi et al., 2017). In the context of METH abuse, it is plausible that oxytocin may activate GABAergic neurons within the PrL, facilitating enhanced control over pyramidal cells and consequently reducing glutamatergic output in downstream brain regions.

The current study utilised DREADD technology in a genetically modified GAD-Cre rat to investigate the interaction between systemic oxytocin and GABAergic neurons within the PrL. DREADDs were used to chemogenetically inactivate GABAergic neurons prior to systemic oxytocin treatment, during cue-induced and METH-primed reinstatement. First, it was hypothesised that systemic oxytocin treatment will attenuate reinstatement of METH-seeking behaviours in both DREADD-expressing and control rats. Additionally, CNO administration will inactivate PrL GABAergic neurons in DREADD-expressing, but not control rats, reducing the inhibitory effects of systemic oxytocin treatment.

3.2 Materials and Methods

3.2.1 Animals

All experimental procedures were conducted in accordance with the Australian Code of Practice for the Care and Use of Animals for Scientific Purposes (8th Edition, 2013) and were approved by the Macquarie University Animal Ethics Committee (Animal Research Authority: 2017/043; Appendix 2).

In order to selectively manipulate the activity of GABAergic neurons in the PrL, a transgenic GAD-Cre rat was utilised (LE-Tg (Gad1-iCre) 3Ottc). This transgenic model expresses the enzyme Cre recombinase (Cre) under a glutamate decarboxylase (GAD1) promoter, meaning Cre is expressed in place of the GAD67 protein, which is normally encoded by the GAD1 gene (Sharpe et al., 2017). Twelve male GAD-Cre rats (weighing 250-350g upon arrival) were obtained from the Australian Resources Centre (Perth, WA). Rats were pair or group-housed (cage size: 40 x 27 x 16cm for pair housing, 64 x 20 x 40cm for group housing) for the entirety of the experiment excluding two days of individual housing post-surgery. Red Perspex tunnels, wooden blocks, straws, sunflower seeds and shredded paper were provided in home cages for environmental enrichment.

Rats were maintained in a temperature and light-controlled room (21 $\pm$ 1^{o} C, 12-hour light/dark cycle) and all experiments were conducted during the light cycle. Food and water were available *ad libitum* in home cages and not during experimental sessions. Rats were acclimated to the facility for seven days and were handled daily by the experimenter for an additional three days prior to surgery.

3.2.2 Drugs

Methamphetamine hydrochloride (METH, 99% purity) powder was purchased and prepared as previously described (Chapter 2.2.4). Animals were administered 0.1mg/kg of METH (IV) per infusion for intravenous self-administration (IVSA) experiments and 1mg/kg (IP) for reinstatement experiments. Clozapine-N-oxide (CNO) was purchased from HelloBio (Bristol, United Kingdom) and was dissolved in 0.9% isotonic saline and administered at a dose

of 3mg/kg (IP) for chemogenetic inactivation experiments. Oxytocin was synthesised by China Peptides (Jiangsu, China) and was dissolved in 0.9% isotonic saline at a dose of 1mg/kg (IP).

3.2.3 Viral Vectors

An adeno-associated virus serotype 2 vector containing a double-floxed inverted open reading frame (DIO) sequence for mCherry fused to hM4Di (AAV2-hSyn-DIO-hM4D(Gi)-mCherry, titre 4.6 x 10^{12}, Addgene catalogue #44362) was microinjected into animals randomly assigned to the experimental group (n = 8). An adeno-associated virus serotype 1 vector containing a FLEX (FLip and EXcise) approach to express tdTomato in the cytoplasm and EGFP in presynaptic terminals (AAV1-phSyn(1)-FLEX-tdTomato -T2A-SypEGFP-WPRE, titre 1.12 x 10^{12}, custom vector supplied by Salk Vector Core) was used as a control virus (n = 4). Viral vectors were previously validated in a pilot cohort of Cre^{+} (n = 4) and Cre^{-} rats (n = 2), where immunohistochemistry was previously used to demonstrate hyperpolarization of DREADD-transfected neurons following administration of CNO (3mg/kg, IP; Appendix 7). Both viral vectors are Cre-dependent and are therefore exclusively expressed in GABAergic neurons when injected into transgenic GAD-Cre rats. Six weeks were allowed between viral microinjection and administration of the DREADD activator CNO for reinstatement testing, providing sufficient time for viral transfection.

3.2.4 Surgeries

Rats were anaesthetised with 3% isoflurane in oxygen (2L/min) as previously outlined (Chapter 2.2.2). Once anaesthetised, the head, upper back and neck was shaved and the skin was cleaned three times with betadine solution and three times with 70% ethanol. Animals were

treated with carprofen (5mg/kg/, SC) for analgesia and 0.9% saline (2mL, SC) to ensure hydration.

Rats were then positioned in a stereotaxic frame (Kopf Instruments, CA, USA) in the skull flat position with incisors resting on a nose bar adjusted to 3.3mm below the ear bars in preparation for bilateral viral microinjection into the PrL. The depth of anaesthesia and breathing rate was routinely monitored throughout the surgery. A midline incision was made on the skull and a hole was drilled through the bone above the prelimbic area. The dura was pierced using a 26G needle. The Rat Brain Atlas (Paxinos & Watson, 2007) was used to obtain coordinates for the PrL (AP: + 3.2mm, ML: $\pm$ 0.7mm and DV: -3.3mm relative to Bregma). A glass pipette (approximately 5μm diameter) attached to polyethylene tubing and a 1mL syringe for pressure injection was slowly lowered into the brain above the coordinates using a micromanipulator (Narishige, Japan). As the PrL extends substantially on the dorsal-ventral axis, virus was delivered at two different ventral levels relative to Bregma. First, approximately 100nL was microinjected at a ventral depth of -3.5mm, then 250nL was injected at -3.3mm, for a total of 350nL. Viral injections were delivered over a 5-10 minute period and the glass pipette was left in position for a further 5-10 minutes. Following injection, the glass pipette was slowly removed from the brain, returned to Bregma and the injection processes was repeated on the contralateral side. The skull wound was closed using stainless steel surgical staples and anointed with betadine. Immediately following viral microinjection, animals underwent implantation of a chronic indwelling catheter into the right jugular vein (as described in Chapter 2.2.2). Following surgery, rats were placed into a heated recovery chamber (27^{o} C) for 45 minutes and monitored until ambulatory.

3.2.5 Post-Operative Care

For the first two days post-surgery, rats were treated with cephazolin sodium (IV) and carprofen (SC) as previously described (2.2.3). Rats were allowed to recover for at least five days prior to commencing IVSA training and catheters were flushed daily with cephazolin sodium in heparinised saline to maintain catheter patency. The post-operative weight and behaviour of the animal were monitored and recorded daily during this period.

3.2.6 Self-Administration Apparatus

Behavioural testing was conducted in twelve standard operant response chambers (as described in Chapter 2.2.5). Active and inactive lever presses, number of drug infusions and locomotor activity was recorded using MED-PC software (Med Associates, St Albans, VT, USA).

3.2.7 Self-Administration Paradigm

Rats underwent experimentation as one cohort (Figure 3.1).

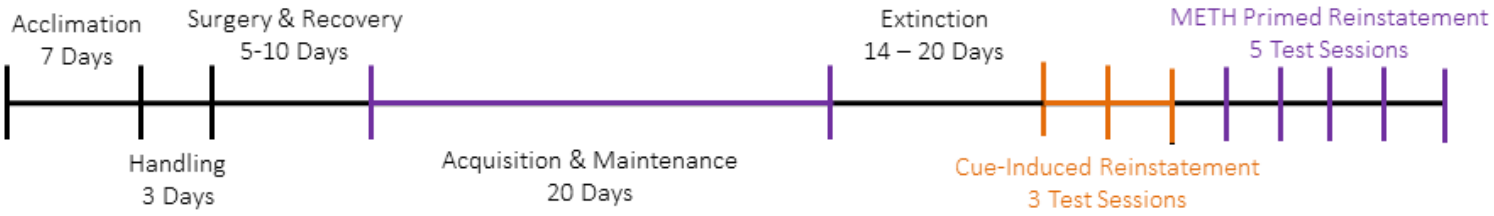

Figure 3.1. Schematic diagram depicting the experimental timeline and order of reinstatement testing.

3.2.7.1 Acquisition and Maintenance of METH Self-administration

Acquisition of self-administration was undertaken for a total of 20 days. Rats were allowed to acquire self-administration of METH during 3-hour fixed ratio 1 (FR1) schedule sessions conducted seven days a week. Levers were allocated as active or inactive, where the location of active lever was counterbalanced across chambers and experimental groups. The

number of lever presses, infusions and locomotor activity was recorded during each session using MED-PC software (Med Associates, St Albans, VT, USA).

Prior to the commencement of each IVSA session, infusion lines were flushed 70% ethanol followed by METH solution. Catheters were flushed with 0.1mL of heparinised saline (10IU/mL) and infusion line tubing was threaded onto the back mount (Bioscientific, Kirawee, NSW) located on the animal's back. Rats were then placed inside the operant chamber. Lever extension and house light illumination indicated the initiation of the session. Depression of the active lever resulted in consequences such drug infusion, elimination of the house light and illumination of the cue light as previously described (Chapter 2.2.6.1). Depression of the inactive leaver had no consequences.

To avoid drug overdose, rats were limited to a maximum of 100 infusions per session (10mg/kg). The session ended when 180 minutes had elapsed or the rat had received the maximum number of infusions. Completion of the session was indicated via retraction of the levers and elimination of the house light. At the end of the session, rats were disconnected from infusion lines and catheters were flushed with 0.2mL of heparinised cephazolin sodium solution.

3.2.7.2 Extinction of METH Self-administration

Following 20 days of IVSA, rats were exposed to daily extinction sessions. Extinction sessions were gradually shortened from 180 minutes to 60 minutes in length (duration: 180mins days 1-3, 150min day 4, 120min day 5 – 6, 90min day 7, 60min days 8 – 20). Rats underwent 14-20 days of extinction training and were deemed to have met extinction criteria if responding on the drug-paired lever was reduced (< 12 active presses) and not significantly different to responding on the

inactive lever. All programmed consequences of active lever depression, such as illumination of the cue light, extinction of the house light and drug infusion, were removed to allow separation of cue-induced reinstatement from drug-primed reinstatement. On the final day of extinction, rats were administered 1mL/kg of vehicle IP to habituate to drug injections during reinstatement.

3.2.7.3 Reinstatement of METH Self-administration

A total of eight reinstatement sessions were conducted, each separated by a minimum of two extinction days (72 hours) to ensure the reinstated lever pressing had re-extinguished, and that the behavioural effects of the preceding drug administration had dissipated. All rats were required to meet extinction criteria (<12 active presses) before each reinstatement test.

METH-seeking behaviour was examined after exposure to drug-associated cues or a non-contingent injection of METH. During reinstatement testing, rats received 2-3 IP pre-treatments depending on the relapse condition (Table 3.1). As cue-induced responding diminishes with repeated exposure, cue-induced testing was limited to three reinstatement sessions, with pretreatment with CNO/vehicle acting as the control for the CNO/oxytocin and vehicle/oxytocin conditions. The inclusion of DREADD-free animals acted as the control for non-specific effects of CNO administration. Animals underwent four counterbalanced METH-primed reinstatement test sessions, and a final METH-primed reinstatement test to determine if responding had gradually declined following repeated reinstatement testing.

During cue-induced reinstatement, depression of the active lever resulted in 3-second illumination of a cue light located directly above the active lever. During this time, the house

Table 3.1

Experiment 2 treatment schedule (IP administration).

Reinstatement Test	IP Pretreatment 1 (-40 minutes)	IP Pretreatment 2 (-20 minutes)	Prime (0 minutes)
1	Vehicle	Oxytocin	Drug-associated Cue
2	CNO	Vehicle	Drug-associated Cue
3	CNO	Oxytocin	Drug-associated Cue
4	Vehicle	Vehicle	METH
5	Vehicle	Oxytocin	METH
6	CNO	Vehicle	METH
7	CNO	Oxytocin	METH
8	Vehicle	Vehicle	METH

light was also turned off for 3 seconds then illuminated signaling drug availability however no drug infusion was delivered. One non-contingent cue exposure was delivered at 30-seconds into the session. The 20-second time out period was not implemented during cue-induced reinstatement testing. Depression of the inactive lever was recorded but had no consequences. During METH-primed reinstatement, parameters were identical to extinction sessions. Across each form of reinstatement testing, treatments were counterbalanced across animals in order to prevent the possibility of treatment order effects. Each pre-treatment incurred a unique pretreatment time before the rat was placed in the IVSA chamber (CNO or vehicle = 40 minutes prior; oxytocin or vehicle = 20 minutes prior; METH = immediately placed in chamber). Any animals that did not reinstate to METH-seeking behaviour under vehicle/vehicle conditions were excluded from the final analyses (> 12 active lever presses).

3.2.8 Euthanasia and Histology

Upon the completion of reinstatement testing, rats were heavily anaesthetised with sodium pentobarbitone (135mg/mL, IP) and perfused with DMEM and 4% PFA. Brains were

harvested, post-fixed and cryopreserved as previously described (Chapter 2.2.7). The PFC was coronally sectioned used a vibratome (1:5 serial 40μm sections) and immunohistochemistry was used to determine if DREADD expression was localised with GAD67 immunoreactivity (antibody details are provided in Appendix 4; immunohistochemistry protocol provided in Appendix 5).

PFC sections were initially imaged under epifluorescence (Zeiss AxioImager Z2 microscope 10x/0.30M27 objective lens running ZEN 2011) at consistent exposure times. This enabled identification of regional spread of viral transfection. Tiled images of each coronal section were captured using Zen Blue image acquisition software (Zeiss, Gottingen, Germany). Confocal microscopy was used to image random samples of DREADD expression (n = 3 per animal). Images were obtained using a Zeiss LSM-880 confocal microscope (Plan-Apochromat 63x/1.5 oil DIC M27 objective) running Zen Black software (Zeiss, Gottingen, Germany). In order to visualize GAD67 immunoreactivity, an argon laser was used (3% laser power, detector gain: 750). In order to visualize mCherry expression, a DPSS561 laser was used (laser power 0.18-0.50%, detector gain: 750). Images were processed using Airyscan mode in an identical manner.

3.2.9 Statistical Analysis

To ensure rats had acquired METH self-administration, the number of drug infusions, active and inactive lever presses and locomotor activity counts were compared using a repeated measures ANOVA, with the first day of acquisition and final day of IVSA directly compared. In order to ensure rats had acquired a preference for the drug-paired lever, the number of active and inactive lever presses on the final day of IVSA was compared using a paired t-test.

In order to determine if the preference for the drug-paired lever had been extinguished, the mean number of active and inactive lever presses was compared to the final three days of IVSA with the final three days of extinction using a paired t-test. Paired t-tests were used to compare METH consumption (mg/kg), active lever presses during IVSA and active lever during extinction across DREADD-expressing and control animals.

Cue-induced reinstatement data was analysed using a 2x3 repeated measures ANOVA. The between subjects factor was virus (DREADD-expressing or control), whilst the within subjects factor was pretreatment (three levels - 1 x pretreatment combination per cue-induced reinstatement test; CNO/vehicle, vehicle/oxytocin and CNO/oxytocin). METH-primed reinstatement data was collected using a 3-factor repeated measures ANOVA (2x2x2 design) containing one between-subjects factor (DREADD-expressing or control) and two within-subjects factors; CNO treatment (CNO or vehicle) and oxytocin treatment (oxytocin or vehicle).

Main effects and interaction effects were examined. In order to address the main hypothesis, CNO/oxytocin pretreatment was directly contrasted with vehicle/oxytocin and CNO/vehicle pretreatment in DREADD-expressing animals. All contrasts were considered *a priori*. Pearson's correlation coefficient was used to correlate DREADD transfection area (μm^2) with behaviour following CNO/oxytocin treatment; this correlation enables investigation of a relationship between higher transfection efficiency and reduced efficacy of oxytocin. All statistical analyses were performed using SPSS Version 20 (SPSS Incorporated, Chicago, IL, USA). Data are presented as mean ± SEM. Differences were considered significant when $p < 0.05$. Bonferroni corrections were used to correct for multiple comparisons.

3.3 Results

3.3.1 Excluded Animals

Upon histological analysis, one animal was removed due to off-target DREADD-expression and a second animal failed to yield any DREADD expression. As a result, the data from the animal with no DREADD-expression was placed into the DREADD-free control group for statistical analyses.

3.3.2 METH Self-Administration

All rats acquired METH IVSA, as evidenced by significant increases in the number of delivered drug infusions over a 20-day period ($F(1, 19) = 1.714$, $p = 0.037$; Figure 3.2A). Due to the rapid acquisition of drug-paired responding, the number of active lever presses did not significantly differ from Day 1 to Day 20 ($F(1, 19) = 0.793$, $p = 0.714$), nor did the number of inactive lever presses ($F(1, 19) = 1.358$, $p = 0.152$; Figure 3.2B). However, on the final day of METH self-administration, the number of responses on the active lever was significantly increased compared to the inactive lever ($t\ (11) = 6.242$, $p = 0.000$; Figure 3.2C), indicating rats had acquired a preference for the drug-paired lever. Locomotor activity also steadily increased ($F(1, 19) = 1.725$, $p = 0.035$; Figure 3.2D).

Importantly, there were no significant differences in METH intake ($t(4) = -2.150$; $p = 0.098$; Figure 3.3A), active lever presses during the final three days of METH self-administration ($t(4) = -0.868$; $p = 0.434$; Figure 3.3B) or active lever presses during the final three days of extinction ($t(4) = -2.271$; $p = 0.086$; Figure 3.3C) between groups. This suggests both groups of animals were equally likely to reinstate to METH-seeking behaviour.

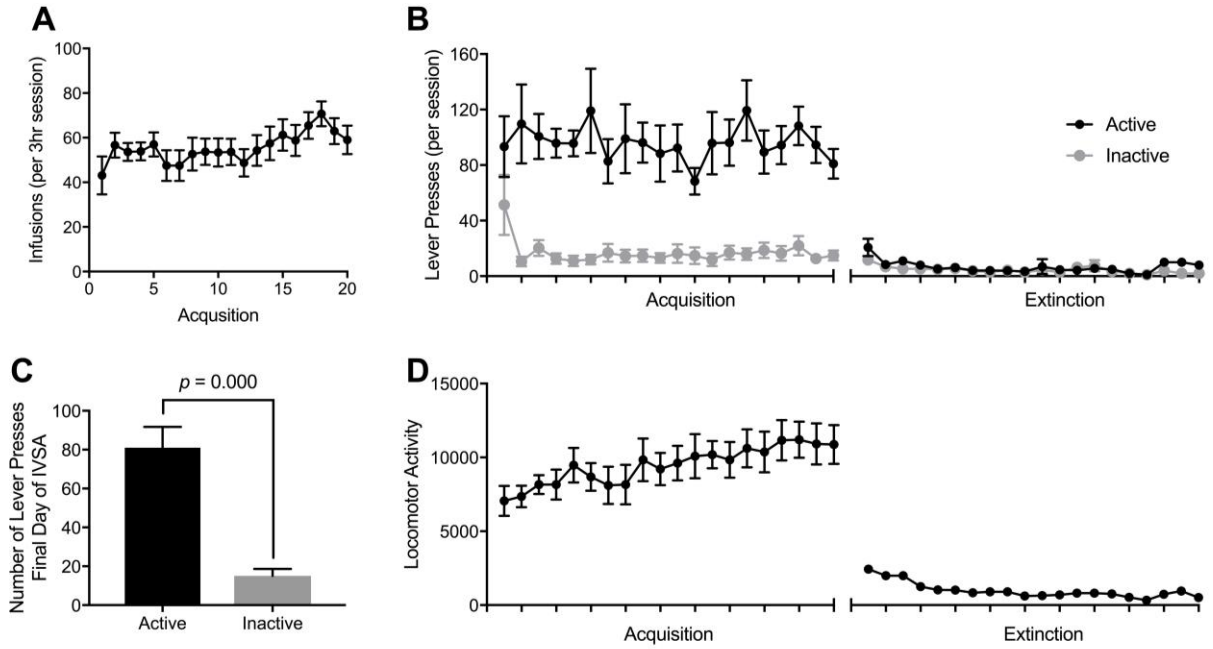

Figure 3.2. Mean (+ SEM) number of infusions (A), lever presses (B), lever presses on the final day of IVSA and locomotor activity counts (D). Data from one animal (control group) was removed from acquisition graphs for the purpose of clarity (lever pressing > 2 SD away from the cohort mean).Data displayed from n = 11 animals.

3.3.3 Behavioural Extinction

The number of active lever presses during the final three days of extinction was significantly reduced when compared to the final three days of IVSA (t (11) = -3.115 ; p = 0.010). A reduction in locomotor activity was also observed from the final day of self-administration to the final day of extinction (t (11) = 7.886; p = 0.000). Animals continued on extinction training until there was a non-significant difference in responding on the active and inactive lever (t (11) = 0.000; p = 1.000); suggesting preference for the drug-paired lever had been extinguished.

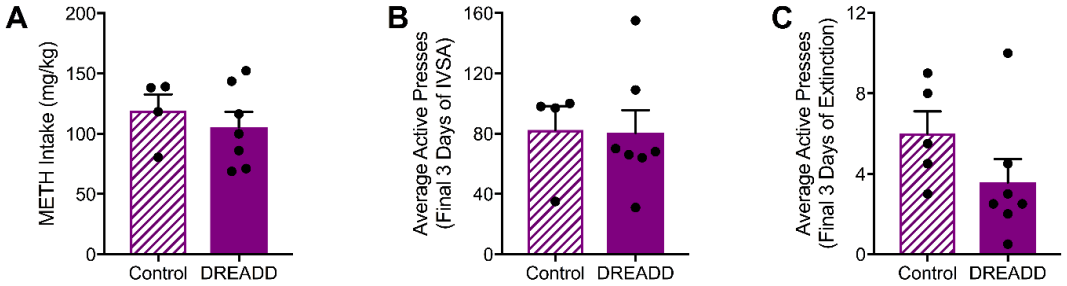

Figure 3.3. There were no significant differences in total METH intake (A), the number of active presses during IVSA (B) or the number of active presses during extinction (C) across groups. All data is presented as mean + SEM, with each dot representing one experimental animal.

3.3.4 Reinstatement of Drug-seeking Behaviour

3.3.4.1 Cue-Induced Reinstatement

Re-exposure to drug-associated cue lights elicited increased active lever pressing following pretreatment with CNO/vehicle, which was statistically significant when compared to the extinction day prior (t (9) = -2.991; p = 0.015). Overall, there was a significant main effect of pretreatment on cue-induced active lever pressing [F (2, 16) = 12.347, p = 0.001] and locomotor activity [F (2, 16) = 4.050, p = 0.038], but not inactive lever presses [F (1, 10) = 0.92, p = 0.768]. Further analysis of pretreatment effects across both virus groups revealed that compared with CNO/vehicle control treatment, active lever pressing was significantly attenuated following vehicle/oxytocin pretreatment [F (2, 16) = 17.565, p = 0.003] and CNO/oxytocin pretreatment [F (2, 16) = 10.225, p = 0.013; Figure 3.4A]. This trend was also observed in locomotor behaviour, with significant attenuation of cue-induced locomotor activity following vehicle/oxytocin pretreatment [F (2, 16) = 6.098, p = 0.039] and CNO/oxytocin pretreatment [F (2, 16) = 4.950, p = 0.057; Figure 3.4B], when compared to CNO/vehicle control pretreatment. There were no significant interactions of virus x pre-treatment for active lever pressing [F (2, 16) = 2.709, p = 0.097] or locomotor activity [F (2, 16) = 0.015, p = 0.984]. Analysis within DREADD-expressing animals revealed no statistically significant differences in reinstatement behaviours when CNO/oxytocin pretreatment was compared with CNO/vehicle [Actives: t (5) = 2.446; p = 0.058; Locomotor: t (5) = 2.083; p = 0.092] and vehicle/oxytocin pretreatment [Actives: t (5) = 0.323; p = 0.759; Locomotor: t (5) = 0.177; p = 0.866].

3.3.4.2 METH-Primed Reinstatement

Administration of a non-contingent METH-prime, under vehicle/vehicle conditions, produced statistically significant increases in active lever pressing (t(10) = -4.657, p =0.001)

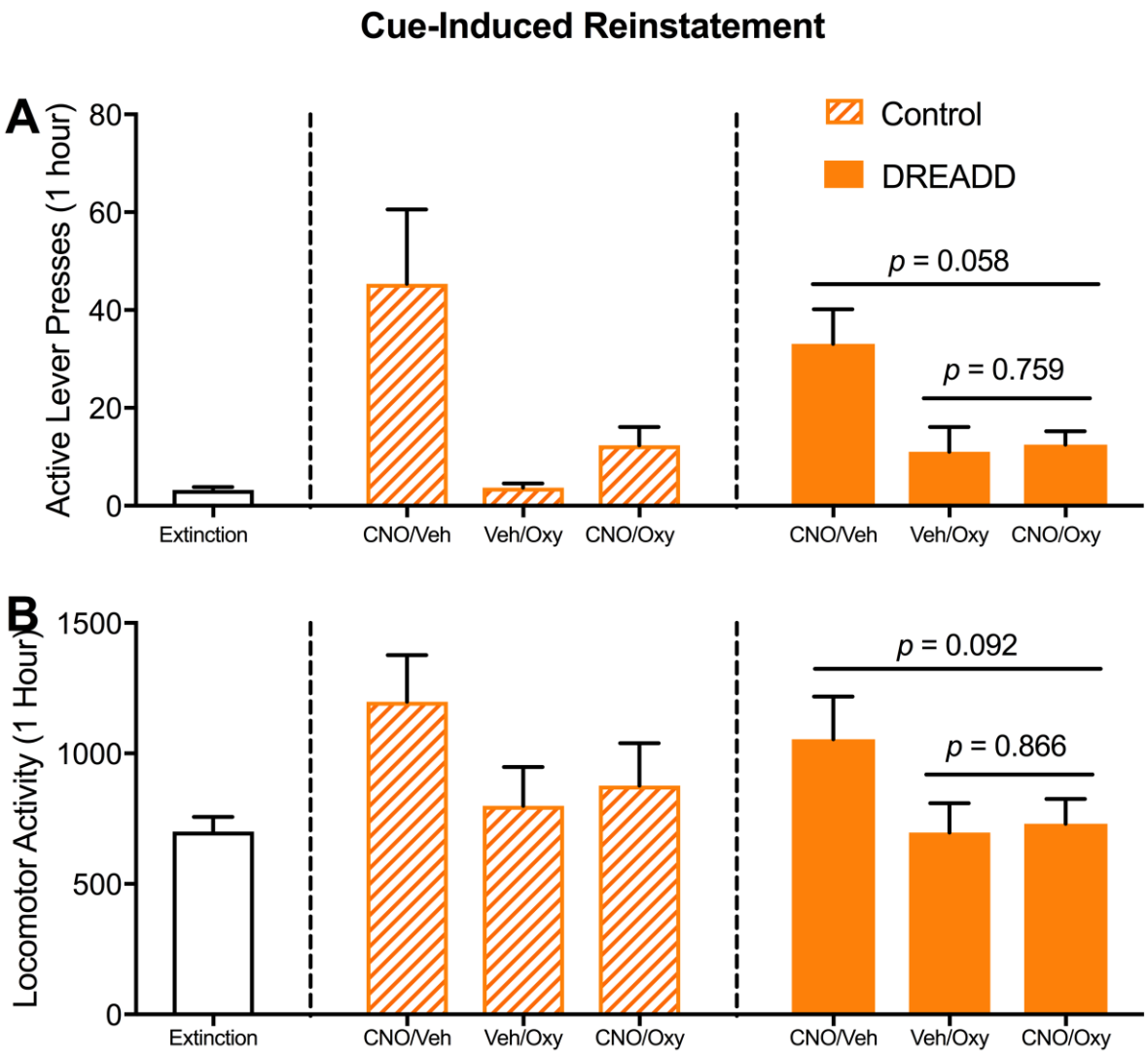

Figure 3.4. Cue-induced responding on the active lever (A) and locomotor activity (B). There was a significant main effect of oxytocin, with a priori contrasts results depicted for DREADD-expressing rats. Data presented as mean + SEM. Data displayed from n = 6 DREADD-expressing animals and n = 4 control animals.

when compared to the extinction day prior. Independent t-tests revealed no statistically significant differences in the METH-induced reinstatement behaviours across DREADD-expressing and control animals when treated with vehicle/vehicle (Actives: $t(4) = -0.259$, $p = 0.809$; Locomotor: $t(4) = 0.250$, $p = 0.815$). The 2x2x2 ANOVA revealed a significant main effect of oxytocin on reducing active lever pressing [$F(1, 8) = 53.919$, $p = 0.000$; Figure 3.5A] and locomotor activity [$F(1, 8) = 33.177$, $p = 0.001$; Figure 3.5B] compared with vehicle treatment. Additionally, there

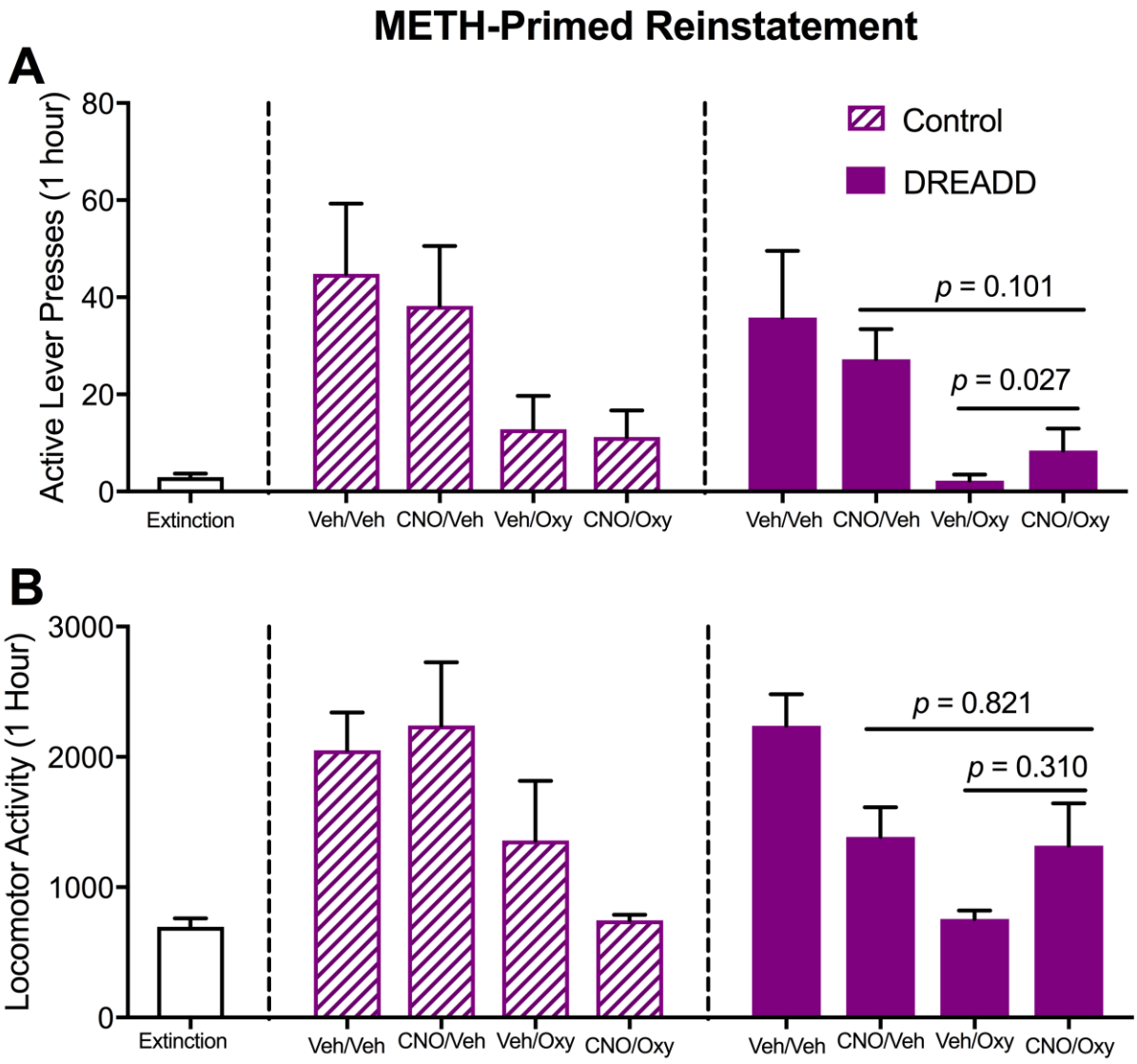

Figure 3.5 Mean (+ SEM) active lever presses (A) and locomotor activity (B) in response to presentation with a METH-prime. A priori contrasts are depicted for DREADD-expressing rats. Data displayed from n = 5 DREADD-expressing animals and n = 5 control animals

was no significant main effect of CNO pretreatment on active lever pressing [$F(1, 8) = 0.166$, $p = 0.694$] or locomotor activity [$F(1, 8) = 0.776$, $p = 0.404$]. Planned contrasts across both virus groups revealed no difference in reinstatement behaviours following pretreatment with vehicle/vehicle and CNO/vehicle [Actives: $t(9) = 0.269$, $p = 0.618$; Locomotor: $t(9) = 1.192$, $p = 0.264$], suggesting no effect of CNO treatment alone. Furthermore, when directly compared with vehicle/oxytocin pretreatment, CNO/oxytocin pretreatment resulted in significantly higher active

lever presses during METH-primed reinstatement [Actives: $t(4) = -3.396$, $p = 0.027$], but did not differ in locomotor activity [$t(4) = 1.162$; $p = 0.310$]. However, as Bonferoni corrections were used, resulting in $\propto = 0.017$, the effect on active lever pressing was not significant after controlling for multiple comparisons.

Analysis of interaction effects failed to yield any significant findings in active lever pressing behaviour [virus x CNO pretreatment: $F(1, 8) = 0.050$, $p = 0.829$; virus x oxytocin pretreatment: $F(1, 8) = 0.189$, $p = 0.675$; CNO pretreatment x oxytocin pretreatment: $F(1, 8) = 0.302$, $p = 0.598$; virus x CNO pretreatment x oxytocin pretreatment: $F(1, 8) = 0.074$, $p = 0.793$] or METH-induced locomotor activity [virus x CNO pretreatment: $F(1, 8) = 0.978$, $p = 0.352$; virus x oxytocin pretreatment: $F(1, 8) = 0.117$, $p = 0.741$; CNO pretreatment x oxytocin pretreatment: $F(1, 8) = 0.884$, $p = 0.375$; virus x CNO pretreatment x oxytocin pretreatment: $F(1, 8) = 2.519$, $p = 0.151$]. Animals were exposed to a final METH-primed reinstatement session (under vehicle/vehicle conditions) at the completion of the experiment. Reinstatement of active lever pressing did not significantly differ from the initial vehicle/vehicle responding (First Session: $M = 37.25$, SEM = 8.290; Final Session: $M = 34.58$, SEM = 8.746, $t(11) = 0.284$, $p = 0.781$), indicating no impairment to the ability to reinstate METH-paired responding.

3.3.5 Histological Analysis

Brains were sectioned in order to verify viral transfection location and colocalisation with GAD67 immunoreactivity. Histological examination resulted in the exclusion of two animals from the DREADD-expressing group. Only rats with bilateral DREADD-expression were included in the final analyses (n = 6). Viral spread varied in rostral-caudal location, ranging from +4.2mm to +3.2mm (Figure 3.6A). When visualised at low magnification (10x objective),

mCherry expression did not appear to be colocalised with GAD67 immunoreactivity. In contrast, when tissue sections were visualized at a higher magnification (63x objective), mCherry expression was entirely colocalised with GAD67 immunoreactivity, confirming specific manipulation of GABAergic neurons within the PrL (Figure 3.6B-D). Similar levels of colocalisation were also observed in control animals. To determine whether the effects of CNO depended upon individual differences in viral-mediated DREADD expression, the total area of DREADD expression (mm^2) was calculated (M = 1.91; SEM = 0.378, n = 6), and included in a correlation with active lever pressing and locomotor activity during cue-induced and METH-primed reinstatement. Modest positive correlations between DREADD expression and active lever pressing were found, however these correlations were not statistically significant (Cue-induced active lever pressing: r = 0.251, p = 0.631; METH-primed active lever pressing: r = 0.251, p = 0.685; Appendix 8).

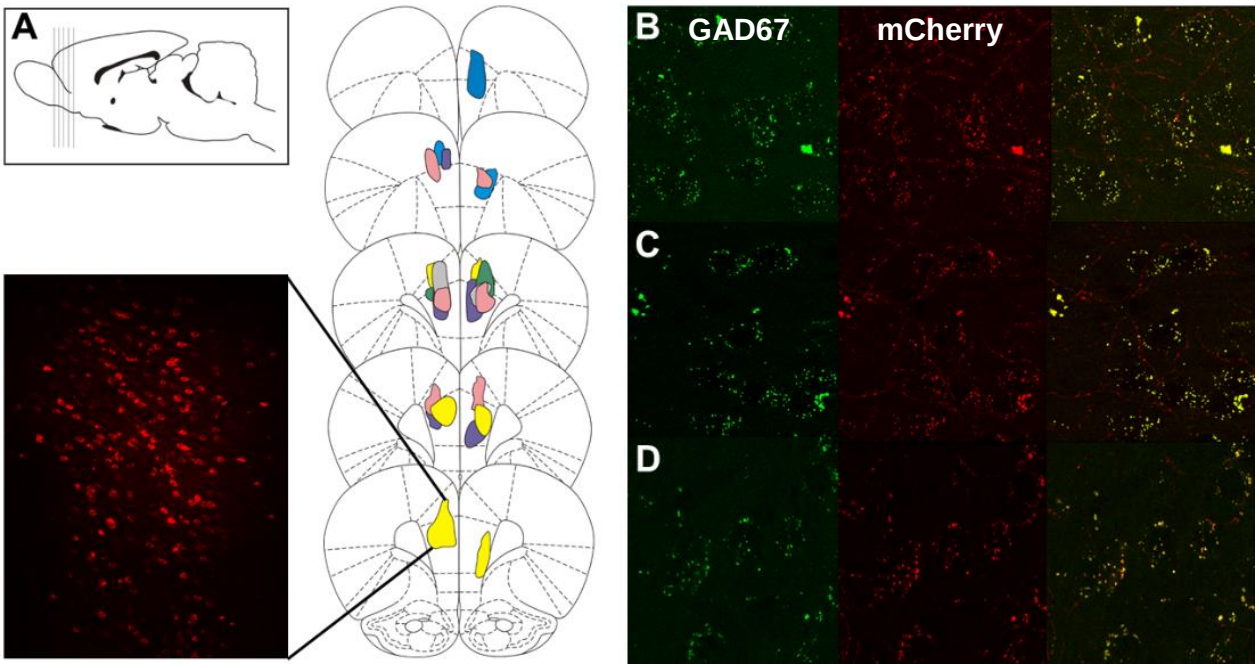

Figure 3.6. Coronal brain sections adapted from the Rat Brain Atlas of (Paxinos and Watson, 2007) displaying the anterior-posterior spread of DREADD expression within the prelimbic cortex (A). Each colour represents DREADD expression in each animal (n = 6). Representative (n = 3 animals) confocal images (taken at 63x) displaying GAD67 immunoreactivity, mCherry expression and colocalisation (B-D).

3.4 Discussion

3.4.1 Main Findings

The aim of this study was to determine whether the inhibitory effects of systemic oxytocin administration on reinstatement to METH-seeking behaviours required activity of GABA-releasing neurons in the PrL. It was hypothesised that firstly, animals would reinstate to METH-seeking behaviours following METH-priming or cue re-exposure. Secondly, it was hypothesized that systemic oxytocin administration would attenuate METH reinstatement behaviours. Lastly, it was hypothesised that the efficacy of systemic oxytocin would be blunted following inactivation of GABAergic neurons within the PrL, eliciting robust reinstatement.

The main significant finding of this study was that systemic oxytocin treatment attenuated both cue-induced and METH-primed reinstatement of active lever pressing and locomotor activity. These findings support initial hypotheses and align with a wealth of existing published literature (Bernheim, Leong, Berini, & Reichel, 2017; Carson, Cornish, Guastella, Hunt, & McGregor, 2010; Everett et al., 2018). Results also revealed a non-significant effect of CNO on reinstatement of METH-seeking behavior in both DREADD-expressing, and DREADD-free control animals, supporting the use of CNO/vehicle pretreatment as a control treatment condition for cue-induced reinstatement testing. Importantly, the present findings indicate that inactivation of PrL GABAergic neurons did not reduce the efficacy of systemic oxytocin treatment to reduce relapse to METH-seeking behaviour. Therefore, oxytocin may not be interacting with GABAergic neurons and thus may be working via alternative neurobiological mechanisms, such as GABA receptors, glutamate systems and dopamine systems.

3.4.2 Alternative Neurobiological Mechanisms of Oxytocin

The findings from the present study suggest oxytocin is not working via GABAergic neurons, however oxytocin may still be interacting with GABA receptors to exert inhibitory effects. Experiments conducted by Kaneko, Pappas, Tajiri, and Borlongan (2016) revealed oxytocin pretreatment exerted neuroprotective effects in an *in vitro* model of ischemic stroke via modulation of $GABA_AR$ subunits expression. Ischemic stroke and addiction share similar pathophysiologies, including disruptions to the excitatory/inhibitory balance within the brain (Kaneko et al., 2016). Kaneko et al. (2016) found bathing primary rat neural cells in oxytocin increased expression of α_4, β_3, δ, and ε $GABA_AR$ subunits and simultaneously decreased γ_2 $GABA_AR$ subunit expression. This lead the authors to hypothesise that oxytocin may upregulate expression of $GABA_AR$ subtypes, leading to increased inhibitory tone and restoration of the excitatory/inhibitory balance (Kaneko et al., 2016). Furthermore, research conducted by Bowen and colleagues (2015) demonstrated direct actions of oxytocin on δ-subunits of the $GABA_AR$, independent of the OTR. This suggests that in the present study, the inhibitory effects of oxytocin on reinstatement may not be due to increasing the activity of GABA-releasing neurons, but by binding to δ-subunits of the $GABA_AR$, which are typically extrasynaptic and responsible for increasing tonic inhibition (Brickley & Mody, 2012). Thus, approaches that selectively inhibit or modulate expression of GABA receptors may blunt the effects of oxytocin on METH-seeking behaviours.

Whilst Qi et al. (2012) demonstrated attenuation of METH-induced increases in glutamate within the PrL following intracerebroventricular oxytocin treatment, earlier electrophysiology experiments conducted by Jo, Stoeckel, Freund-Mercier, and Schlichter (1998) suggested

oxytocin may act to increase glutamate release. More recently, Weber et al. (2018) found direct administration of oxytocin into the NAc core significantly increased extracellular glutamate during reinstatement of cocaine-seeking behaviour. The authors suggest oxytocin may bind with receptors located on glutamatergic terminals, modulating extracellular glutamate release. Recent evidence gathered by Tan et al. (2017) revealed 54% of OTR-expressing neurons within the murine mPFC were glutamatergic in nature, suggesting oxytocin may interact directly with glutamatergic pyramidal cells. There is also evidence to suggest an interaction between oxytocin and dopaminergic systems in reward-associated brain regions (Baracz et al., 2014; Baskerville & Douglas, 2010; Kovacs, Sarnyai, Barbarczi, Szabo, & Telegdy, 1990; Sarnyai, 2011; Yang, Qi, Han, Wang, & Wu, 2010). Thus, it is possible oxytocin may be acting via OTRs to indirectly modulate release of dopamine in the NAc, through modulation of glutamate neurotransmission from the PrL to the NAc (Yang et al., 2010).

Lastly, administration of oxytocin may interact with PrL activity and drug-seeking behaviours through mechanisms beyond classical receptor binding actions. For example, oxytocin has been associated with neuroprotective effects, including anti-oxidant and anti-apoptotic effects (Erbas, Oltulu, & Taskiran, 2012; Kaneko et al., 2016; Vargas-Martinez, Uvnas-Moberg, Petersson, Olausson, & Jimenez-Estrada, 2014). Furthermore, findings by Erbas et al. (2012) indicate oxytocin may act to enhance expression of tyrosine hydroxylase, the enzyme responsible for dopamine synthesis. Therefore, oxytocin may potentially be acting to ameliorate METH-induced neurotoxic effects, by reducing the depletion of monoamine stores and level of oxidative stress.

3.4.3 Limitations, Methodological Considerations and Future Directions

In this study, chemogenetic inactivation of GABA neurons within the PrL did not affect reinstatement of METH-seeking behavior and did not reduce the effect of oxytocin to attenuate METH-seeking behaviour. The rodent PrL is a relatively large brain region, expanding approximately 2.5mm in the anterior/posterior direction (Paxinos & Watson, 2007). Firstly, discrepancies in rostro-caudal location of DREADD-expression within the PrL may have confounded the effect of chemogenetic inactivation. Secondly, it is possible only a small proportion of GABAergic neurons within the PrL were DREADD-expressing, meaning a significant proportion of GABAergic neurons may still interact with oxytocin. Correlational analysis of virally transfected area with active lever presses during CNO/oxytocin treatment revealed a very modest and non-significant positive correlation (Appendix 8), suggesting null results may not be attributed to transfection efficiency alone.

Another important methodological consideration is the dose of CNO administered. It has previously been suggested that relatively higher doses of CNO are required to hyperpolarise hM4D(Gi)-transfected neurons compared with the dose required to depolarise hM3D(Gq)-transfected neurons (Roth, 2016). It is plausible that 3mg/kg of CNO (IP) was not sufficient to elicit strong hyperpolarisation of GABAergic neurons. Whilst responding on the active lever was slightly higher in DREADD-expressing animals following treatment with CNO/oxytocin compared with vehicle/oxytocin, this effect was not large enough to reach significance. Therefore, the dose of administered CNO is an important consideration for future DREADD experiments.

The present study utilised a genetically modified animal, LE-Tg(GAD1-iCre)3Ottc, which expresses the enzyme Cre recombinase under a GAD1 promotor. Previously, high co-expression of Cre and GAD1 mRNA has been observed in the hypothalamus (80 ± 6%) and midbrain (76 ± 11%; Sharpe et al., 2017). However, markedly decreased co-expression was reported in the anterior cingulate cortex (32 ± 8%), a brain region in close anatomical proximity to the PrL (Sharpe et al., 2017). In the present study, preliminary analysis revealed poor localization of mCherry with GAD67 immunoreactivity, however, visualization at high magnification revealed very high co-expression of mCherry with GAD67 (Figure 3.6B-D). Despite confinement to GABAergic neurons, each GABAergic interneuron subpopulation has unique structural and functional characteristics (Kawaguchi & Kondo, 2002; Kawaguchi & Kubota, 1997; Tremblay, Lee, & Rudy, 2016). The mPFC is highly heterogeneous, with recent reports revealing 10 genetically distinct inhibitory neuronal subtypes within the mPFC (Wang et al., 2018). Given that oxytocin is unlikely to act equally at all GABA receptor subtypes, broad chemogenetic inactivation of all GABAergic subpopulations may limit the interpretation of the present findings. Future experiments could adopt parvalbumin-Cre or somatostatin-Cre transgenic rats, as interactions between oxytocin and these GABAergic interneuron populations have previously been evidenced (Marlin, Mitre, D'amour, Chao, & Froemke, 2015; Owen et al., 2013).

Lastly, due to the limited availability of transgenic animals at the time of this experiment, relatively small sample sizes for the DREADD (n = 8) and DREADD-free control (n = 4) groups were possible. As such, this enabled the present pilot study which revealed broad inhibition of GABAergic neurons within the PrL does not reduce the efficacy of oxytocin in attenuating METH-relapse behaviours. Furthermore, this pilot study also revealed higher than anticipated Cre

expression within the PrL, despite previous reports of relatively low expression in the adjacent anterior cingulate cortex (Sharpe et al., 2017). However, the sample size certainly limited the statistical power of the present analyses, making some near-significant findings difficult to interpret. Furthermore, follow up studies with larger cohorts will enable investigation of higher CNO doses to ensure sufficient chemogenetic inhibition.

In conclusion, this study suggests that the ability for oxytocin to reduce relapse to METH-seeking behavior does not occur through the activation of GABAergic neurons in the PrL. Although not surprising, these data do provide further information on the neurobiology of methamphetamine addiction, indicating that reinstatement to METH-seeking behaviours does not require activity of PrL GABAergic neurons. However, the specific mechanisms of oxytocin in the PrL still remain unknown. To continue this investigation, the present findings need to be replicated using a higher dose of CNO to ensure sufficient chemogenetic inhibition. Furthermore, the receptor mechanisms of oxytocin in the PrL should be determined using a pharmacological approach. Improvements in our understanding of the mechanistic actions of oxytocin may lead to development of oxytocin-based treatments for METH abuse.

References

Baracz, S. J., Everett, N. A., & Cornish, J. L. (2015). The involvement of oxytocin in the subthalamic nucleus on relapse to methamphetamine-seeking behaviour. *PLOS One, 10*(8), e0136132. doi:doi:10.1371/ journal.pone.0136132

Baracz, S. J., Everett, N. A., McGregor, I. S., & Cornish, J. L. (2014). Oxytocin in the nucleus accumbens core reduces reinstatement of methamphetamine-seeking behaviour in rats. *Addiction Biology, 21*, 316-325.

Baskerville, T. A., & Douglas, A. J. (2010). Dopamine and oxytocin interactions underlying behaviors: potential contributions to behavioral disorders. *CNS Neurosci Ther, 16*(3), e92-123. doi:10.1111/j.1755-5949.2010.00154.x

Bernheim, A., Leong, K. C., Berini, C., & Reichel, C. M. (2017). Antagonism of mGlu2/3 receptors in the nucleus accumbens prevents oxytocin from reducing cued methamphetamine seeking in male and female rats. *Pharmacol Biochem Behav, 161*, 13-21. doi:10.1016/j.pbb.2017.08.012

Bowen, M. T., Peters, S. T., Absalom, N., Chebib, M., Neumann, I. D., & McGregor, I. S. (2015). Oxytocin prevents ethanol actions at δ subunit-containing GABA_A receptors and attenuates ethanol-induced motor impairment in rats. *Proceedings of the National Academy of Sciences, 112*, 3104-3109.

Brickley, S. G., & Mody, I. (2012). Extrasynaptic GABA(A) receptors: their function in the CNS and implications for disease. *Neuron, 73*(1), 23-34. doi:10.1016/j.neuron.2011.12.012

Carson, D. S., Cornish, J. L., Guastella, A. J., Hunt, G. E., & McGregor, I. S. (2010). Oxytocin decreases methamphetamine self-administration, methamphetamine hyperactivity, and relapse to methamphetamine-seeking behaviour in rats. *Neuropharmacology, 58*(1), 38-43. doi:https://doi.org/10.1016/j.neuropharm.2009.06.018

Courtney, K. E., & Ray, L. A. (2014). Methamphetamine: an update on epidemiology, pharmacology, clinical phenomenology and treatment literature. *Drug Alcohol Dependence, 143*, 11-21.

Cox, B. M., Young, A. B., See, R. E., & Reichel, C. M. (2013). Sex differences in methamphetamine seeking in rats: impact of oxytocin. *Psychoneuroendocrinology, 38*(10), 2343-2353. doi:10.1016/j.psyneuen.2013.05.005

Cruickshank, C. C., & Dyer, K. R. (2009). A review of the clinical pharmacology of methamphetamine. *Addiction, 104*(7), 1085-1099. doi:10.1111/j.1360-0443.2009.02564.x

Erbas, O., Oltulu, F., & Taskiran, D. (2012). Amelioration of rotenone-induced dopaminergic cell death in the striatum by oxytocin treatment. *Peptides, 38*(2), 312-317. doi:10.1016/j.peptides.2012.05.026

Everett, N. A., McGregor, I. S., Baracz, S. J., & Cornish, J. L. (2018). The role of the vasopressin V1A receptor in oxytocin modulation of methamphetamine primed reinstatement. *Neuropharmacology, 133*, 1-11. doi:https://doi.org/10.1016/j.neuropharm.2017.12.036

Everitt, B. J., Giuliano, C., & Belin, D. (2018). Addictive behaviour in experimental animals: prospects for translation. *Philos Trans R Soc Lond B Biol Sci, 373*(1742). doi:10.1098/rstb.2017.0027

Everitt, B. J., & Robbins, T. W. (2005). Neural systems of reinforcement for drug addiction: from actions to habits to compulsion. *Nat Neurosci, 8*(11), 1481-1489. doi:10.1038/nn1579

Goldstein, R. Z., & Volkow, N. D. (2011). Dysfunction of the prefrontal cortex in addiction: neuroimaging findings and clinical implications. *Nat Rev Neurosci, 12*(11), 652-669. doi:10.1038/nrn3119

Hicks, C., Cornish, J. L., Baracz, S. J., Suraev, A., & McGregor, I. S. (2016). Adolescent pre-treatment with oxytocin protects against adult methamphetamine-seeking behaviour in female rats. *Addiction Biology, 21*, 304-315.

Jo, Y.-H., Stoeckel, M.-E., Freund-Mercier, M.-J., & Schlichter, R. (1998). Oxytocin Modulates Glutamatergic Synaptic Transmission between Cultured Neonatal Spinal Cord Dorsal Horn Neurons. *The Journal of Neuroscience, 18*, 2377-2386.

Kaneko, Y., Pappas, C., Tajiri, N., & Borlongan, C. V. (2016). Oxytocin modulates GABAAR subunits to confer neuroprotection in stroke in vitro. *Scientific Reports, 6*, 35659. doi:10.1038/srep35659

Kawaguchi, Y., & Kondo, S. (2002). Parvalbumin, somatostatin and cholecystokinin as chemical markers for specific GABAergic interneuron types in the rat frontal cortex. *J Neurocytol, 31*(3-5), 277-287.

Kawaguchi, Y., & Kubota, Y. (1997). GABAergic cell subtypes and their synaptic connections in rat frontal cortex. *Cereb Cortex, 7*(6), 476-486.

Kovacs, G. L., Sarnyai, Z., Barbarczi, E., Szabo, G., & Telegdy, G. (1990). The role of oxytocin-dopamine interactions in cocaine-induced locomotor hyperactivity. *Neuropharmacology, 29*(4), 365-368.

Marlin, B. J., Mitre, M., D'amour, J. A., Chao, M. V., & Froemke, R. C. (2015). Oxytocin enables maternal behaviour by balancing cortical inhibition. *Nature, 520*, 499. doi:10.1038/nature14402 https://www.nature.com/articles/nature14402 - supplementary-information

Martín-García, E., Courtin, J., Renault, P., Fiancette, J.-F., Wurtz, H., Simonnet, A., . . . Deroche-Gamonet, V. (2014). Frequency of Cocaine Self-Administration Influences Drug Seeking in the Rat: Optogenetic Evidence for a Role of the Prelimbic Cortex. *Neuropsychopharmacology, 39*, 2317. doi:10.1038/npp.2014.66 https://www.nature.com/articles/npp201466 - supplementary-information

Ninan, I. (2011). Oxytocin suppresses basal glutamatergic transmission but facilitates activity-dependent synaptic potentiation in the medial prefrontal cortex. *J Neurochem, 119*(2), 324-331. doi:10.1111/j.1471-4159.2011.07430.x

Owen, S. F., Tuncdemir, S. N., Bader, P. L., Tirko, N. N., Fishell, G., & Tsien, R. W. (2013). Oxytocin enhances hippocampal spike transmission by modulating fast-spiking interneurons. *Nature, 500*(7463), 458-462. doi:10.1038/nature12330

Panenka, W. J., Procyshyn, R. M., Lecomte, T., MacEwan, G. W., Flynn, S. W., Honer, W. G., & Barr, A. M. (2013). Methamphetamine use: a comprehensive review of molecular, preclinical and clinical findings. *Drug Alcohol Depend, 129*(3), 167-179. doi:10.1016/j.drugalcdep.2012.11.016

Paxinos, G., & Watson, C. (2007). The Rat Brain in Stereotaxic Coordinates *123Library* (6 ed.): Academic Press.

Qi, J., Han, W., Yang, J., Wang, L., Dong, Y., Wang, F., . . . Wu, C. (2012). Oxytocin regulates changes in extracellular glutamate and GABA levels induced by methamphetamine in the mouse brain. *Addiction Biology, 17*, 758-769.

Robinson, T. E., & Berridge, K. C. (1993). The neural basis of drug craving: an incentive-sensitization theory of addiction. *Brain Res Brain Res Rev, 18*(3), 247-291.

Rocha, A., & Kalivas, P. W. (2010). Role of the prefrontal cortex and nucleus accumbens in reinstating methamphetamine seeking. *Eur J Neurosci, 31*(5), 903-909. doi:10.1111/j.1460-9568.2010.07134.x

Roth, B. L. (2016). DREADDs for Neuroscientists. *Neuron, 89*(4), 683-694. doi:10.1016/j.neuron.2016.01.040

Sabihi, S., Dong, S. M., Maurer, S. D., Post, C., & Leuner, B. (2017). Oxytocin in the medial prefrontal cortex attenuates anxiety: Anatomical and receptor specificity and mechanism of action. *Neuropharmacology, 125*, 1-12. doi:https://doi.org/10.1016/j.neuropharm.2017.06.024

Sabihi, S., Durosko, N. E., Dong, S. M., & Leuner, B. (2014). Oxytocin in the prelimbic medial prefrontal cortex reduces anxiety-like behavior in female and male rats. *Psychoneuroendocrinology, 45*, 31-42. doi:10.1016/j.psyneuen.2014.03.009

Sarnyai, Z. (2011). Oxytocin as a potential mediator and modulator of drug addiction. *Addict Biol, 16*(2), 199-201. doi:10.1111/j.1369-1600.2011.00332.x

Sarnyai, Z., & Kovacs, G. L. (1994). Role of oxytocin in the neuroadaptation to drugs of abuse. *Psychoneuroendocrinology, 19*(1), 85-117.

Sharpe, M. J., Marchant, N. J., Whitaker, L. R., Richie, C. T., Zhang, Y. J., Campbell, E. J., . . . Schoenbaum, G. (2017). Lateral Hypothalamic GABAergic Neurons Encode Reward Predictions that Are Relayed to the Ventral Tegmental Area to Regulate Learning. *Curr Biol, 27*(14), 2089-2100.e2085. doi:10.1016/j.cub.2017.06.024

Tan, Y., Singhal, S., Hiller, H., Nguyen, D.-T., Colon-Perez, L. M., Febo, M., . . . Krause, E. G. (2017). Oxytocin Receptors are expressed on Neurons within the Prefrontal Cortex that Control Preference for Social Novelty. *The FASEB Journal, 31*(1_supplement), 1076.1013-1076.1013. doi:10.1096/fasebj.31.1_supplement.1076.13

Tremblay, R., Lee, S., & Rudy, B. (2016). GABAergic Interneurons in the Neocortex: From Cellular Properties to Circuits. *Neuron, 91*(2), 260-292. doi:10.1016/j.neuron.2016.06.033

Vargas-Martinez, F., Uvnas-Moberg, K., Petersson, M., Olausson, H. A., & Jimenez-Estrada, I. (2014). Neuropeptides as neuroprotective agents: Oxytocin a forefront developmental player in the mammalian brain. *Prog Neurobiol, 123c*, 37-78. doi:10.1016/j.pneurobio.2014.10.001

Wang, X., Allen, W. E., Wright, M. A., Sylwestrak, E. L., Samusik, N., Vesuna, S., . . . Deisseroth, K. (2018). Three-dimensional intact-tissue sequencing of single-cell transcriptional states. *Science, 361*.

Weber, R. A., Logan, C. N., Leong, K. C., Peris, J., Knackstedt, L., & Reichel, C. M. (2018). Regionally Specific Effects of Oxytocin on Reinstatement of Cocaine Seeking in Male and Female Rats. *Int J Neuropsychopharmacol, 21*(7), 677-686. doi:10.1093/ijnp/pyy025

Yang, J.-y., Qi, J., Han, W.-y., Wang, F., & Wu, C.-f. (2010). Inhibitory role of oxytocin in psychostimulant-induced psychological dependence and its effects on dopaminergic and glutaminergic transmission. *Acta Pharmacologica Sinica, 31*(9), 1071-1074. doi:10.1038/aps.2010.140

Chapter 4: General Discussion

4.1 Summary of Findings

The present thesis aimed to reveal new insights relating to the neurobiological mechanisms underlying METH addiction and the mechanistic action of oxytocin. The findings of Chapter 2 build on existing literature, suggesting METH elicits increased neuronal activity in subregions of the NAc, mPFC and OFC, as indicated by increased Fos immunoreactivity. Lack of colocalisation of Fos with nNOS or PV GABAergic interneurons suggests activation of excitatory populations. Fos immunoreactivity was correlated across examined subregions, indicating of direct or indirect functional connections. METH-exposed animals revealed reduced correlated activity, indicating potential reductions in functional connectivity.

In parallel experiments, Chapter 3 employed a chemogenetic approach to investigate the interaction between oxytocin and GABAergic neurons within the PrL during METH-relapse. Chemogenetic inactivation of GABAergic neurons within the PrL did not blunt the effect of systemic oxytocin, suggesting alternative mechanisms of action. Whilst this thesis has shed light on METH-induced neuroadaptations within the NAc and PFC and enhanced understanding of GABA-oxytocin interactions, there are still many avenues of research that require further investigation.

4.2 What is the Behavioural Impact of METH-induced Alterations to Functional Connectivity?

Correlational analysis of Fos immunoreactivity across subregions of the NAc and PFC revealed a reduction in the number of statistically significant correlations in METH-exposed animals (Figure 4.1). This finding could suggest reduced functional connectivity following METH

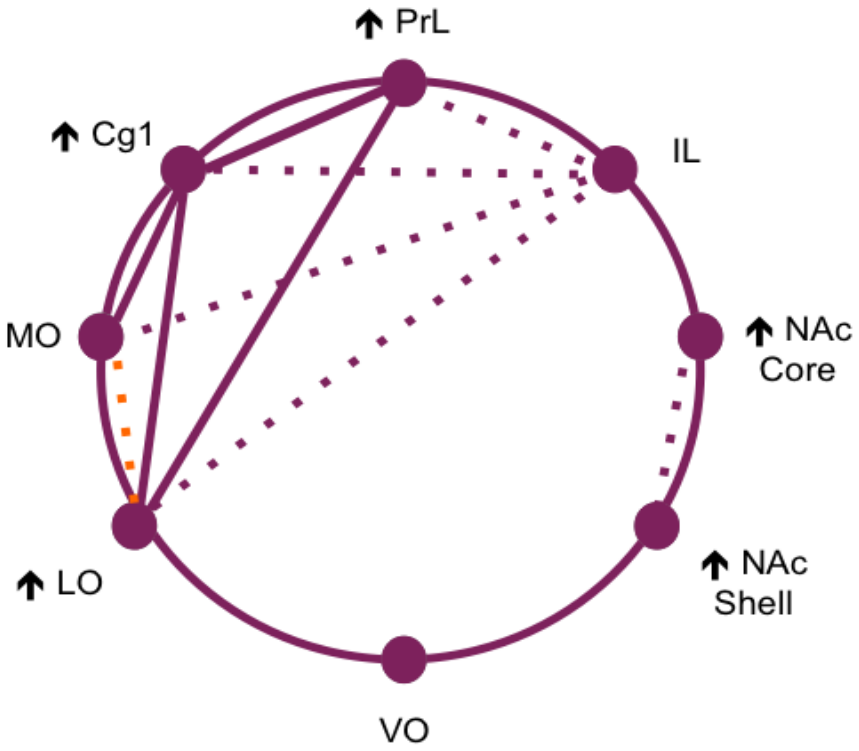

Figure 4.1. Diagram depicts possible functional connections between subregions of the NAc, mPFC and OFC. Solid lines represent statistically significant Fos correlations present across all examined groups. Broken purple lines represent statistically significant correlations which were present in control animals but absent in METH-exposed animals. Broken orange line represents a statistically significant correlation that was present in all treatment groups except animals which had relapsed to METH. Arrows depict increases in neuronal activation, as evidenced by increased Fos immunoreactivity, in METH-treated groups.

exposure. Interestingly, animals that were METH-experienced, but currently in withdrawal, also exhibited decreased correlated activity, suggesting that METH-induced changes to functional connectivity may persist despite cessation of drug-use. In addition, correlated neuronal activity between MO and LO subregions was absent in METH-relapse animals. This finding is interesting, particularly in light of recent findings by Lopatina et al. (2017) which suggest the MO and LO work together to encode information about the perceived value of a stimulus. Accordingly, disruption to the function of MO-LO connections may drive addicts to overvalue administered drugs. Disruption to MO-LO connectivity was only observed in METH-relapse animals, suggesting disruption to this functional pathway may be specific to relapse. To address this, future experiments could utilise optogenetic stimulation of MO terminals to transiently silence or excite this OFC microcircuit prior to METH reinstatement.

Such an approach could determine whether the change in correlated activity in these regions has functional consequences relating to addiction behaviours. The current findings, whilst useful, are of limited scope. It is possible functional connectivity and neuronal activity may be altered in additional reward-associated brain regions such as the dorsal striatum or VTA.

4.2.1 Could Functional Connections with the Dorsal Striatum be Altered?

The rodent striatum is composed of two critical components; the ventral nucleus accumbens and the dorsal caudate putamen (Yager, Garcia, Wunsch, & Ferguson, 2015). The nucleus accumbens is critical for the establishment of drug-seeking behaviours (Hyman, Malenka, & Nestler, 2006; Yager et al., 2015). However, once drug-seeking behaviours have been established, recruitment shifts from the nucleus accumbens to the dorsal striatum, which is involved in established habit-like drug-taking behaviours (Hyman et al., 2006; Yager et al., 2015). Analysis of the dorsal striatum has previously revealed increased concentrations of neurotransmitters and increased immediate early gene expression following acute and chronic drug exposure (Liu et al., 2014; Yager et al., 2015); however it remains unclear if functional connectivity between the dorsal striatum and other reward substrates is impacted upon. Further investigation of altered functional connectivity between the PFC, NAc and dorsal striatum may be aided by the adoption of fibre photometry. Fibre photometry enables real-time investigation of neuronal activity, and by extension functional connectivity, across multiple ROIs within the same experimental animal (Kim et al., 2016); these data may yield critical insights into compulsive drug-taking and recruitment of the dorsal striatum.

4.2.2 Could Functional Connections with the Ventral Tegmental Area be Altered?

Drug-induced increases in neuronal activation in the striatum and PFC may also be driven by increased activation of the VTA. The VTA provides dopaminergic input to many reward-associated substrates (Hyman & Malenka, 2001; Volkow, Wang, Fowler, & Tomasi, 2012; Yager et al., 2015), where dopamine and glutamate are hypothesized to act synergistically to modulate neuronal activity (Cruz, Javier Rubio, & Hope, 2015). Therefore, aberrant firing within the VTA may act to increase neuronal activity in all regions which receive projections from the VTA. Furthermore, VTA dysfunction could underlie altered dopamine and glutamate neurotransmission within many brain regions, including increased activation of VTA-PFC and PFC-NAc projections (Scofield et al., 2016). Hence, further investigation of METH-induced changes to striatal and VTA output is warranted.

4.3 Are GABA Systems Altered Following Exposure to METH?

Loss of inhibitory control within the PFC has previously been attributed to dysfunction of GABAergic interneurons which tightly control pyramidal activity (Ferguson & Gao, 2018; Tremblay, Lee, & Rudy, 2016). Findings from Chapter 2 do not directly support this theory, as chronic METH exposure did not result in a reduction of nNOS or PV interneurons, or altered activation of these GABA subpopulations. This finding suggests that the increased neuronal activation observed in METH-exposed rats is confined to other neuronal populations. It is possible then, that other GABAergic interneuron subpopulations such as somatostatin- or calretinin-expressing interneurons may be impacted by a history of METH self-administration, and thus contribute to METH-induced dysfunctions. Further investigation of other GABAergic interneuron populations could reveal changes to the number or activity of other interneuron populations following METH exposure. However, the broad chemogenetic inactivation of GABAergic PrL neurons employed in Chapter 3 did not

significantly increase METH reinstatement, as one would expect if tonic GABAergic activity in the PrL is acting as a brake on glutamate output and relapse. Therefore, this may suggest that specific interneuron subtypes need to be targeted, which is consistent with the literature indicating that PrL interneurons have distinct neuromodulatory roles (Markram et al., 2004; Rudy, Fishell, Lee, & Hjerling-Leffler, 2011; Tremblay et al., 2016). Further research is needed to identify how these other PrL interneurons are affected by METH, and whether manipulating their activity has consequences for addictive behaviours.

4.4 How and where is Oxytocin Acting in the Brain?

Chapter 3 investigated if systemic oxytocin was acting directly via GABAergic neurons within the PrL to increase inhibitory tone and restore the excitatory/inhibitory balance within the PrL and its pathways (Owen et al., 2013; Sabihi, Dong, Maurer, Post, & Leuner, 2017). In light of the findings of Chapter 2, it may not be surprising that chemogenetic inactivation of GABAergic neurons within the PrL did not blunt the effect of oxytocin, as the function of nNOS and PV interneurons within the PrL (40-50% of mPFC GABAergic interneurons) does not appear to be impaired. Hence if the majority of GABAergic neurons are not impaired in the PrL, it is plausible that systemic oxytocin is working via an alternative mechanism within the PrL, or acts on other brain regions to regulate addiction-related neurotransmission (Figure 4.2).

Previous published experiments have implicated the role of the PrL in the effects of oxytocin (Sabihi et al., 2017; Weber et al., 2018). Sabihi et al. (2017) revealed significant reductions in the anxiolytic effect of oxytocin when co-administered directly into the PrL with either bicuculline methiodide a $GABA_AR$ antagonist, or desGly-NH2,d(CH2)5[D-Tyr2,Thr4]OVT, an OTR antagonist (OTR-A). Taken collectively with the results from

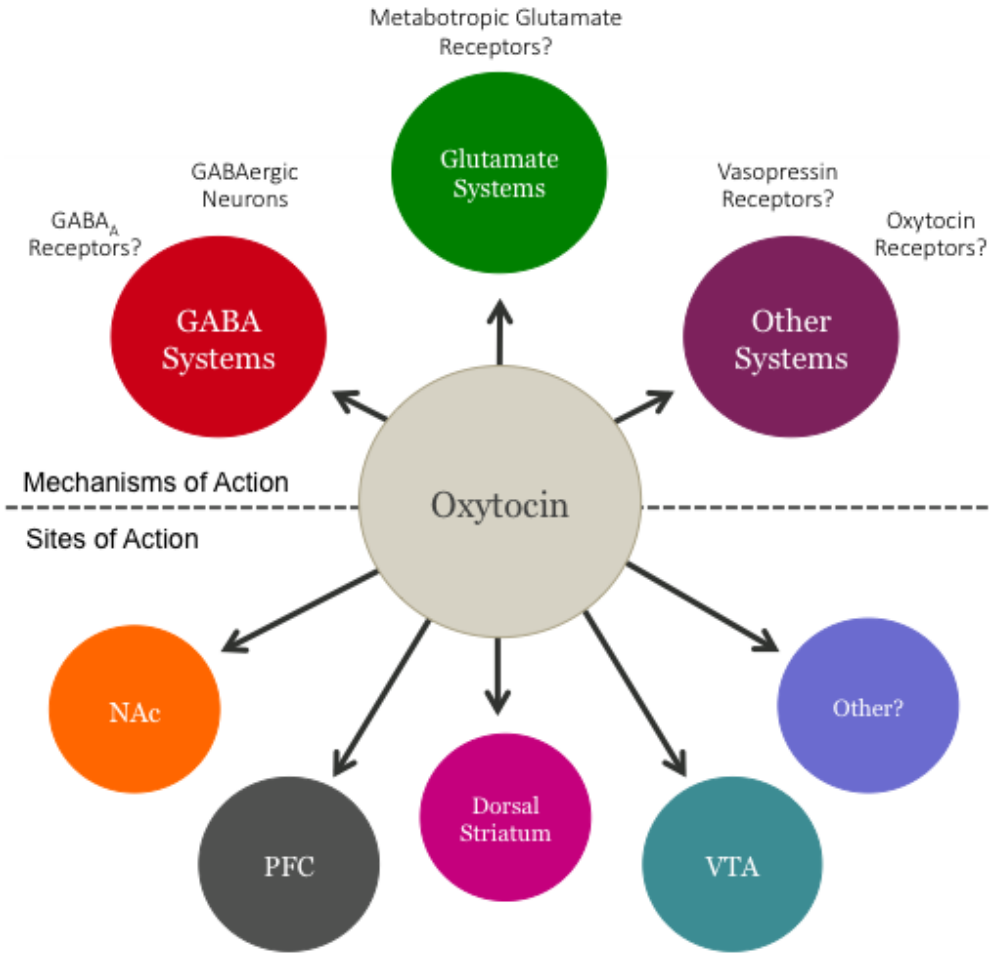

Figure 4.2. Diagram depicting the hypothesised mechanisms of action and possible substrates in which oxytocin could be acting to attenuated drug-seeking behaviour.

Chapter 3, oxytocin may still be acting directly in the PrL to attenuate drug-seeking behaviour, however this interaction is most likely via direct agonistic activity at $GABA_A$Rs or OTRs. Previous research has also investigated other sites of action of oxytocin, as co-administration with OTR-A into the NAc core (Baracz, Everett, McGregor, & Cornish, 2014) and the subthalamic nucleus (Baracz, Everett, & Cornish, 2015) failed to prevent the inhibitory effects of oxytocin on METH-primed relapse. Conversely, antagonism of metabotropic glutamate (Bernheim, Leong, Berini, & Reichel, 2017) and vasopressin V1A receptors (Everett, McGregor, Baracz, & Cornish, 2018) reduced the efficacy of oxytocin, eliciting robust reinstatement of drug-seeking behaviour. This clearly indicates that oxytocin interacts with various receptor systems other than its own, and that this may differ according to brain region.

It is plausible that oxytocin administration may also be acting in other reward-associated substrates, such as the VTA (Weber et al., 2018). Experiments conducted by Tang et al. (2014) and Xiao, Priest, Nasenbeny, Lu, and Kozorovitskiy (2017) indicate oxytocin may act to modulate dopaminergic neurons within the VTA, inhibiting release of dopamine and glutamate in reward circuitry. Further investigation is required to elucidate the site of action within the brain and the receptor systems responsible for oxytocin-induced attenuation of drug-seeking behaviours. Currently, our limited understanding of the neurobiological mechanisms of oxytocin to reduce METH-relapse hinders the development, and application, of novel oxytocin-based pharmacotherapies.

4.5 Concluding Remarks

In summary, exposure to METH alters the function of reward circuitry within the brain. Administration of METH elicits aberrant neuronal activity in key reward-associated areas, such as the mPFC and NAc, and further highlights an important role for MO-LO connections in the addiction process. Findings from the present study suggest that METH self-administration increases neuronal activation in the PrL, however there is minimal activation of nNOS or PV interneurons, indicating GABAergic systems in the PrL, at least nNOS and PV populations, may not be impeded following drug administration. However, the mPFC is highly heterogeneous with recent reports suggesting 15 genetically distinct cell types (Wang et al., 2018). Further research is required to elucidate the mechanisms driving increased excitatory activity, as direct loss of inhibitory input may not be directly implicated. There is a critical need to develop pharmacotherapies that restore the excitatory/inhibitory balance within the brain; oxytocin may be one such treatment, however further research is required to understand the precise mechanistic and site of actions of oxytocin to reduce relapse to METH-seeking behaviour.

References

Baracz, S. J., Everett, N. A., & Cornish, J. L. (2015). The involvement of oxytocin in the subthalamic nucleus on relapse to methamphetamine-seeking behaviour. *PLOS One, 10*(8), e0136132. doi:doi:10.1371/ journal.pone.0136132

Baracz, S. J., Everett, N. A., McGregor, I. S., & Cornish, J. L. (2014). Oxytocin in the nucleus accumbens core reduces reinstatement of methamphetamine-seeking behaviour in rats. *Addiction Biology, 21*, 316-325.

Bernheim, A., Leong, K. C., Berini, C., & Reichel, C. M. (2017). Antagonism of mGlu2/3 receptors in the nucleus accumbens prevents oxytocin from reducing cued methamphetamine seeking in male and female rats. *Pharmacol Biochem Behav, 161*, 13-21. doi:10.1016/j.pbb.2017.08.012

Cruz, F. C., Javier Rubio, F., & Hope, B. T. (2015). Using c-fos to study neuronal ensembles in corticostriatal circuitry of addiction. *Brain Res, 1628*(Pt A), 157-173. doi:10.1016/j.brainres.2014.11.005

Everett, N. A., McGregor, I. S., Baracz, S. J., & Cornish, J. L. (2018). The role of the vasopressin V1A receptor in oxytocin modulation of methamphetamine primed reinstatement. *Neuropharmacology, 133*, 1-11. doi:https://doi.org/10.1016/j.neuropharm.2017.12.036

Ferguson, B. R., & Gao, W. J. (2018). PV Interneurons: Critical Regulators of E/I Balance for Prefrontal Cortex-Dependent Behavior and Psychiatric Disorders. *Front Neural Circuits, 12*, 37. doi:10.3389/fncir.2018.00037

Hyman, S. E., & Malenka, R. C. (2001). Addiction and the brain: the neurobiology of compulsion and its persistence. *Nat Rev Neurosci, 2*(10), 695-703. doi:10.1038/35094560

Hyman, S. E., Malenka, R. C., & Nestler, E. J. (2006). Neural mechanisms of addiction: the role of reward-related learning and memory. *Annu Rev Neurosci, 29*, 565-598. doi:10.1146/annurev.neuro.29.051605.113009

Kim, C. K., Yang, S. J., Pichamoorthy, N., Young, N. P., Kauvar, I., Jennings, J. H., . . . Deisseroth, K. (2016). Simultaneous fast measurement of circuit dynamics at multiple sites across the mammalian brain. *Nat Methods, 13*(4), 325-328. doi:10.1038/nmeth.3770

Liu, Q.-R., Rubio, F. J., Bossert, J. M., Marchant, N. J., Fanous, S., Hou, X., . . . Hope, B. T. (2014). Detection of molecular alterations in methamphetamine-activated Fos-expressing neurons from a single rat dorsal striatum using fluorescence-activated cell sorting (FACS). *J Neurochem, 128*(1), 173-185. doi:10.1111/jnc.12381

Lopatina, N., Sadacca, B. F., McDannald, M. A., Styer, C. V., Peterson, J. F., Cheer, J. F., & Schoenbaum, G. (2017). Ensembles in medial and lateral orbitofrontal cortex construct cognitive maps emphasizing different features of the behavioral landscape. *Behav Neurosci, 131*(3), 201-212. doi:10.1037/bne0000195

Markram, H., Toledo-Rodriguez, M., Wang, Y., Gupta, A., Silberberg, G., & Wu, C. (2004). Interneurons of the neocortical inhibitory system. *Nat Rev Neurosci, 5*(10), 793-807. doi:10.1038/nrn1519

Owen, S. F., Tuncdemir, S. N., Bader, P. L., Tirko, N. N., Fishell, G., & Tsien, R. W. (2013). Oxytocin enhances hippocampal spike transmission by modulating fast-spiking interneurons. *Nature, 500*(7463), 458-462. doi:10.1038/nature12330

Rudy, B., Fishell, G., Lee, S., & Hjerling-Leffler, J. (2011). Three groups of interneurons account for nearly 100% of neocortical GABAergic neurons. *Dev Neurobiol, 71*(1), 45-61. doi:10.1002/dneu.20853

Sabihi, S., Dong, S. M., Maurer, S. D., Post, C., & Leuner, B. (2017). Oxytocin in the medial prefrontal cortex attenuates anxiety: Anatomical and receptor specificity and mechanism of action. *Neuropharmacology, 125*, 1-12. doi:https://doi.org/10.1016/j.neuropharm.2017.06.024

Scofield, M. D., Heinsbroek, J. A., Gipson, C. D., Kupchik, Y. M., Spencer, S., Smith, A. C., . . . Kalivas, P. W. (2016). The Nucleus Accumbens: Mechanisms of Addiction across Drug Classes Reflect the Importance of Glutamate Homeostasis. *Pharmacol Rev, 68*(3), 816-871. doi:10.1124/pr.116.012484

Tang, Y., Chen, Z., Tao, H., Li, C., Zhang, X., Tang, A., & Liu, Y. (2014). Oxytocin activation of neurons in ventral tegmental area and interfascicular nucleus of mouse midbrain. *Neuropharmacology, 77*, 277-284. doi:10.1016/j.neuropharm.2013.10.004

Tremblay, R., Lee, S., & Rudy, B. (2016). GABAergic Interneurons in the Neocortex: From Cellular Properties to Circuits. *Neuron, 91*(2), 260-292. doi:10.1016/j.neuron.2016.06.033

Volkow, N. D., Wang, G.-J., Fowler, J. S., & Tomasi, D. (2012). Addiction Circuitry in the Human Brain. *Annual review of pharmacology and toxicology, 52*, 321-336. doi:10.1146/annurev-pharmtox-010611-134625

Wang, X., Allen, W. E., Wright, M. A., Sylwestrak, E. L., Samusik, N., Vesuna, S., . . . Deisseroth, K. (2018). Three-dimensional intact-tissue sequencing of single-cell transcriptional states. *Science, 361*.

Weber, R. A., Logan, C. N., Leong, K. C., Peris, J., Knackstedt, L., & Reichel, C. M. (2018). Regionally Specific Effects of Oxytocin on Reinstatement of Cocaine Seeking in Male and Female Rats. *Int J Neuropsychopharmacol, 21*(7), 677-686. doi:10.1093/ijnp/pyy025

Xiao, L., Priest, M. F., Nasenbeny, J., Lu, T., & Kozorovitskiy, Y. (2017). Biased Oxytocinergic Modulation of Midbrain Dopamine Systems. *Neuron, 95*(2), 368-384.e365. doi:10.1016/j.neuron.2017.06.003

Yager, L. M., Garcia, A. F., Wunsch, A. M., & Ferguson, S. M. (2015). The ins and outs of the striatum: role in drug addiction. *Neuroscience, 301*, 529-541. doi:10.1016/j.neuroscience.2015.06.033

Appendix 1: Detailed explanation of preclinical models of addiction.

The field of addiction primarily aims to enhance our understanding of the behavioural, environmental and neurochemical changes contributing to the addiction processes, and develop effective treatments to prevent relapse to addictive drugs (Epstein et al., 2006; Everitt et al., 2018; Van den Oever et al., 2010). Whilst many experiments are conducted on humans, studies of human addiction are limited by ethical concerns and confounding factors including comorbid neuropsychological disorders, poly drug use, environmental and genetic influences (Hall, Carter, & Morley, 2004). Animal models of addiction are a useful tool for studying drug-induced changes in physiology, behaviour and brain neurochemistry. Moreover, the use of animal models enables examination of addiction processes under controlled laboratory conditions (Panlilio & Goldberg, 2007). Preclinical animal models of drug addiction can yield critical information relating to altered reward circuitry and the development of targeted pharmacotherapies (Deroche-Gamonet et al., 2004; Everitt et al., 2018; Panlilio & Goldberg, 2007).

Animal models of addiction can be subdivided into two distinct categories based on the method of drug administration; non-contingent, experimenter-delivered drug paradigms and contingent, self-administration paradigms (Kalivas, 2009). Examples of non-contingent drug administration models include behavioural sensitisation (Pierce & Kalivas, 1997) and conditioned place preference, which can be used to examine learnt contextual associations (Tzschentke, 2007). In contrast, contingent self-administration models of addiction require experimental animals to perform a trained operant response in order to receive delivery of an addictive drug (Kalivas, 2008; Panlilio & Goldberg, 2007). Drug self-administration paradigms exhibit the highest correlation with human drug administration (Epstein et al., 2006; Panlilio & Goldberg, 2007), including a similar incidence of addiction-like behaviours in a drug-using population (Deroche-Gamonet et al., 2004). Drug self-administration models are highly regarded as a valid animal model of human addiction behaviour (Deroche-Gamonet et al., 2004; Kalivas, 2009; Panlilio & Goldberg, 2007; Shaham et al., 2003).

Animal Models of Drug Self-administration

Drug self-administration models are built on operant conditioning paradigms, where experimental animals are trained to perform a particular response, for example press a lever or poke their nose into a hole, in order to receive reinforcement in the form of administered drug (Panlilio & Goldberg, 2007; Shaham et al., 2003). Drug-self administration is a form of operant conditioning as drug administration acts as a reinforcement, increasing the likelihood of repeating the response which triggered drug delivery (Kalivas, 2009; Panlilio & Goldberg, 2007). Furthermore, drug self-administration paradigms often incorporate environmental cues such as lights and/or tones which act to predict the availability of drug, utilising classical conditioning principles to strengthen the association between the performed response and drug reward (Panlilio & Goldberg, 2007). Most commonly, drugs are administered via intravenous catheters (Deroche-Gamonet et al., 2004), however oral routes can also be used (Panlilio & Goldberg, 2007).

Self-administration models can incorporate varying schedules of reinforcement (Kalivas, 2009; Panlilio & Goldberg, 2007). These training schedules outline the number of times a response must be performed to receive reinforcement (Everitt et al., 2018; Panlilio & Goldberg, 2007). Requirements to receive reinforcement can be constant (fixed ratio) or variable (variable ratio) (Panlilio & Goldberg, 2007). Fixed ratio reinforcement schedules are typically used to detect the reinforcing properties of the stimulus and facilitate examination of the relationship between the performed response and drug administration, whilst progressive ratio schedules offer examination of the motivation of responding, as animals must continue performing the response whilst the ratio of responses required to receive drug administration increases (Panlilio & Goldberg, 2007).

Reinstatement Models

The reinstatement model of drug-seeking is widely used to emulate human relapse behaviours following a period of behavioural extinction or abstinence from drug-seeking (Panlilio & Goldberg, 2007; Shaham et al., 2003). Extinction training exposes the animal to the environmental context in which they previously received drug administration, for example an operant conditioning box with levers, but no longer rewards operant responses with drug delivery (Kalivas, 2008; Shaham et al., 2003). As the operant drug-seeking response is no longer reinforced by drug delivery, the behaviour will diminish over several days, providing forced abstinence from drug-taking (Kalivas, 2008; Panlilio & Goldberg, 2007).

Reinstatement of drug-seeking behaviour is initiated via presentation with one of three stimuli; a non-contingent drug injection, drug-associated cue such as a light and/or tone or an acute stressor such as a foot shock (Epstein et al., 2006; Kalivas, 2008). Once presented with this stimulus, drug-seeking behaviour will dominate over extinction-induced inhibition of responding, causing the animal to initiate previously learnt behaviours associated with drug administration, ‘relapse to drug-seeking behaviour’, despite no drug delivery (Kalivas, 2009; Shaham et al., 2003). Reinstatement models of addiction yield critical information, enhancing our understanding of the neural mechanisms driving relapse and assisting in the development of effective pharmacotherapies which may reduce the high incidence of relapse in human addicts attempting to abstain from continued drug-seeking (Epstein et al., 2006; Everitt et al., 2018; Van den Oever et al., 2010).

References:

Deroche-Gamonet, V., Belin, D., & Piazza, P. V. (2004). Evidence for addiction-like behavior in the rat. *Science, 305*(5686), 1014-1017. doi:10.1126/science.1099020

Epstein, D. H., Preston, K. L., Stewart, J., & Shaham, Y. (2006). Toward a model of drug relapse: an assessment of the validity of the reinstatement procedure. *Psychopharmacology (Berl), 189*(1), 1-16. doi:10.1007/s00213-006-0529-6

Everitt, B. J., Giuliano, C., & Belin, D. (2018). Addictive behaviour in experimental animals: prospects for translation. *Philos Trans R Soc Lond B Biol Sci, 373*(1742). doi:10.1098/rstb.2017.0027

Hall, W., Carter, L., & Morley, K. (2004). Neuroscience research on the addictions: a prospectus for future ethical and policy analysis. *Addictive Behaviours, 29*, 1481-1495.

Kalivas, P. W. (2008). Addiction as a pathology in prefrontal cortical regulation of corticostriatal habit circuitry. *Neurotoxicity Research, 14*(2), 185-189. doi:10.1007/bf03033809

Kalivas, P. W. (2009). The glutamate homeostasis hypothesis of addiction. *Nature Reviews Neuroscience, 10*, 561. doi:10.1038/nrn2515

Panlilio, L., & Goldberg, A. (2007). Self-administration of drugs in animals and humans as a model and an investigative tool. *Addiction, 102*, 1863-1870.

Pierce, R. C., & Kalivas, P. W. (1997). A circuitry model of the expression of behavioral sensitization to amphetamine-like psychostimulants. *Brain Research Reviews, 25*(2), 192-216. doi:https://doi.org/10.1016/S0165-0173(97)00021-0

Shaham, Y., Shalev, U., Lu, L., de Wit, H., & Stewart, J. (2003). The reinstatement model of drug relapse: history, methodology and major findings. *Psychopharmacology (Berl), 168*(1-2), 3-20. doi:10.1007/s00213-002-1224-x

Tzschentke, T. M. (2007). Measuring reward with the conditioned place preference (CPP) paradigm: update of the last decade. *Addict Biol, 12*(3-4), 227-462. doi:10.1111/j.1369-1600.2007.00070.x

Van den Oever, M. C., Spijker, S., Smit, A. B., & De Vries, T. J. (2010). Prefrontal cortex plasticity mechanisms in drug seeking and relapse. *Neuroscience & Biobehavioral Reviews, 35*(2), 276-284. doi:https://doi.org/10.1016/j.neubiorev.2009.11.016

Appendix 2: Animal Research Authority 2017/043

MACQUARIE University

ANIMAL RESEARCH AUTHORITY (ARA)

AEC Reference No.: 2017/043-8 — Date of Expiry: 22 October 2018

Full Approval Duration: 23 October 2017 to 30 September 2020

This ARA remains in force until the Date of Expiry (unless suspended, cancelled or surrendered) and will only be renewed upon receipt of a satisfactory Progress Report before expiry (see Approval email for submission details).

Principal Investigator:
Associate Professor Jennifer Cornish
Department of Psychology
Macquarie University, NSW 2109
jennifer.cornish@mq.edu.au
0404 807 175

Associate Investigators:
Sarah Baracz 0410 324 069
Nick Everett 0447 285 037
Erin Lynch 0431 106 315
Anita Turner 0411 283 223

Others Participating:
Katherine Robinson 0402 734 322
Teodora Nedelkoska 0423 397 306

In case of emergency, please contact:
the Principal Investigator / Associate Investigator named above
or Manager, CAF: 9850 7780 / 0428 861 163 and Animal Welfare Officer: 9850 7758 / 0439 497 383

The above-named are authorised by MACQUARIE UNIVERSITY ANIMAL ETHICS COMMITTEE to conduct the following research:

Title of the project: Does oxytocin reduce relapse to methamphetamine seeking through modulating GABA signaling in the prelimbic cortex?

Purpose: 4 - Research: Human or Animal Biology

Aims: To determine whether oxytocin acts directly in the Prelimbic Cortex (PLC) to reduce relapse to METH-seeking; the receptors which mediate oxytocin's effect in the PLC; and whether modulation of GABA neurons is necessary for oxytocin to reduce relapse.

Surgical Procedures category: 5 - Major Surgery with Recovery

All procedures must be performed as per the AEC-approved protocol, unless stated otherwise by the AEC and/or AWO.

Maximum numbers approved (for the Full Approval Duration):

Species	Strain	Age/Weight/Sex	Total	Supplier/Source
02 – Rat	Long Evans (GAD-Cre Transgenic)	Any/Any/Male	56	ARC, Perth
	Sprague Dawley (Wild-Type)		152	
	Long Evans		32	
			240	

Location of research:

Location	*Full street address*
Central Animal Facility	Building F9A, Research Park Drive, Macquarie University, NSW 2109

Amendments approved by the AEC since initial approval:

1. ***Amendment #1*** *– Add Katherine Robinson as Student (Executive approved. Ratified by AEC 14 December 2017).*
2. ***Amendment #2(a)*** *- Additional experiment to train 20 male rats to self-administer intravenous methamphetamine in up to 6 hour sessions, 5 days per week (2 days off a week) on a fixed ratio-1 (Approved by AEC 14 December 2017).*
3. ***Amendment #2(b)*** *- Add 32 Male Wild Type Rats (taking total no. of Male Wild Type Rats on protocol to 184) (Approved by AEC 14 December 2017) (Approved by AEC 14 December 2017).*
4. ***Amendment #3(a)*** *- Add 16 Sprague Dawley rats (taking total number of SD rats on protocol to 200) (Executive approved. To be ratified by AEC 15 February 2018).*
5. ***Amendment #3(b)*** *- Additional experiment to include infusion of the virus (experiment #8) into the paraventricular nucleus of the hypothalamus (Executive approved. To be ratified by AEC 15 February 2018).*
6. ***Amendment #4(a)*** *- Use 32 male Long Evans rats instead of Sprague Dawley rats (Executive approved. To be ratified by AEC 15 February 2018).*
7. ***Amendment #4(b)*** *- Use 56 GAD-cre transgenic rats originating from Long Evans rats (Executive approved. To be ratified by AEC 15 February 2018).*
8. ***Amendment #5*** *- Add Anita Turner as Associate Investigator (Executive approved. Ratified by AEC 15 February 2018).*
9. ***Amendment*** *– 25/07/2018 – Add Teodora Nedelkoska to Protocol (Executive approved. To be ratified by AEC 23/08/2018).*

Conditions of Approval:

1. ***Amendment*** *– 25/07/2018 – Subject to submission of a revised Personnel Expertise document confirming no suspensions have occurred.*

A/Prof. Nathan Hart (Chair, Animal Ethics Committee) — Approval Date: 02 August 2018

Adapted from Form C (issued under part IV of the Animal Research Act, 1985)

Appendix 3: Cornish Behavioural Neuropharmacology Laboratory guide to constructing intravenous catheters.

Construction of Intravenous Catheters

Materials needed:

- Right angled cannulas 26 gauge *(Plastics One, Wallingford, Connecticut, USA)*
- Silastic tubing *(Dow Corning Australia Pty Ltd, North Ryde, NSW, Australia)*
  - Small tubing cut to 14.0 cm long
    - 0.33mm internal diameter (ID) x 0.64mm outside diameter (OD)
  - Medium tubing cut to 2.0 cm long
    - 0.64 mm ID x 1.19 mm OD
  - Large tubing cut to 1.5 cm long
    - 1.022 mm ID x 2.16 mm OD
- D-limonene citrus solvent *(Barnes, Moorebank, NSW, Australia)*
  - Aliquot ~30ml into a specimen jar
- Polypropylene mesh *(Small Parts, Lexington, Kentucky, USA)*
  - 500 micron opening; 300 micron thread diameter
- Silicone sealant *(Selleys, Padstow, NSW / Bunnings / Woolies)*
- Superglue *(Selleys, Padstow, NSW / Bunnings / Woolies)*
- Brass caps *(Macquarie Engineering and Technology Services)*
- Plastic fishing line
- Tygon tubing
- 1 ml syringe with 23 gauge needle (tip removed) for testing
- Saline
- Permanent marker
- Scalpel blade (any)
- Ruler
- 5 specimen jars

Construction:

1. **Test:** Test patency of each right-angled cannula by flushing with saline (using needle + tygon tubing)
2. **Cut Tubing:** Cut small, medium and long tubing to correct lengths (1 per catheter), and separate into 3 labelled specimen jars
3. Soak one end of the small diameter tubing in D-Limonene for at least 5 minutes to give it time to expand.
4. **Small Tubing:** Fit the expanded section of the small tubing to the long arm of the right-angled guide cannula. Allow at least an hour for the tubing to dry and shrink over the cannula. You should occasionally check to ensure that the small tubing has not slid down the cannula as it shrinks. Once the D-limonene has fully evaporated, the tubing will be secured firmly to the cannula.
5. **Medium Tubing:** To reinforce the section of small tubing that covers the cannula, we add further layers of progressively larger tubing. This protects

against leaks, and ensures long-term catheter patency. To do this, first soak medium diameter tubing in D-Limonene for about 5 minutes.

6. Using fingers or forceps, thread the small tubing of the cannula through the medium tubing. You may find it helps to collaborate with gravity at this step, and hold the medium tubing above the small, then slowly slide the medium over the small. Before sliding the medium tubing up onto the arm of the cannula, apply silicon sealant along the length of the small tubing covering the arm, then slide the medium tubing all the way up. It may be easiest to do this with your fingers, and slowly, as the grip of forceps can be too tight. Wipe away any excess silicone with paper towel. Again, allow about one hour of drying time.
7. IMPORTANT: Ensure that the small tubing underneath has not been scrunched up underneath the medium tubing. Lightly tug on the end of the small tubing to ensure it isn't stuck. Skipping this step may result in the small tubing bunching up and causing a blockage!
8. **Large Tubing**: Repeat steps 5-7 to fit the large tubing, and again allow one hour of drying time.
9. **Test**: Once the three layers of tubing have been fitted and dried, flush the catheter with saline to ensure it is clear (i.e. no silicone leaked into it, and the small tubing isn't bunched up)
10. **Mesh Back-mount**: Cut the polypropylene mesh into 2.5cm squares, and then shape it into a circle/ellipse to remove any sharp edges. Avoid removing too much of the mesh though, as a small back-mount may not stand up straight!
11. Using forceps make a small hole in the centre of the mesh, being careful to only pry the threads apart, without actually severing them. The hole only needs to be big enough for the plastic cap on the bottom of the cannula to fit through.
12. Remove the plastic cap from the cannula and place it into the hole on the mesh. Add a few droplets of superglue to the tip of the cap, and then refit it to the cannula. Wait at least 15 minutes for it to dry.
13. **Silicone Bead**: Apply a bead of silicon 3.5 cm up from the end of the small tubing (the end furthest from the catheter). This will prevent the tubing from entering too far into the jugular vein of the rat. To do this, use the wooden end of a cotton tip and make little meringue-like peaks. Roll the tubing around the smallest part of the peak to get it to catch and bead. It's not an issue if it's not a perfect sphere, but smoother edges are better. Try to avoid making it too large, and ensure there is no debris (i.e. little bits of silicone) on the rest of the small tubing, especially the 3.5 cm which will enter the vein. Allow at least 1 hour for the silicone to dry (hang from edge of a desk).
14. **Test**: Test each catheter thoroughly, ensuring a relatively effortless flow of saline. If a catheter is noticeably 'stiffer' than the others, you can trouble shoot this by:
    a. Flushing saline through at high pressure (might need a 10ml syringe) to remove any debris
    b. Lightly tugging on the small tubing to ensure it isn't bunched up
15. If a catheter isn't perfect, <u>don't use it!</u> You can always remove the tubing and start again ☺

Catheter construction in 6 stages!

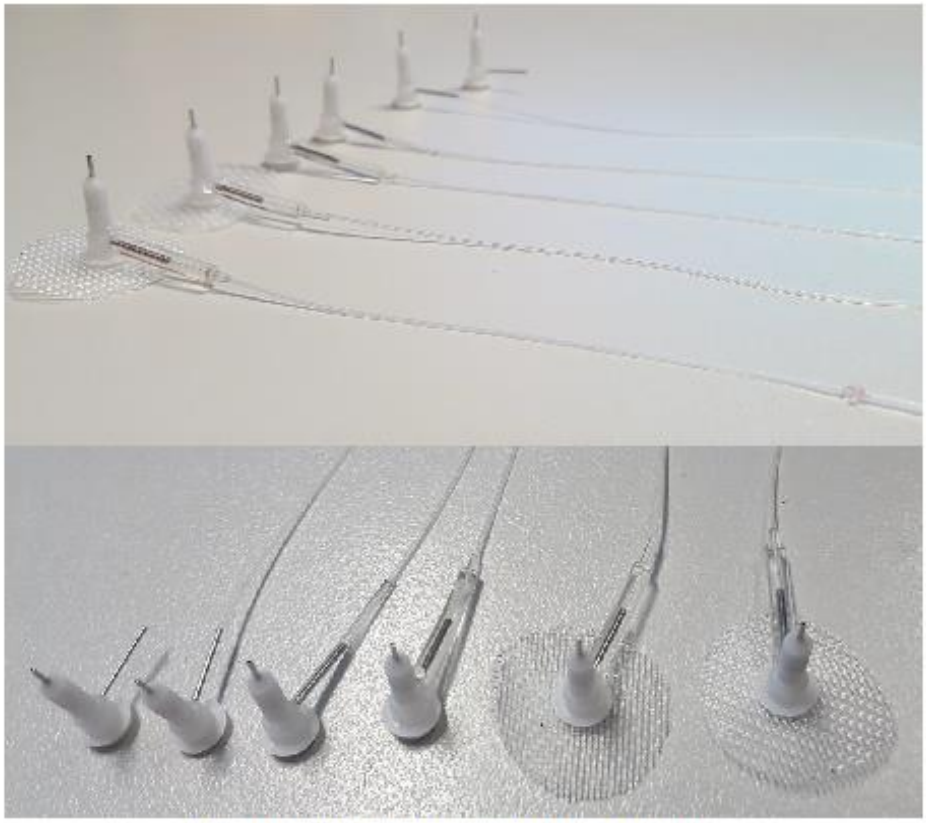

Completed intravenous catheter

1 = Right angled cannula

2 = Small tubing

3 = Medium tubing

4 = Large tubing

5 = Polypropylene mesh back mount

6 = Silicone bead

Plastic caps

1. For each catheter you use, you will also need to make a small plastic cap to close it, for when the rat is in its home cage. Note that these are different than the 'plastic caps' referred to in step 12 above, which secure the mesh to the cannula.
2. Cut a length of Tygon tubing, and a length of plastic fishing wire. The length will depend on how many plastic caps you need to make. As a guide, 15cm of Tygon and 10cm of fishing wire will comfortably make 16 plastic caps.
3. Using fingers or forceps, insert one end of the fishing wire into one end of the Tygon tubing, so that about 3-4mm of fishing wire is now inside the Tygon. This can be frustrating, as it is a very tight fit. Be patient!
4. Using scissors or wire cutters, snip the end of the fishing wire where it enters the Tygon, so you are now holding a long piece of Tygon with a small length of fishing wire inserted into one end.
5. Colour the end of the fishing wire/tygon using a permanent marker (red works best)
6. Using scissors or wire cutters, cut the tygon to about 5-6mm, so that half of the piece of Tygon is empty, and the other half is the fishing wire insert.
7. Repeat for each catheter – and perhaps make a few spares... They are very easy to drop, and you will handle each plastic cap at least twice per day during IVSA.

Appendix 4: List of primary antibodies used for immunohistochemistry.

Table 3

Antibodies used for immunohistochemistry experiments.

Antibody	Type	Concentration	Catalogue #	Company
Goat anti c-Fos	1°	1:1000	sc-52-G	Santa Cruz Biotechnology, Santa Cruz, CA, USA.
Rabbit anti nNOS	1°	1:500	SAB4502010	Sigma Aldrich, Castle Hill, NSW.
Mouse anti Parvalbumin	1°	1:1000	P3088	Sigma Aldrich, Castle Hill, NSW.
Mouse anti GAD67	1°	1:1000	MAB5406	Merck Millipore, Bayswater, VIC.
Donkey anti goat Cyanine 3	2°	1:500	705-165-147	Jackson ImmunoResearch, West Grove, PA, USA.
Donkey anti rabbit Alexa Fluor 647	2°	1:500	711-605-152	Jackson ImmunoResearch, West Grove, PA, USA.
Donkey anti mouse 488	2°	1:500	715-545-150	Jackson ImmunoResearch, West Grove, PA, USA.

Appendix 5: Detailed immunohistochemistry protocol.

1. Permeabilise free floating tissue sections in 50% ethanol (Chem Supply, Gillman, Australia) diluted in 0.1M phosphate buffered saline (PBS) shaking for 30 minutes at room temperature.

2. Rehydrate sections via 3 x 10 minute washes in 0.1M PBS, shaking at room temperature.

3. Block tissue for non-specific binding in 0.1M Tris-PBS (10mM Tris, 0.9% sodium chloride, 0.05% thermiserol and 10mM phosphate buffer) containing 10% normal horse serum (NHS) and 10% normal rat serum. Incubate at room temperature for 1-2 hours with gentle agitation.

4. Add primary antibody to blocking solution. Incubate for a total of 68 hours (including 24 hours at room temperature). Agitate gently to ensure antibody circulation.

6. Remove primary antibody solution and was tissue sections 3 x 10 minutes in 0.1M PBS.

7. Incubate tissue sections in solution containing in 0.1M Tris-PBS and 2% NHS with fluorescent-conjugated secondary antibodies. Cover pots in foil to protect from light and incubate at 4^{o}C for 24 hours (gentle shaking).

9. Store tissue in PBSm at 4^{o}C until ready for mounting and visualisation. Avoid light during storage and mounting.

10. Mount tissue sections onto glass slides using 0.1M PBS with 3% Tween-20 and Dako fluorescence mounting media (Agilent, Mulgrave, Victoria, Australia).

Neurons were considered to be immunoreactive for Fos when fluorescent signals were confined to oval or round-shaped nuclei. Neurons were considered to immunoreactive for nNOS and PV when fluorescent signals were present throughout the cytoplasm of the neuron.

Appendix 6: Number of immunoreactive neurons in regions of interest.

Table 5

Mean number (± SEM) of c-Fos immunoreactive neurons.

Region	Bregma	Vehicle/Vehicle (n = 5)	Vehicle/METH (n = 5)	METH/Vehicle (n = 4)	METH/METH (n = 5)
NAc	1.7mm	9.80 ± 4.76	16.00 ± 9.16	3.25 ± 2.02	37.20 ± 9.63
Core	2.2mm	6.00 ± 2.95	9.40 ± 2.25	4.75 ± 3.12	32.60 ± 12.06
	2.7mm	0.80 ± 0.37	5.20 ± 1.74	1.75 ± 1.18	6.25 ± 5.27
	3.2mm	1.00 ± 0.78	0.60 ± 0.60	0.00 ± 0.00	0.40 ± 0.40
	Total	17.60 ± 5.25	31.20 ± 9.95	9.75 ± 5.31	75.20 ± 11.48
NAc	1.7mm	5.60 ± 2.84	17.20 ± 8.99	1.00 ± 1.00	25.40 ± 11.06
Shell	2.2mm	4.20 ± 2.27	10.60 ± 2.91	2.75 ± 1.25	22.40 ± 11.95
	2.7mm	0.00 ± 0.00	1.80 ± 0.80	3.50 ± 2.36	2.75 ± 1.11
	Total	9.80 ± 3.48	29.60 ± 0.31	7.25 ± 4.27	50.00 ± 14.62
Cg1	1.7mm	5.80 ± 1.88	16.40 ± 8.41	6.50 ± 2.47	42.40 ± 12.86
	2.2mm	9.20 ± 5.45	22.80 ± 8.73	9.50 ± 4.63	44.20 ± 18.98
	2.7mm	8.60 ± 6.62	40.00 ± 20.83	16.25 ± 9.03	42.25 ± 17.68
	3.2mm	7.00 ± 2.85	8.80 ± 3.90	4.75 ± 1.03	50.60 ± 19.01
	3.7mm	4.50 ± 2.72	8.60 ± 2.87	5.33 ± 2.33	37.40 ± 9.271
	4.2mm	0.60 ± 0.60	8.00 ± 2.43	1.00 ± 0.48	15.50 ± 13.85
	Total	34.80 ± 16.55	104.60 ± 30.81	42.00 ± 16.16	220.80 ± 53.29
PrL	2.7mm	14.60 ± 5.43	39.00 ± 11.10	24.00 ± 10.79	25.25 ± 8.92
	3.2mm	21.20 ± 7.89	14.60 ± 5.64	3.75 ± 1.44	41.80 ± 4.72
	3.7mm	10.75 ± 7.83	15.60 ± 6.17	13.67 ± 5.24	26.80 ± 6.18
	4.2mm	4.00 ± 2.14	23.00 ± 10.82	5.67 ± 2.40	40.50 ± 30.19
	4.7mm	1.80 ± 0.66	18.50 ± 8.25	8.33 ± 5.90	18.20 ± 3.02
	Total	48.40 ± 19.12	87.60 ± 25.83	42.25 ± 12.42	121.20 ± 31.69
IL	2.7mm	4.20 ± 1.80	6.50 ± 2.60	5.25 ± 3.59	7.25 ± 2.69
	3.2mm	5.60 ± 2.09	3.40 ± 1.60	1.75 ± 0.85	5.60 ± 0.87
	3.7mm	4.25 ± 2.63	3.60 ± 0.93	4.33 ± 1.86	7.40 ± 1.86
	Total	13.20 ± 4.66	12.20 ± 2.56	10.25 ± 3.57	18.80 ± 1.32
LO	2.7mm	7.00 ± 2.85	29.00 ± 7.87	7.75 ± 2.43	42.75 ± 12.98
	3.2mm	13.00 ± 5.13	23.20 ± 9.23	5.75 ± 1.80	72.80 ± 15.16
	3.7mm	2.75 ± 1.60	33.20 ± 13.66	43.33 ± 18.44	79.80 ± 10.43
	4.2mm	5.20 ± 1.83	36.80 ± 19.18	12.75 ± 1.80	74.00 ± 22.33
	4.7mm	2.80 ± 2.06	25.75 ± 8.83	20.25 ± 10.91	73.80 ± 8.86
	Total	27.40 ± 40	122.20 ± 44.53	58.75 ± 17.18	246.00 ± 53.41
VO	3.2mm	15.80 ± 5.23	27.00 ± 10.73	5.50 ± 2.53	78.60 ± 17.70
	3.7mm	14.00 ± 9.72	23.80 ± 10.64	21.33 ± 8.68	47.80 ± 7.79
	4.2mm	11.40 ± 4.39	28.60 ± 13.07	8.50 ± 3.52	92.00 ± 60.14
	4.7mm	4.60 ± 2.04	24.50 ± 10.49	14.50 ± 5.07	40.80 ± 11.36
	Total	13.40 ± 3.33	14.20 ± 5.15	24.50 ± 5.90	20.40 ± 3.52
MO	4.2mm	1.60 ± 0.81	6.00 ± 3.49	3.33 ± 1.45	15.75 ± 9.33
	4.7mm	3.40 ± 1.86	6.50 ± 2.18	2.67 ± 1.45	12.00 ± 5.31
	Total	5.00 ± 1.92	10.00 ± 4.56	4.50 ± 0.87	22.20 ± 8.06

Table 6

Mean number (± SEM) of nNOS immunoreactive neurons.

Region	Bregma	Vehicle/Vehicle (n = 5)	Vehicle/METH (n = 5)	METH/Vehicle (n = 5)	METH/METH (n = 5)
NAc	1.7mm	29.40 ± 8.04	27.80 ± 9.536	38.20 ± 12.01	41.20 ± 10.91
Core	2.2mm	23.40 ± 6.23	26.20 ± 4.40	22.80 ± 9.22	31.80 ± 6.97
	2.7mm	13.00 ± 3.80	12.80 ± 4.10	6.20 ± 2.13	12.00 ± 5.26
	3.2mm	2.60 ± 1.33	2.20 ± 1.02	4.40 ± 2.16	2.00 ± 0.949
	Total	68.40 ± 15.00	69.00 ± 15.00	71.60 ± 22.68	84.60 ± 14.49
NAc	1.7mm	43.60 ± 6.70	56.20 ± 10.96	29.60 ± 5.34	63.00 ± 10.56
Shell	2.2mm	30.80 ± 8.37	46.20 ± 11.84	26.40 ± 4.61	40.40 ± 10.20
	2.7mm	6.40 ± 2.50	9.20 ± 1.74	3.80 ± 1.69	4.75 ± 0.85
	Total	80.80 ± 13.05	111.60 ± 17.84	59.80 ± 8.09	107.20 ± 16.22
Cg1	1.7mm	4.40 ± 0.93	4.60 ± 1.29	4.80 ± 1.07	5.40 ± 0.68
	2.2mm	3.40 ± 0.68	3.20 ± 0.92	4.00 ± 1.79	5.60 ± 1.33
	2.7mm	3.20 ± 1.32	5.40 ± 1.29	3.40 ± 0.51	5.00 ± 1.29
	3.2mm	2.80 ± 0.58	6.20 ± 1.99	5.20 ± 1.69	3.40 ± 0.49
	3.7mm	1.25 ± 0.47	1.40 ± 0.510	4.40 ± 2.77	4.20 ± 0.66
	4.2mm	1.00 ± 0.32	2.60 ± 1.17	3.20 ± 1.59	0.75 ± 0.25
	Total	15.80 ± 2.42	23.40 ± 4.81	25.00 ± 6.77	23.20 ± 2.78
PrL	2.7mm	6.00 ± 1.70	3.00 ± 1.00	8.20 ± 3.74	4.25 ± 1.44
	3.2mm	2.40 ± 1.12	2.80 ± 1.39	5.60 ± 1.40	5.00 ± 0.89
	3.7mm	5.00 ± 1.78	3.20 ± 1.83	7.20 ± 5.21	4.80 ± 2.35
	4.2mm	3.20 ± 1.32	4.50 ± 1.71	7.25 ± 4.40	1.25 ± 0.75
	4.7mm	0.80 ± 0.37	5.25 ± 1.97	3.25 ± 1.32	2.80 ± 0.66
	Total	16.40 ± 3.23	16.80 ± 6.29	29.40 ± 14.20	17.00 ± 4.40
IL	2.7mm	3.40 ± 1.54	2.25 ± 0.25	4.50 ± 2.60	3.00 ± 1.68
	3.2mm	1.80 ± 0.66	2.00 ± 1.52	2.60 ± 1.47	0.80 ± 0.49
	3.7mm	2.25 ± 0.95	0.80 ± 0.37	3.00 ± 2.07	3.80 ± 2.15
	Total	7.00 ± 2.53	4.60 ± 1.80	9.20 ± 5.56	7.00 ± 2.70
LO	2.7mm	1.20 ± 0.37	1.20 ± 0.74	7.80 ± 6.62	2.75 ± 1.55
	3.2mm	3.00 ± 1.00	4.20 ± 1.16	12.60 ± 8.05	7.80 ± 2.63
	3.7mm	2.75 ± 0.48	5.40 ± 1.36	5.20 ± 0.97	7.00 ± 1.14
	4.2mm	7.40 ± 2.79	5.20 ± 1.32	6.40 ± 2.87	4.00 ± 1.47
	4.7mm	2.40 ± 1.60	5.75 ± 2.17	7.25 ± 4.40	5.60 ± 2.13
	Total	16.20 ± 4.01	20.60 ± 4.39	37.80 ± 21.65	25.80 ± 3.68
VO	3.2mm	3.60 ± 1.29	3.40 ± 1.33	7.80 ± 5.24	3.80 ± 1.60
	3.7mm	3.75 ± 0.48	5.20 ± 1.46	5.40 ± 3.34	4.00 ± 1.38
	4.2mm	4.80 ± 1.32	4.40 ± 1.50	5.60 ± 1.72	3.25 ± 1.25
	4.7mm	3.80 ± 0.86	4.25 ± 1.49	7.50 ± 3.66	4.40 ± 1.69
	Total	15.20 ± 3.17	16.40 ± 4.46	24.80 ± 12.79	14.80 ± 3.00
MO	4.2mm	1.60 ± 0.68	1.75 ± 0.63	3.50 ± 1.85	1.50 ± 1.19
	4.7mm	1.80 ± 0.66	3.25 ± 1.97	2.75 ± 1.03	1.75 ± 0.48
	Total	3.40 ± 1.03	4.00 ± 2.10	5.00 ± 2.41	2.60 ± 0.98

Table 7

Mean number (± SEM) of parvalbumin immunoreactive neurons.

Region	Bregma	Vehicle/Vehicle (n = 5)	Vehicle/METH (n = 5)	METH/Vehicle (n = 5)	METH/METH (n = 5)
NAc	1.7mm	6.40 ± 3.78	7.80 ± 3.23	0.40 ± 0.40	3.00 ± 0.84
Core	2.2mm	4.40 ± 2.25	7.40 ± 3.36	0.20 ± 0.20	6.60 ± 3.34
	2.7mm	2.20 ± 1.43	5.20 ± 2.85	0.00 ± 0.00	1.50 ± 1.50
	3.2mm	0.00 ± 0.00	0.00 ± 0.00	0.00 ± 0.00	0.00 ± 0.00
	Total	13.00 ± 7.02	20.40 ± 8.81	0.60 ± 0.40	10.80 ± 3.65
NAc	1.7mm	7.20 ± 3.41	4.80 ± 1.86	0.20 ± 0.20	6.80 ± 4.09
Shell	2.2mm	2.00 ± 1.05	7.60 ± 6.14	0.20 ± 0.20	3.80 ± 2.40
	2.7mm	0.00 ± 0.00	3.00 ± 3.00	0.00 ± 0.00	1.50 ± 1.50
	Total	9.20 ± 4.22	15.40 ± 7.87	0.40 ± 0.40	11.80 ± 3.87
Cg1	1.7mm	17.40 ± 5.97	44.80 ± 16.15	33.80 ± 4.66	26.80 ± 4.21
	2.2mm	31.40 ± 16.69	28.20 ± 8.87	29.40 ± 13.74	36.20 ± 16.64
	2.7mm	24.20 ± 18.05	28.40 ± 7.69	28.20 ± 10.57	29.25 ± 3.82
	3.2mm	10.00 ± 3.33	31.40 ± 12.00	20.20 ± 7.59	20.40 ± 3.84
	3.7mm	8.00 ± 4.04	10.80 ± 5.54	4.50 ± 1.44	21.80 ± 6.51
	4.2mm	1.80 ± 0.74	12.20 ± 9.24	2.20 ± 1.16	1.25 ± 0.75
	Total	92.80 ± 37.46	155.80 ± 52.44	117.40 ± 31.67	129.60 ± 29.33
PrL	2.7mm	57.80 ± 19.938	59.20 ± 14.88	22.60 ± 6.73	36.25 ± 10.29
	3.2mm	21.20 ± 6.37	46.80 ± 13.94	15.40 ± 4.65	42.40 ± 5.84
	3.7mm	21.80 ± 15.70	31.80 ± 9.50	18.25 ± 8.49	16.20 ± 6.28
	4.2mm	9.00 ± 4.57	26.75 ± 12.95	2.50 ± 1.66	4.25 ± 2.10
	4.7mm	4.40 ± 1.81	10.50 ± 3.38	1.00 ± 0.58	3.20 ± 1.77
	Total	114.20 ± 45.34	167.60 ± 43.39	55.20 ± 17.59	94.20 ± 19.03
IL	2.7mm	6.80 ± 2.13	5.50 ± 2.18	1.40 ± 1.40	0.25 ± 0.25
	3.2mm	5.80 ± 3.37	2.00 ± 0.95	0.60 ± 0.60	2.00 ± 1.30
	3.7mm	2.80 ± 2.31	3.40 ± 1.47	6.50 ± 4.91	1.60 ± 0.68
	Total	15.40 ± 7.30	9.80 ± 4.10	7.20 ± 4.35	3.80 ± 1.69
LO	2.7mm	7.20 ± 4.21	11.20 ± 3.22	1.00 ± 1.00	11.75 ± 4.82
	3.2mm	40.20 ± 12.80	47.40 ± 11.52	17.80 ± 7.83	50.80 ± 11.31
	3.7mm	32.20 ± 13.91	73.00 ± 17.55	47.00 ± 25.85	51.60 ± 14.41
	4.2mm	40.00 ± 11.57	50.00 ± 16.89	44.20 ± 28.14	26.75 ± 12.887
	4.7mm	13.20 ± 8.576	55.00 ± 23.41	9.00 ± 4.97	28.40 ± 11.47
	Total	132.80 ± 44.86	225.60 ± 54.95	109.60 ± 54.44	161.60 ± 29.57
VO	3.2mm	19.40 ± 6.86	41.60 ± 17.48	4.20 ± 2.58	20.40 ± 5.52
	3.7mm	31.80 ± 19.85	50.20 ± 17.71	28.00 ± 13.04	27.80 ± 10.74
	4.2mm	22.80 ± 12.34	56.20 ± 20.00	17.80 ± 7.65	15.50 ± 11.27
	4.7mm	25.60 ± 13.70	51.00 ± 22.92	25.80 ± 10.48	6.00 ± 3.29
	Total	99.60 ± 47.11	188.80 + 59.46	70.20 ± 23.96	66.60 ± 17.24
MO	4.2mm	5.80 ± 3.56	9.00 ± 5.12	2.75 ± 1.80	1.25 ± 0.75
	4.7mm	10.20 ± 5.55	15.75 ± 9.71	2.25 ± 0.85	8.50 ± 7.23
	Total	16.00 ± 9.04	19.80 ± 11.90	4.00 ± 2.02	7.80 ± 5.70

Table 8

Mean number (± SEM) of neurons colocalised for nNOS and Fos.

Region	Bregma	Vehicle/Vehicle (n = 5)	Vehicle/METH (n = 5)	METH/Vehicle (n = 4)	METH/METH (n = 5)
NAc	1.7mm	0.40 ± 0.40	0.40 ± 0.25	0.80 ± 0.58	1.00 ± 0.55
Core	2.2mm	0.20 ± 0.20	0.20 ± 0.20	1.40 ± 0.87	1.80 ± 1.11
	2.7mm	0.00 ± 0.00	0.20 ± 0.20	0.00 ± 0.00	0.25 ± 0.25
	3.2mm	0.00 ± 0.00	0.00 ± 0.00	0.00 ± 0.00	0.00 ± 0.00
	Total	1.00 ± 1.00	1.20 ± 0.58	1.60 ± 1.03	2.00 ± 1.55
NAc	1.7mm	0.00 ± 0.00	0.60 ± 0.25	0.40 ± 0.40	2.20 ± 1.74
Shell	2.2mm	0.60 ± 0.60	0.20 ± 0.20	0.40 ± 0.40	1.00 ± 0.63
	2.7mm	0.00 ± 0.00	0.00 ± 0.00	0.00 ± 0.00	0.00 ± 0.00
	Total	0.00 ± 0.00	0.00 ± 0.00	0.00 ± 0.00	0.00 ± 0.00
Cg1	1.7mm	0.40 ± 0.40	0.40 ± 0.25	0.60 ± 0.40	0.40 ± 0.40
	2.2mm	0.00 ± 0.00	0.20 ± 0.20	0.60 ± 0.40	0.00 ± 0.00
	2.7mm	0.00 ± 0.00	0.20 ± 0.20	0.80 ± 0.58	0.25 ± 0.25
	3.2mm	0.20 ± 0.20	0.00 ± 0.00	0.00 ± 0.00	0.00 ± 0.00
	3.7mm	0.00 ± 0.00	0.50 ± 0.50	0.20 ± 0.20	0.75 ± 0.48
	4.2mm	0.00 ± 0.00	0.50 ± 0.50	0.00 ± 0.00	0.25 ± 0.25
	Total	0.33 ± 0.33	1.60 ± 0.51	2.20 ± 1.16	1.40 ± 0.40
PrL	2.7mm	0.00 ± 0.00	0.00 ± 0.00	1.60 ± 0.98	0.25 ± 0.25
	3.2mm	0.00 ± 0.00	0.00 ± 0.00	0.20 ± 0.20	0.20 ± 0.20
	3.7mm	0.00 ± 0.00	0.00 ± 0.00	0.40 ± 0.40	0.25 ± 0.25
	4.2mm	0.00 ± 0.00	0.00 ± 0.00	0.80 ± 0.58	0.00 ± 0.00
	4.7mm	0.00 ± 0.00	0.40 ± 0.40	1.00 ± 1.00	0.75 ± 0.48
	Total	0.00 ± 0.00	0.40 ± 0.40	3.80 ± 0.74	1.20 ± 0.37
IL	2.7mm	0.40 ± 0.245	0.00 ± 0.00	0.00 ± 0.00	0.00 ± 0.00
	3.2mm	0.20 ± 0.20	0.00 ± 0.00	0.40 ± 0.40	0.00 ± 0.00
	3.7mm	0.00 ± 0.00	0.00 ± 0.00	0.20 ± 0.20	0.50 ± 0.50
	Total	0.60 ± 0.40	0.00 ± 0.00	0.60 ± 0.40	0.40 ± 0.40
LO	2.7mm	0.00 ± 0.00	0.00 ± 0.00	0.00 ± 0.00	0.00 ± 0.00
	3.2mm	0.60 ± 0.40	0.00 ± 0.00	0.00 ± 0.00	1.00 ± 0.78
	3.7mm	0.00 ± 0.00	0.25 ± 0.25	0.40 ± 0.40	0.50 ± 0.50
	4.2mm	0.00 ± 0.00	0.40 ± 0.40	1.00 ± 0.78	0.25 ± 0.25
	4.7mm	0.00 ± 0.00	0.00 ± 0.00	2.50 ± 1.66	0.20 ± 0.20
	Total	0.60 ± 0.40	0.60± 0.40	3.40 ± 2.09	1.80 ± 0.58
VO	3.2mm	0.20 ± 0.20	0.00 ± 0.00	0.60 ± 0.60	0.00 ± 0.00
	3.7mm	1.50 ± 1.50	0.25 ± 0.25	0.20 ± 0.20	1.00 ± 1.00
	4.2mm	0.00 ± 0.00	0.20 ± 0.20	1.20 ± 0.97	0.50 ± 0.29
	4.7mm	0.33 ± 0.33	0.00 ± 0.00	2.75 ± 2.43	0.20 ± 0.20
	Total	1.00 ± 0.55	0.40 ± 0.40	4.20 ± 2.78	1.40 ± 0.93
MO	4.2mm	0.00 ± 0.00	0.00 ± 0.00	0.20 ± 0.20	0.00 ± 0.00
	4.7mm	0.33 ± 0.33	0.00 ± 0.00	0.75 ± 0.75	0.00 ± 0.00
	Total	0.20 ± 0.20	0.00 ± 0.00	0.80 ± 0.80	0.00 ± 0.00

Table 9

Mean number (± SEM) of neurons colocalised for parvalbumin and Fos.

Region	Bregma	Vehicle/Vehicle (n = 5)	Vehicle/METH (n = 5)	METH/Vehicle (n = 4)	METH/METH (n = 5)
NAc	1.7mm	0.20 ± 0.20	0.00 ± 0.00	0.00 ± 0.00	0.00 ± 0.00
Core	2.2mm	0.00 ± 0.00	0.20 ± 0.20	0.00 ± 0.00	0.00 ± 0.00
	2.7mm	0.00 ± 0.00	0.20 ± 0.20	0.00 ± 0.00	0.00 ± 0.00
	3.2mm	0.00 ± 0.00	0.00 ± 0.00	0.00 ± 0.00	0.00 ± 0.00
	Total	0.00 ± 0.00	0.40 ± 0.40	0.00 ± 0.00	0.00 ± 0.00
NAc	1.7mm	0.40 ± 0.40	0.00 ± 0.00	0.60 ± 0.40	0.00 ± 0.00
Shell	2.2mm	0.20 ± 0.20	0.40 ± 0.40	0.00 ± 0.00	0.20 ± 0.20
	2.7mm	0.00 ± 0.00	0.20 ± 0.20	0.00 ± 0.00	0.00 ± 0.00
	Total	0.60 ± 0.60	0.40 ± 0.40	0.60 ± 0.40	0.20 ± 0.20
Cg1	1.7mm	0.00 ± 0.00	0.00 ± 0.00	0.20 ± 0.20	0.50 ± 0.50
	2.2mm	0.00 ± 0.00	0.00 ± 0.00	0.00 ± 0.00	0.60 ± 0.60
	2.7mm	0.20 ± 0.20	0.40 ± 0.25	0.00 ± 0.00	0.00 ± 0.00
	3.2mm	0.00 ± 0.00	0.00 ± 0.00	0.20 ± 0.20	0.00 ± 0.00
	3.7mm	0.00 ± 0.00	0.20 ± 0.20	0.00 ± 0.00	0.20 ± 0.20
	4.2mm	0.00 ± 0.00	0.00 ± 0.00	0.25 ± 0.25	0.00 ± 0.00
	Total	0.20 ± 0.20	0.60 ± 0.40	0.60 ± 0.60	1.20 ± 0.80
PrL	2.7mm	1.40 ± 0.75	0.20 ± 0.20	0.00 ± 0.00	0.00 ± 0.00
	3.2mm	1.40 ± 0.98	0.00 ± 0.00	0.60 ± 0.60	0.00 ± 0.00
	3.7mm	0.00 ± 0.00	0.00 ± 0.00	0.00 ± 0.00	0.00 ± 0.00
	4.2mm	0.60 ± 0.60	0.00 ± 0.00	0.00 ± 0.00	0.00 ± 0.00
	4.7mm	0.00 ± 0.00	0.00 ± 0.00	0.00 ± 0.00	0.00 ± 0.00
	Total	3.40 ± 2.18	0.20 ± 0.20	0.60 ± 0.60	0.00 ± 0.00
IL	2.7mm	0.40 ± 0.40	0.00 ± 0.00	0.00 ± 0.00	0.00 ± 0.00
	3.2mm	0.00 ± 0.00	0.00 ± 0.00	0.00 ± 0.00	0.00 ± 0.00
	3.7mm	0.00 ± 0.00	0.00 ± 0.00	0.00 ± 0.00	0.00 ± 0.00
	Total	0.40 ± 0.40	0.00 ± 0.00	0.00 ± 0.00	0.00 ± 0.00
LO	2.7mm	0.20 ± 0.20	0.20 ± 0.20	0.00 ± 0.00	0.50 ± 0.50
	3.2mm	0.00 ± 0.00	0.00 ± 0.00	0.00 ± 0.00	0.60 ± 0.40
	3.7mm	0.00 ± 0.00	0.00 ± 0.00	0.00 ± 0.00	0.20 ± 0.20
	4.2mm	0.40 ± 0.40	0.60 ± 0.60	0.00 ± 0.00	0.00 ± 0.00
	4.7mm	0.00 ± 0.00	0.00 ± 0.00	0.00 ± 0.00	0.00 ± 0.00
	Total	0.60 ± 0.60	1.00 ± 0.55	0.00 ± 0.00	1.20 ± 0.49
VO	3.2mm	0.00 ± 0.00	0.00 ± 0.00	0.00 ± 0.00	0.20 ± 0.20
	3.7mm	0.25 ± 0.25	0.00 ± 0.00	0.25 ± 0.25	0.00 ± 0.00
	4.2mm	0.40 ± 0.40	0.00 ± 0.00	0.00 ± 0.00	0.25 ± 0.25
	4.7mm	0.00 ± 0.00	0.00 ± 0.00	0.20 ± 0.20	0.00 ± 0.00
	Total	0.60 ± 0.60	0.00 ± 0.00	0.40 ± 0.25	0.40 ± 0.25
MO	4.2mm	0.00 ± 0.00	0.00 ± 0.00	0.00 ± 0.00	0.00 ± 0.00
	4.7mm	0.00 ± 0.00	0.00 ± 0.00	0.00 ± 0.00	0.00 ± 0.00
	Total	0.00 ± 0.00	0.00 ± 0.00	0.00 ± 0.00	0.00 ± 0.00

Appendix 7: Validation of Viral Vectors

Expression of Cre-dependent viral vectors was validated in a pilot cohort of Cre^+ (n = 4) and Cre^- rats (n = 2). Each animal underwent surgery to implant cannulae into the prelimbic cortex (AP: +3.2mm, ML: ±1.0mm, DV: - 2.3mm relative to Bregma). Each animal was injected with viral vectors into the PrL via micro-injectors which extended 1mm beyond cannulae. The left hemisphere of the brain was injected with a Cre-dependent DREADD-expressing virus (AAV2-hSyn-DIO-hM4D(Gi)-mCherry), whilst the right hemisphere of the brain was injected with a control virus (AAV1-phSyn(1)-FLEX-tdTomato -T2A-SypEGFP-WPRE). Blue microbeads (Thermo Fisher Scientific, Australia, Cat# 09980508) were mixed with both viral vectors (6 parts virus: 1 part microbeads) and co-injected. Three to five weeks after viral injection, animals were injected with 3mg/kg of CNO (IP). This was followed by a microinjection of 1ug of oxytocin per hemisphere, via implanted cannulae (25 minutes after CNO injection. Animals were then euthanised 90 minutes following oxytocin microinjected. Intracannulae injection of oxytocin has been shown to increased GABAergic activity within the PrL, whilst CNO administration should chemogenetically inactivate DREADD-transfected GABAergic neurons. Brains were harvested, sectioned and immunohistochemically stained for Fos (a marker of neuronal activity) and GAD67. Analysis of brain sections revealed a lack of viral expression in Cre^- rats, however blue microbeads were visible suggesting successful microinjection. Analysis of Fos immunoreactivity revealed significant colocalisation of GAD67 and Fos in neurons transfected with the control virus (below, left). A distinct lack of Fos colocalisation was observed in neurons positive for both mCherry and GAD67 (below, right); this suggests IP administration of 3mg/kg CNO was sufficient to hyperpolarise DREADD-transfected neurons.

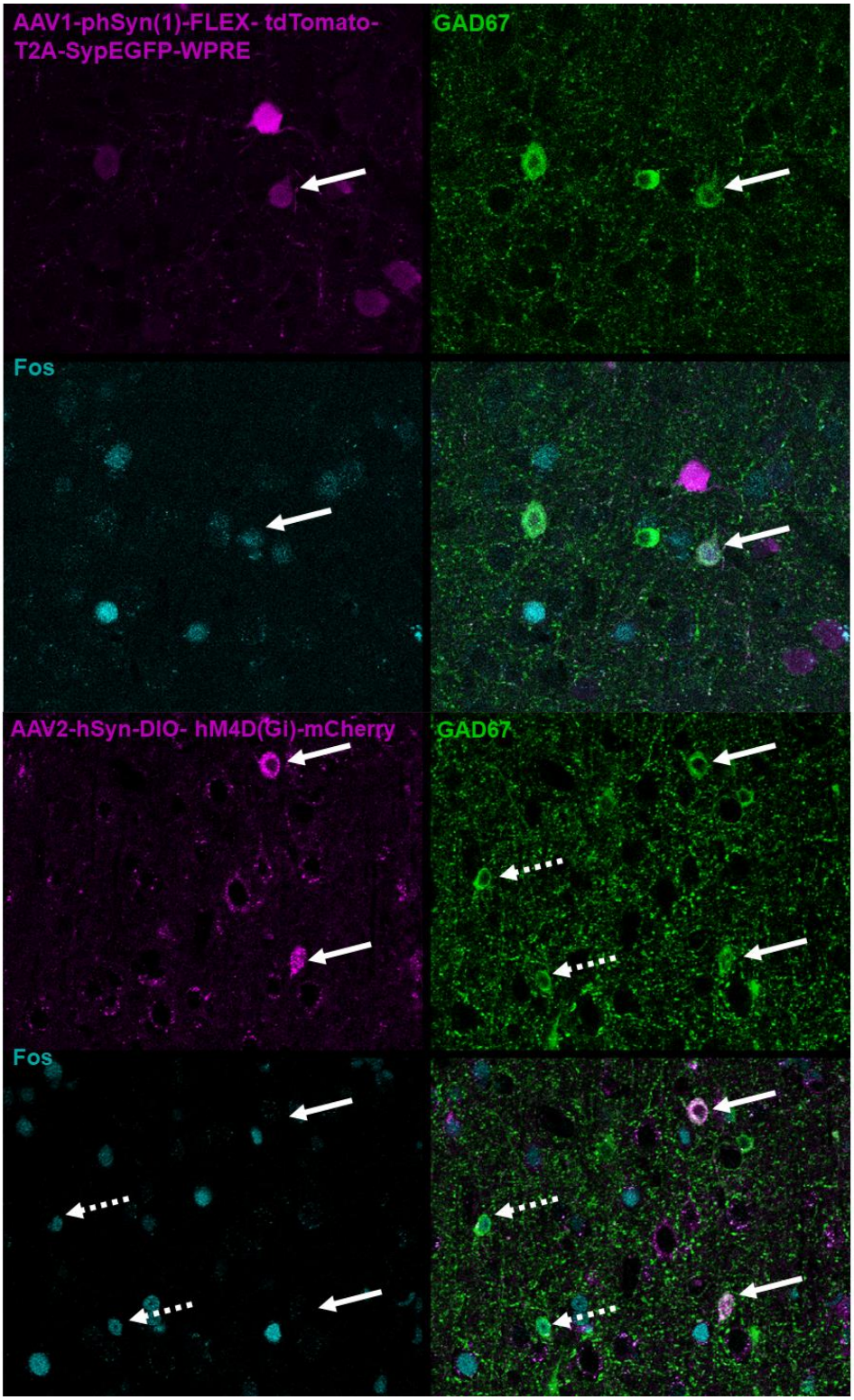

Supplementary Figure 1. Representative images displaying colocalised viral expression with GAD67 immunoreactivity (as represented by a bold arrow). DREADD-expressing neurons displayed a lack of Fos immunoreactivity, whilst non-DREADD transfected GABAergic neurons displayed Fos immunoreactivity (as represented by a broken arrow), suggesting oxytocin was increasing the activation of GAD67 neurons whilst treatment with CNO reduced the activity of DREADD-transfected neurons.

Appendix 8: Correlation Analysis of DREADD-transfection area and behavioural responses following pretreatment with CNO and oxytocin.

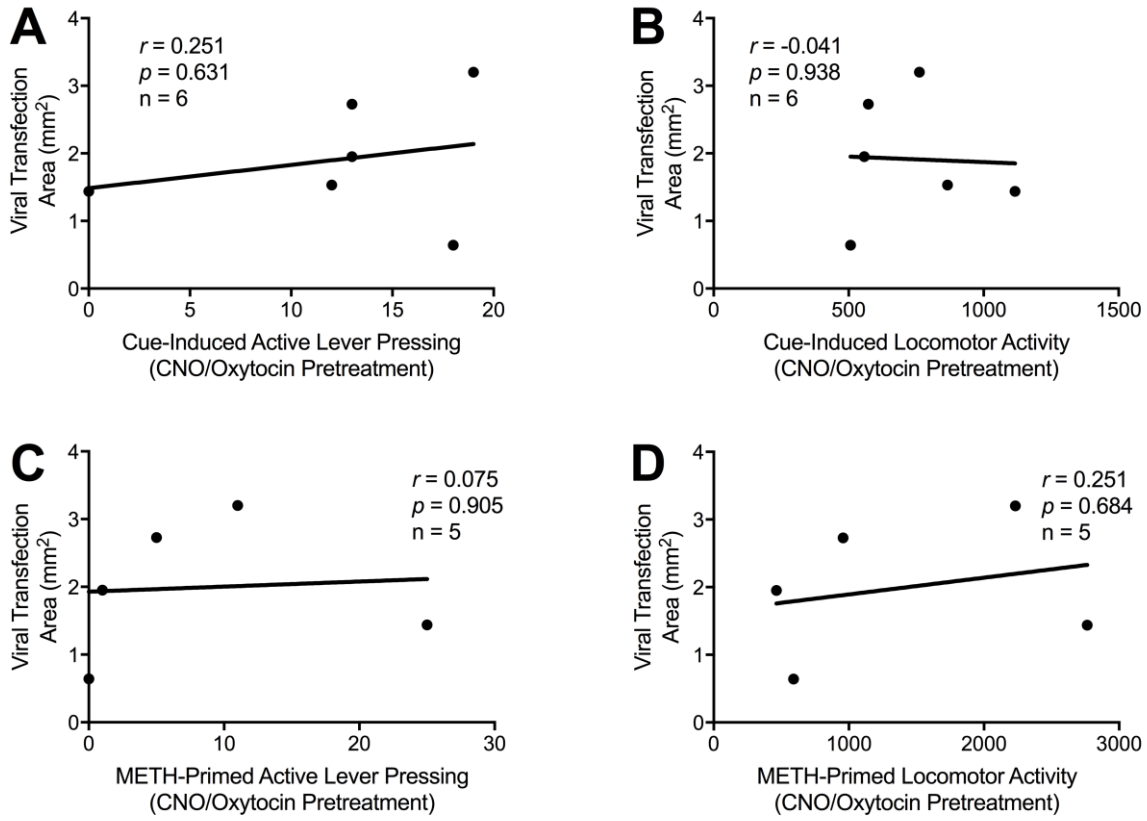

Supplementary Figure 2. To determine whether the effects of CNO depended upon individual differences in viral-mediated DREADD expression, the total area of DREADD expression (mm^2) was correlated with behavioural responses following pretreatment with CNO and oxytocin. (A) demonstrates a mild negative correlation between cue-induced active lever pressing and area of DREADD transfection. (B) demonstrates a mild positive correlation between METH-primed locomotor activity and area of DREADD transfection. (C) demonstrates a mild positive correlation between cue-induced active lever pressing and area of DREADD transfection. (D) demonstrates a mild positive correlation between METH-primed locomotor activity and area of DREADD transfection.